Université de la Méditerranée
AIX-MARSEILLE II
Faculté des Sciences de Luminy
163 Avenue de Luminy
13288 Marseille Cedex 09

Thèse de Doctorat

Specialité: Physique et Sciences de la Matière
Mention: Instrumentation

présentée par

Federico Alessio

en vue d'obtenir le grade de docteur de l'Université de la Méditerranée

Beam, Background and Luminosity Monitoring in LHCb and Upgrade of the LHCb Fast Readout Control

soutenance prévue le 21 juin 2011 devant le jury composé de

Dr.	T. Camporesi	Rapporteur
Dr.	R. Schmidt	Rapporteur
HDR.	R. Le Gac	Directeur de Thése
Dr.	R. Jacobsson	
HDR.	E. Kajfasz	

Contents

Chapter 1

Introduction

Le travail présenté dans cette thèse a été effectué au sein de la collaboration internationale LHCb qui a conçue et qui exploite un détecteur pour la physique des particules auprès de l'accélérateur proton-proton, le LHC, au CERN à Genève. Ces travaux concerne l'opération de l'expérience dans son ensemble. Ils ont montré toutes leurs forces pendant la première année de prise de données qui a débutée fin 2009. Ils couvrent plusieurs systèmes qui sont très dépendant les uns des autres.

Deux systèmes sont plus particulièrement étudiés. Le premier est en charge de la surveillance des faisceaux, du niveau des bruits de fond et de la luminosité. Le second permet la visualisation, l'analyse et l'optimisation des conditions expérimentales. Ces deux systèmes sont fortement interconnectés. En effet, l'amélioration de la qualité des faisceaux de la machine et la diminution du bruit de fond augmentent le nombre de collisions utiles pour la physique. En même temps, comprendre les paramètres clefs qui gouvernent l'opération de l'expérience permet de les optimiser et d'améliorer la qualité des données collectées.

Le complexe des accélérateurs du CERN ainsi que le LHC sont brièvement décrits dans le Chapitre 2. Le détecteur LHCb, ses divers composants et leurs technologies sont ensuite présentés avec le système de distribution des information temporelles et le système d'acquisition des données.

Les paramètres très complexes qui gouvernent les collision proton-proton au point d'interaction de LHCb sont introduis au Chapitre 3.4. Ils sont à l'origine des systèmes étudiés et mise en oeuvre dans cette thèse. Nous décrirons plus particulièrement, les paramètres des faisceau, l'origine des bruits de fond ainsi que la réception des information temporelles fournies par la machine, leurs distributions dans l'expérience et leurs synchronisation avec le passage des particules au point d'interaction. Ce Chapitre inclus une courte description des différent modes de fonctionnement de l'accélérateur et positionne ce travail dans le contexte plus général du LHC. Des comparaisons avec d'autres expériences sont également données afin d'étayer les choix pour les systèmes développés.

Pour satisfaire le cahiers des charges présenté dans le Chapitre 3.4, différents systèmes matériel et logiciels ont été conçus et réalisés. Ils sont décrits dans les Chapitres 4, 5, 6 et 7. Chapitre 3.4 est un chapitre central car il explique les conditions pour le travail présenté dans cette thèse.

Le Chapitre 4 détail le cadre en charge de la surveillance en ligne des paramètres des faisceaux, du niveaux du bruit de fond et de la luminosité ainsi que les instruments impliquées. Notamment, un système de scintillateur, appelé Beam Loss Scintillator, qui joue un rôle central dans la mesure en temps réels des conditions expérimentales. Le système qui surveille l'intensité des faisceaux et la répartition des différents paquets de protons dans la machine sont également décrits. Ces deux systèmes sont des systèmes hardware qui utilisent la même carte d'acquisition et de contrôle développé pour LHCb. Cette carte est également employé pour la surveillance et le contrôle global de la synchronisation des informations temporelles qui est décrit au début du Chapitre 5.

La deuxième partie du Chapitre 5 est consacrée au système optimisant les conditions expérimentales de LHCb. Elle comprend la description des logiciels développés pour le suivit en temps réels et l'analyse des conditions expérimentales de LHCb, la protection du détecteur et les échanges de données avec la machine. Ces outils logiciels s'appellent : *LHCb Experimental Analysis Tool*, *LHCb Run Summary*, *Operation Webpages* et *LHC Programme Coordinator automatic files exchange*. Leurs intégrations dans le système de contrôle PVSS de l'expérience est également présenté.

Un système de synchronisation centralisée a été développé afin de contrôler les instruments dédiées à la mesure des conditions expérimentales et les système d'acquisition des données. La première partie du Chapitre 6 est consacrée à ce système et à son rôle dans les opérations globales de LHCb. Une proposition détaillée pour un système amélioré est décrite dans la deuxième partie du Chapitre. Ce travail prendra tous son sens dans l'amélioration de LHCb prévue à l'horizon 2018.

Le système de synchronisation surveille en temps réels la luminosité délivrée par la machine. La théorie derrière la mesure de la luminosité et les méthodes employées dans LHCb sont développées dans le Chapitre 7. Une méthode alternative est également présentée à la fin du Chapitre. Il est important de noter que la surveillance en ligne de la luminosité dépend fortement des caractéristiques des faisceaux et du bruit du fond. Cette mesure est essentielle dans l'opération de LHCb, car cette expérience a été conçue pour fonctionner dans des conditions particulières.

Le dernier Chapitre est consacré aux résultats obtenus pendant la première année de fonctionnement du LHC à 3.5 TeV par faisceau. Différentes analyses ont été menées. Leurs impacts sur la mise au point de la machine, les opérations globales de LHCb et la compréhension des faisceaux sont soulignés. Les analyses présentées touchent la dynamique de l'injection, les taux d'interaction des protons avec le gaz

résiduel des chambres à vide, la dérive de la phase de l'horloge dus aux effets de la température, la luminosité et l'émittance par bunch. Une étude dédiée pour déterminer l'acceptance du système de scintillateurs est également présentée. Ce dernier a été employé comme source de mesure en ligne de la luminosité indépendamment de celles possible avec le détecteur de LHCb. L'ensemble de ces études montrent le bon fonctionnement des systèmes décrit dans cette thèse et le niveau de performance atteint par l'expérience LHCb.

Chapter 2

The Large Hadron Collider beauty Experiment

The LHCb experiment is one of the four big experiments which is taking place at the Large Hadron Collider at CERN, close to Geneva, in Switzerland. A brief introduction to the LHC experiments will be given in the next section, followed by a detailed description of the LHCb experiment. The physics programme will be highlighted and the various systems of the detectors will be described. A section dedicated to the LHCb readout and the Timing and Fast Control systems is included since they are relevant for the work presented in this thesis.

2.1 The LHC adventure

LHC stands for Large Hadron Collider [1]. It is a 27 km long accelerator, where two beams of protons or ions travelling in opposite directions collide at four points the machine's circumference.

In an accelerator like the LHC, the maximum energy obtainable is a function of the radius and the strength of the dipole magnetic field that keeps the particles on their orbit. Reusing the existing 27 km circumference tunnel of the LEP (Large Electron-Positron) accelerator, the LHC can reach a maximum energy of 7 TeV per proton beam. This is by far the highest energy ever reached in a beam collider. In reality, the energy available is the centre-of-mass energy, that is the sum of the energy of the two counter-circulating beams. The goal for the LHC is to reach 14 TeV of centre-of-mass energy. When a particle is accelerated, it loses a certain amount of energy along the accelerator. The energy lost is called synchrotron radiation and it increases the lighter the particle is. Hence to obtain the highest-energy collisions it is better to accelerate massive particles, like protons, which are 2000 times more massive than electrons.

The physics to be studied at the LHC accelerator is very broad. The reasons why elementary particles have mass and why their masses are different are among the most perplexing questions to be answered by physicists from all over the world. The answer may be the so-called *Higgs Mechanism* which predicts at least one new particle, the Higgs boson. If such a particle exists, the LHC will be able to detect it and measure its mass with very high precision. According to the theory of the Higgs mechanism, the whole of space is filled with a *Higgs field*, and by interacting with this field, particles acquire their masses. Particles that interact strongly with the Higgs field are heavy, while those that have weak interactions are light.

A very popular idea which could partly explain how all the matter we see in the Universe counts for only 4 % of the total mass, is called supersymmetry, or SUSY. SUSY predicts that for each known particle there is a supersymmetric partner. If SUSY is right, then supersymmetric particles should be found at the LHC.

The LHC will try to solve the mystery of antimatter. According to our understanding, particles and anti-particles must have been produced in the same amounts at the time of the Big Bang. However from what we have observed so far, our Universe is made of only matter. It was once thought that anti-particles were a perfect reflection of particles without being able to tell the difference. Actually as first experiments observed in the past, the reflection is imperfect. If one assumes that after the Big Bang, the Universe separated into different domains where either the amount of particles or anti-particles was dominant, then at the boundaries there should be annihilations, producing cosmic gamma rays. The limit proposed by current theories and experiments is practically equivalent to saying that there is no anti-matter left in our Universe. A necessary condition for a matter/anti-matter imbalance to arise according to Sacharov is CP-violation. In physical cosmology, the imbalance of baryons and anti-baryons is called *baryogenesis*. For baryogenesis to have happened, Sacharov postulated three conditions. One of them was effectively to have C-symmetry and CP-symmetry violation.

The technology involved in the design and construction of the LHC facility is the most advanced ever considered. The whole complex consists of a succession of accelerators allowing to reach the beam energy of 7 TeV in the main LHC, as shown in Figure 2.1 and Figure 2.2.

The LHC proton beams are derived from hydrogen atoms taken from a standard hydrogen bottle. Protons can be obtained by stripping orbiting electrons off hydrogen atoms. Then protons are injected into the PS Booster (PSB) at an energy of 50 MeV from Linac2. The booster accelerates them to 1.4 GeV. The beam is then fed to the Proton Synchrotron (PS) where it is accelerated to 25 GeV. Protons are then sent to the Super Proton Synchrotron (SPS) where they are accelerated to 450 GeV. They are finally transferred to the LHC in a clockwise and anticlockwise direction where they are accelerated to their nominal 7 TeV energy. Beams circulate for many hours inside the LHC beam pipes under normal operating conditions and in a well-defined structure of bunches [2]: each proton beam has thousands

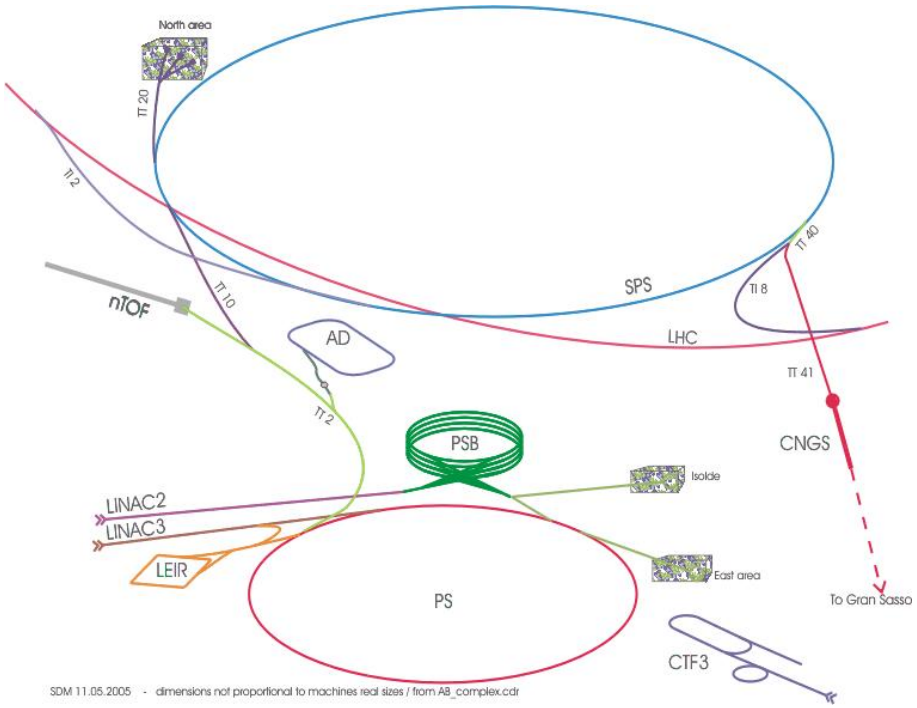

Figure 2.1: The injecting system.

of bunches of particles, where each bunch contains more than 10^{11} particles. A detailed description of the beam structure in bunches will be given later.

The particles circulate in a vacuum tube (10^{-13} atm) and are manipulated using superconducting magnets and radio frequency cavities. The magnetic field is used to curve the trajectory of charged particles and to focus the beam down to the smallest possible size for collisions. The total number of dipoles and quadrupoles magnets in the LHC accelerator is about 9000 and the peak value of the magnetic field is 8.3 T. The LHC dipoles use special cables which become superconducting below a temperature of 10 K. Hence superconducting cavities need a cryogenic system to keep the temperature of the cavity at 1.9 K. To ensure such a low temperature near absolute zero, the LHC superconducting elements sit in a bath of superfluid helium at atmospheric pressure. This bath is cooled by low-pressure helium flowing in heat exchanger tubes threaded along the string of magnets. Radio frequency cavities accelerate the beams in the accelerator. They are also used to keep all the bunches longitudinally tight to ensure high luminosity at the collision point and hence maximize the number of collisions.

There are four experiments as shown in Figure 2.3 which are taking data from the collisions between beams. The collisions will recreate in laboratory similar conditions of those of the very early universe right after the Big Bang in order to study the questions mentioned earlier.

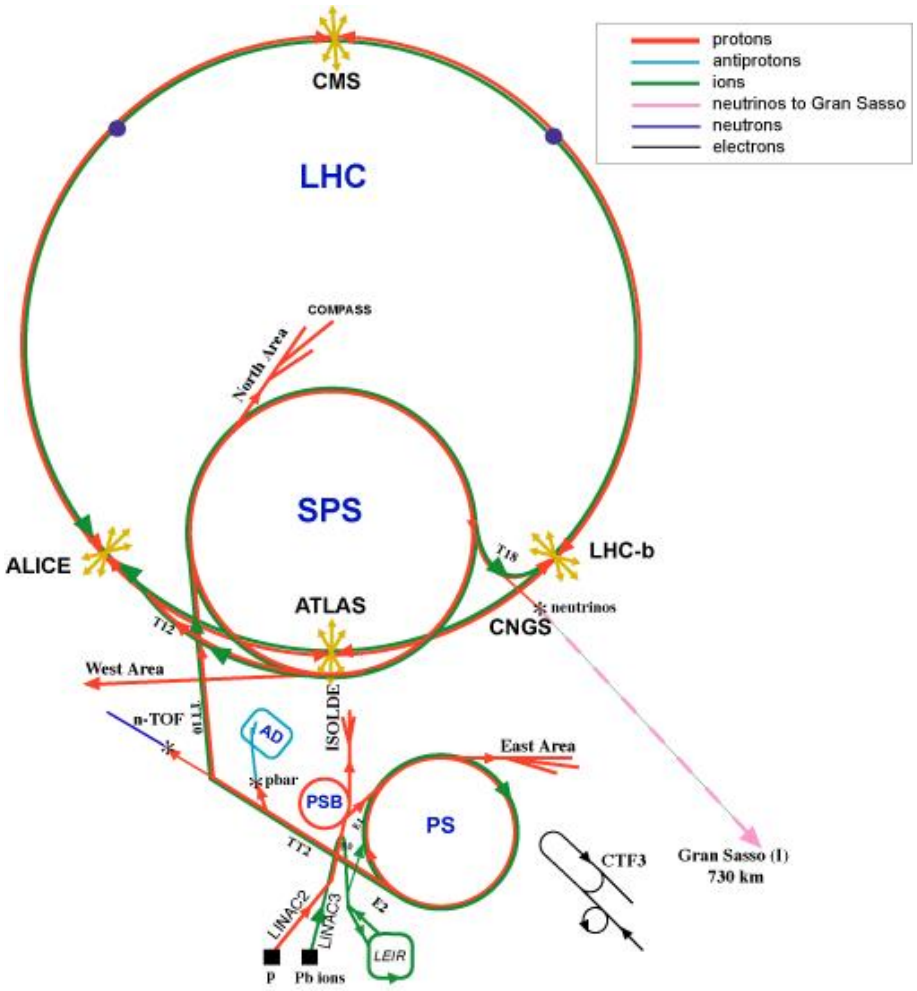

Figure 2.2: The whole accelerator complex.

- ALICE, A Large Ion Collider Experiment, is a general purpose heavy-ion detector designed to study the physics of strongly interacting matter and the quark-gluon plasma in nucleus-nucleus collisions;
- ATLAS, A Toroidal LHC ApparatuS, is a general purpose detector for recording proton-proton collisions, searching for Higgs bosons and spontaneous symmetry-breaking mechanisms, supersymmetric particles, new gauge bosons, leptoquarks, quarks and leptons compositeness indicating extensions to the Standard Model and new physics beyond it;
- CMS, Compact Muon Solenoid, is a general purpose detector for the highest precision identification and tracking of muon and dimuon, seaching for Higgs bosons and symmetry-breaking mechanisms, looking of evidence of physics beyond the standard model, such as suspersymmetry or extra-dimensions;

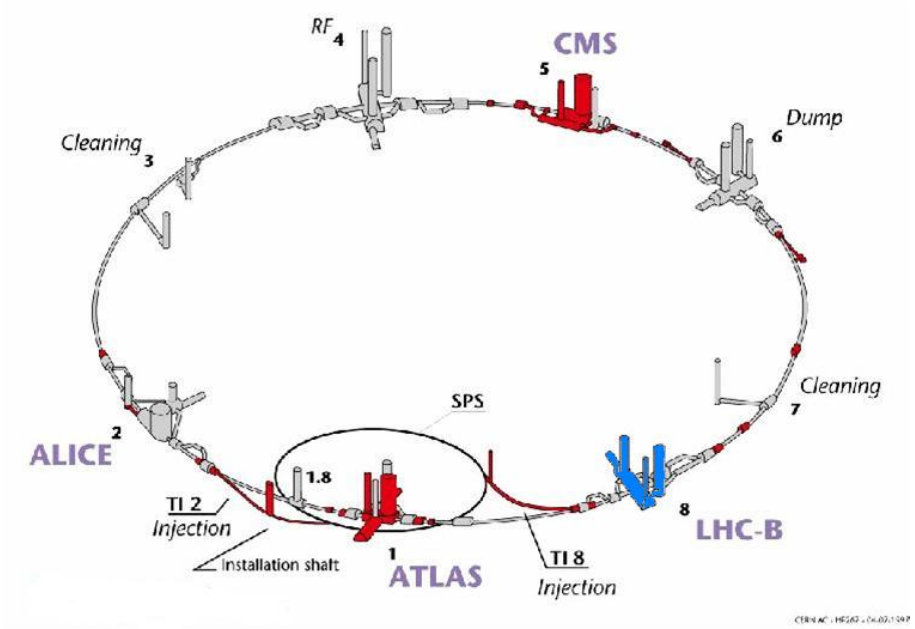

Figure 2.3: Location of the four LHC experiments.

- LHCb, A Large Hadron Collider *beauty* experiment, is a precision detector to study CP-violation and rare decays in its heavy quarks sectors.

2.2 Studying *beauty* and *antibeauty* at LHCb

The physics studied at the LHCb experiment is broader as compared to other precision experiments and B-factories and it attemps answering the most challenging questions at the forefront of knowledge in physics. The final aim of the experiment is to measure precisely decays of $b/\bar{b}$-mesons in order to understand the nature and flavour structure of possible New Physics beyond the current knowledge. New Physics is needed in order to go beyond the formulation of the Standard Model and to build a new theory regarding the unexplored spectra of energies just after the Big Bang.

The physics studies at LHCb can be described by means of the *CPT Theorem*. Each of C, P and T are symmetries. *C, charge conjugation*, represents replacing a particle by its oppositely charged counterpart. *P, parity*, corresponds to mirroring a particle to reverse all three coordinates. Finally, *T* is *time reversal*. Physicists once believed that transformations of anyone of these symmetries would not change the outcome; they said that the symmetries were conserved. In other words, a process in which all particles are exchanged with their anti-particles was assumed

to be equivalent to the mirror image of the original process. However, in the 50's experiments showed that both P and C are broken in the weak interaction. In the 60's, it turned out that the combination of C and P was not conserved. This CP-violation was first observed by James Cronin and Val Fitch in the decays of particles called neutral kaons at the US Brookhaven laboratory.

Symmetries are very important in particle physics because they give fundamental information about particle interactions. Referring to Figure 2.4, telling the difference between the sphere and its mirrored image is impossible, but if the sphere has a little imperfection, like a word written on it, then the difference is clear to see.

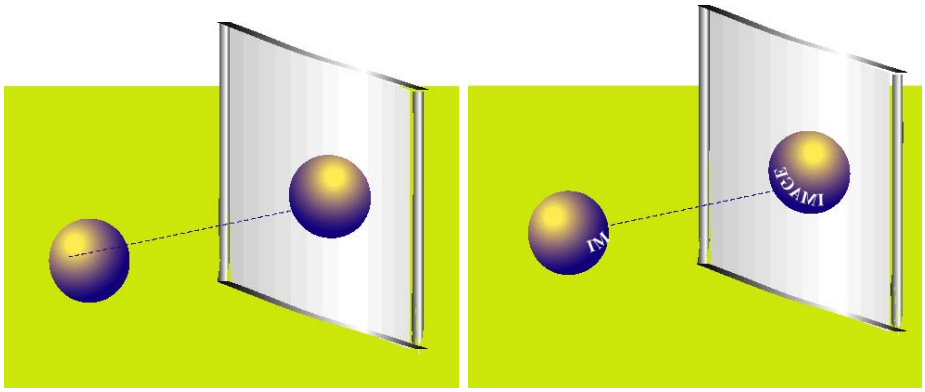

Figure 2.4: CP-Violation seen like a *broken mirror*.

Observing CP-violation is easy at LHCb due to the large productions of b-mesons, but measuring it so precisely that we see incompatibilities with the Standard Model is difficult. The Standard Model is in fact able to accomodate CP-violation as observed by experiments, but does not explain its origin. CP-violation occurs only in the weak interaction, when quarks turn into quarks with different electric charge. All of the possible transitions of this type can be represented by a matrix, known as the *Cabibbo-Kobayashi-Maskawa* (CKM) matrix. The CKM matrix is made up of three rows and columns containing nine *coupling costants*.

$$\text{CKM Matrix} = \begin{pmatrix} V_{ud} & V_{us} & V_{ub} \\ V_{cd} & V_{cs} & V_{cb} \\ V_{td} & V_{ts} & V_{tb} \end{pmatrix}$$

These constants are related to the weak charge of any possible quark transformation, where quarks u, c, t are paired with quarks d,s,b. The transformation of a quark into another quark is possible by changing the charge of the quark by a unit amount e and the strength of these transformations is the CKM matrix. The triumph of the Standard Model is that it predicts a set of relationships between the nine elements of the CKM matrix. These relationship include properties that result in CP-violation.

The CKM matrix has a property known as *unitarity* due to the physical properties it represents. Mathematically, this defines a set of equations that the matrix elements must satisfy:

$$V_{ud}V_{ub}^{*} + V_{cd}V_{cb}^{*} + V_{td}V_{tb}^{*} = 0. \tag{2.1}$$

Dividing by the middle term, it is possible to obtain:

$$\frac{V_{ud}V_{ub}^{*}}{V_{cd}V_{cb}^{*}} + 1 + \frac{V_{td}V_{tb}^{*}}{V_{cd}V_{cb}^{*}} = 0. \tag{2.2}$$

Mathematically, CP-violation is described by complex numbers in the CKM matrix. Each term in the above equation is complex and can be drawn as a vector in the plane. Arranging the three vectors head-to-tail gives the sum described in Figure 2.2. Since the sum is zero, the three vectors should form a closed polygon, that is, a triangle. This is known as the *unitarity triangle*. The three angles ϕ_1, ϕ_2, and ϕ_3 are also known as β, α, and γ, respectively. Figure 2.6 shows how the unitary triangle inserted in the broad picture of measurements of angles and variable of the CKM matrix.

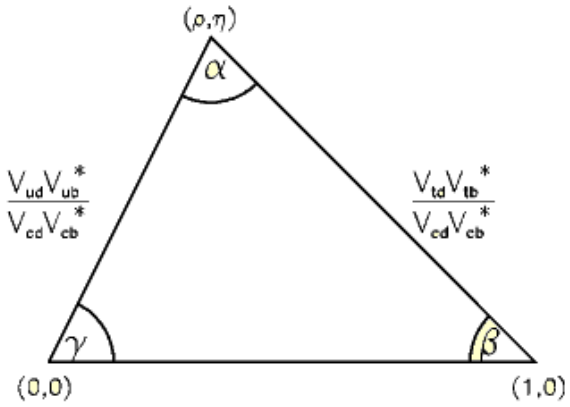

Figure 2.5: The Unitarity triangle.

LHCb has a very challenging task: measuring with the highest precision ever the value of the three angles (β, α, and γ) by profiting from the large production rates of b-mesons at the LHC. Actually, a b-meson consists of a b-antiquark ($\bar{b}$) and either a u- or d-quark; a $\bar{b}$-meson consists of a b-quark and either a u- or d-antiquark ($\bar{u}$ or $\bar{d}$). The b-meson is a relatively heavy particle, having a mass of $5.28\,\mathrm{GeV/c^2}$, which is more than five time the mass of the proton.

When producing b-mesons, the weak interaction allows the quarks inside the mesons to transform themselves. Physically it is said that the mesons decay obeing the basic laws of physics: energy must be conserved and electrical charge must be

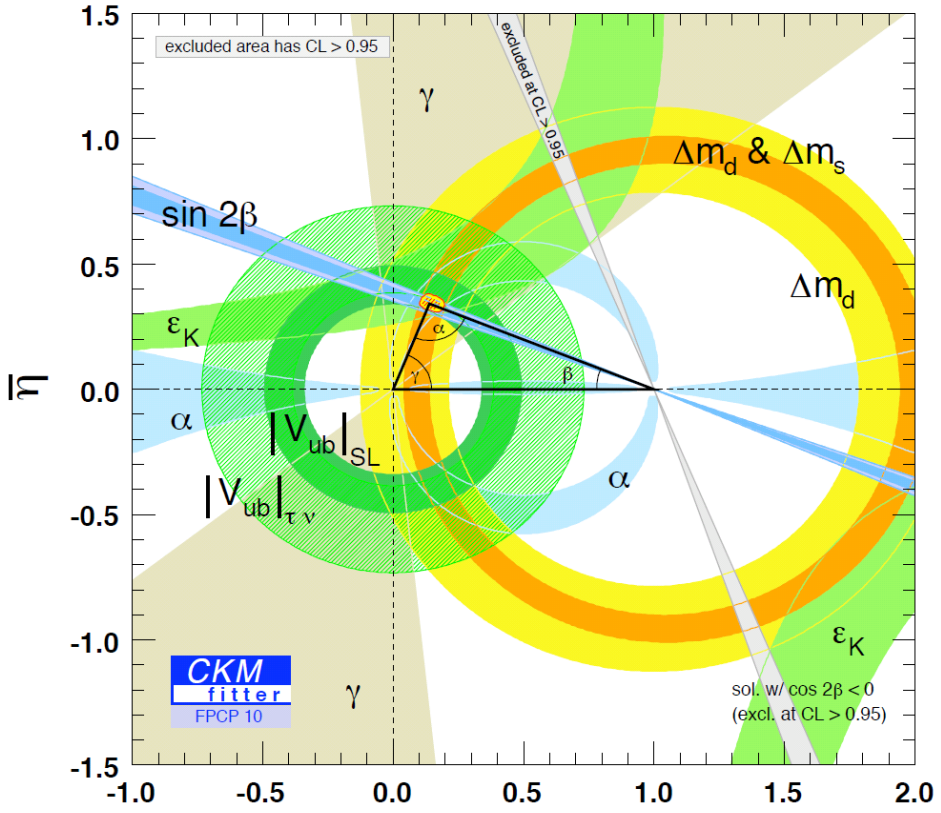

Figure 2.6: The Unitarity triangle in 2011.

conserved. The *b*-meson would be stable if the b-quark and companion antiquark did not have weak charge according to the formulation of the Standard Model. Consequently due to the fact that *b*-mesons are heavier than many other mesons, there are many ways in which they may decay. All of these ways involve the b-quark transforming itself into another quark, which could be a u-, or c-quark. If a t-quark is generated in loops or boxes, the t must then be transformed again. This is because the t-quark it is more massive than the B meson.

In any case, many of these transformations can be detected experimentally. For *b*-mesons is mostly related to the third column of the matrix. CP-violation is evident whenever differences in the decays occurs. Few experiments in the world are currently able to measure CP-violation in B decays:

- BaBar experiment. At PEP-II (electron-positron collider) located at the Stanford Linear Acceleration Center (SLAC) in California, USA.
- BELLE experiment. At KEKB (electron-positron collider) located at the High Energy Accelerator Reasearch Center (KEK) in Tsukuba, Japan.

- D0 and CDF experiments. At Tevatron (proton-antiproton collider) located at the Fermi National Accelerator Laboratory (FNAL) in Illinois, USA.

LHCb will be the only experiment among all the B-factories, to be able to study B meson production at a luminosity of $2 \times 10^{32}\,\mathrm{cm}^{-2}\,\mathrm{s}^{-1}$ and an energy of 7 TeV in the centre of mass.

The LHCb physics programme includes some key measurements which are here only briefly summarized. For more complete descriptions of these measurements, the reader is referred to the published LHCb roadmap paper [3].

For accurate amplitude predictions from the Standard Model, the LHCb experiment is aiming at measuring the parameters of the CKM mass mixing matrix precisely. Semileptonic charm decays can help measurement the V_{ub} and V_{cb} term of the CKM matrix. CP violation measurements can be done with non-leptonic decays as $B \to DK$.

CP violation in the B_s system is still to be explored. CDF and DO at the Tevatron accelerator have put first contraints on the mixing-induced CP-violating phase the flavour-tagged $B_s^0 \to J/\psi\phi$ decays. Since the Standard Model effect is only $O(10^{-2})$ and the current measurement errors are still $O(10^{-1})$, a large contribution from New Physics is not yet excluded.

One of the rare decay modes where there could be still a sizable effect from New Physics is $B_s^0 \to \mu^+\mu^-$. The current limit of the brancing fraction set by the Tevatron experiments is more than an order of magnitude above the Standard Model prediction of $O(10^{-9})$.

2.3 The LHCb experiment

The LHCb experiment is located at the interaction point number 8 along the LHC ring, 103 m undergound [4]. LHCb is a single-arm spectrometer with a forward angular coverage from approximately 10 mrad to 300 mrad. The choice of the detector geometry [5] is motivated by the fact that at high energies both the $b/\bar{b}$-mesons are predominantly produced in the same forward cone. This is also the reason by which the LHCb experiment will not record physics data at a higher luminosity than $2 \times 10^{32}\,\mathrm{cm}^{-2}\,\mathrm{s}^{-1}$, therefore allowing for a small number of interactions per bunch-bunch collisions. At the LHC, the ultimate scenario will provide a maximum of about 30 MHz of bunch-bunch collisions. It is therefore necessary to select events based on their interest for the LHCb physics programme. In LHCb, it was chosen to have a total bandwidth of 1 MHz and store events at a maximum rate of 2 kHz, by means of an electronics Level-0 Trigger which selects events very fast based on few figures of merits and of a software High-Level Trigger running on thousands of CPU cores. The software trigger performs a first analysis of each event and selects only 2 kHz of the interesting ones out of the 1 MHz of events

already selected by the hardware trigger. In order to allow for more flexibility and full control of the readout system, a centralized timing, trigger and readout control system was envisaged. In this Chapter, a brief overview of the LHCb detector and the readout system is given, followed by a description of the timing, trigger and readout control system.

2.3.1 The LHCb detector

The layout of the detector is shown in Figure 2.7. The interaction point is displaced by 11.25 m from the center of the cavern, so that LHCb can fit in the existing cavern from the DELPHI experiment at LEP. LHCb comprises different sub-systems which are based on different technologies and detector principles.

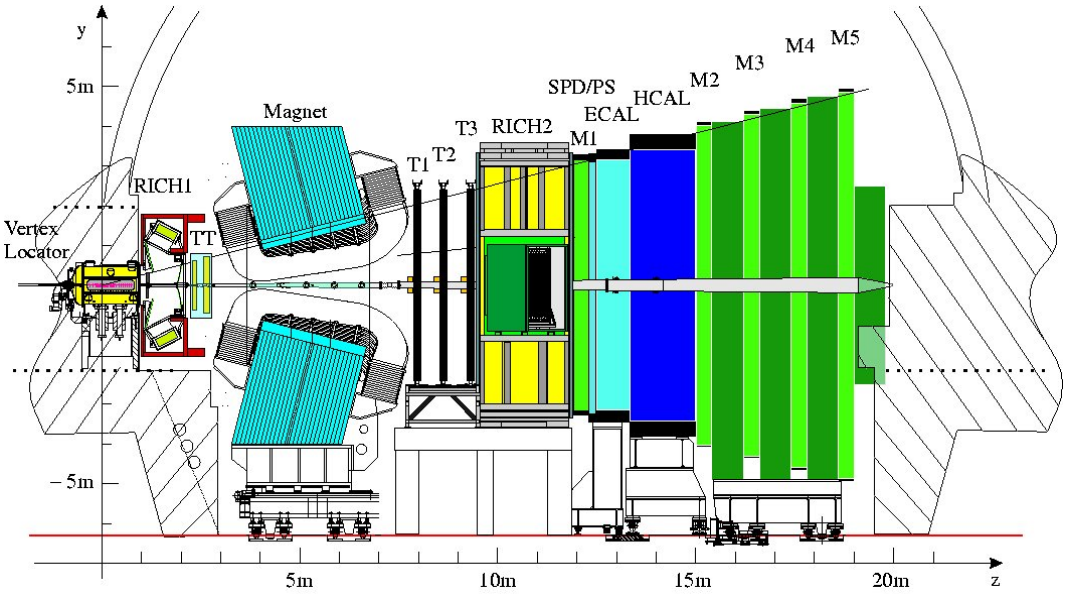

Figure 2.7: The layout of LHCb detector.

The sub-systems are:

- the *Vertex Locator, VELO,* provides precise information on the production and decay vertices of b-mesons. The VELO detector contains a *Pile-Up System* which is used for the Level-0 Trigger and provides a measurement of the number of vertices in each proton-proton interaction;

- the two *Ring Image Cherenkov Counters, RICH1 and RICH2,* have the task of identifying charged particles over a momentum range of 2-150 GeV/c so that it is possible to reduce background in selected final state. They use the Cherenkov effect to detect particles;

- the *Spectrometer Dipole Magnet* curves the particles from the collision in the horizontal plane in order to measure their momentum;
- the *Silicon and the Outer Tracker, ST and OT,* provide efficient track reconstruction and contribute to the momentum measurement of charged tracks and track direction;
- the *Electromagnetic Calorimeter, Hadron Calorimeter and Preshower, ECAL, HCAL, PS/SPD,* provide identification of electrons and hadrons both for for the Level-0 Trigger and offline analysis, with measurements of position and energy. They provide a measurement of the energy of neautral particles;
- the *MUON Detector* provides muon identification and information for the Level-0 Trigger;
- the *Level-0 Trigger* selects events based on the information provided by the MUON and Calorimeter detectors. A signal taken synchronously from the HCAL and ECAL, from the MUON and from the Pile-Up sub-detectors is transmitted to a L0 Decision Unit (L0DU) which is the core of the first-level trigger in LHCb (Level-0 Trigger) [12]. The aim of the Level-0 Trigger is to select leptons, hadrons, and muons with high transverse energy/momentum and the L0DU implemets an intermediate decision to build the master trigger which is submitted to the readout control system.

2.3.2 The LHCb readout system

All subdetectors are connected to the readout system [6] shown in Figure 2.8. The main components of the data readout system are:

- the *Front-End electronics and the Readout Boards*, which record signals from the collision events and generate packets of data which are then sent through the readout network. These events are then processed in the Event Filter Farm by software algorithms;
- the *Level-0 Trigger*, which selects events based on information from the calorimeter system and the muon system;
- the *Timing and Fast Control (TFC) system*, which distributes the clock, the decisions of the Level-0 Trigger and many other synchronous and asynchronous control commands to the front-end electronics. The TFC controls and manages the data-flow of the whole readout system up to the Event Filter Farm;
- a *readout network* which collects data from the Readout Boards (ROBs) and transfers them to a *processing farm* for the execution of the software-based *High Level Trigger (HLT)* algorithms. The whole network is composed

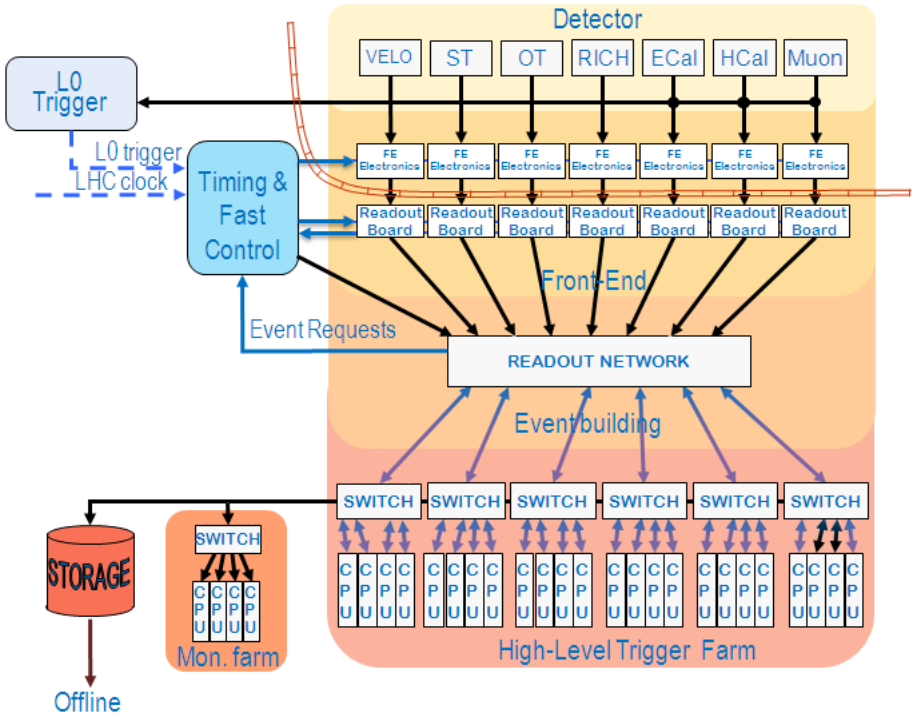

Figure 2.8: Overview of the LHCb readout system.

of a first stage where the bandwidth from the Front-End electronics into the event building network are reduced by aggregating data in packets of successive events. Then, a readout switch routes event fragments from its inputs to a single destination. Finally, a processing farm is composed by all the processing units, called *CPU sub-farms*, available to run the HLT. Data is stored temporarily in a storage system before being transferred to the main disk area at CERN.

The Front-End electronics (FEE) of every sub-detector follows precise requirements to correctly capture and store detector signals from almost a million electronics channels. Moreover the detector signals must be captured with accurate timing, to determine the exact bunch of protons which is crossing the LHCb interaction point and let the detector operate in the optimal conditions [8].

As described in Figure 2.9, the analogue Front-End electronics amplifies the weak signals coming from the corresponding sub-detector with minimum noise and minimum baseline. The analogue signal is then converted through ADC converters into digital data. It is stored in a 160 cells deep *L0 buffer pipeline* at 40 MHz waiting for the Level-0 Trigger decision. Thereafter, the final L0 decision is sent from the TFC system to the output stage of the L0 buffer pipeline with a latency of 160 clock cycles and data is either rejected or written according to the decision made at the

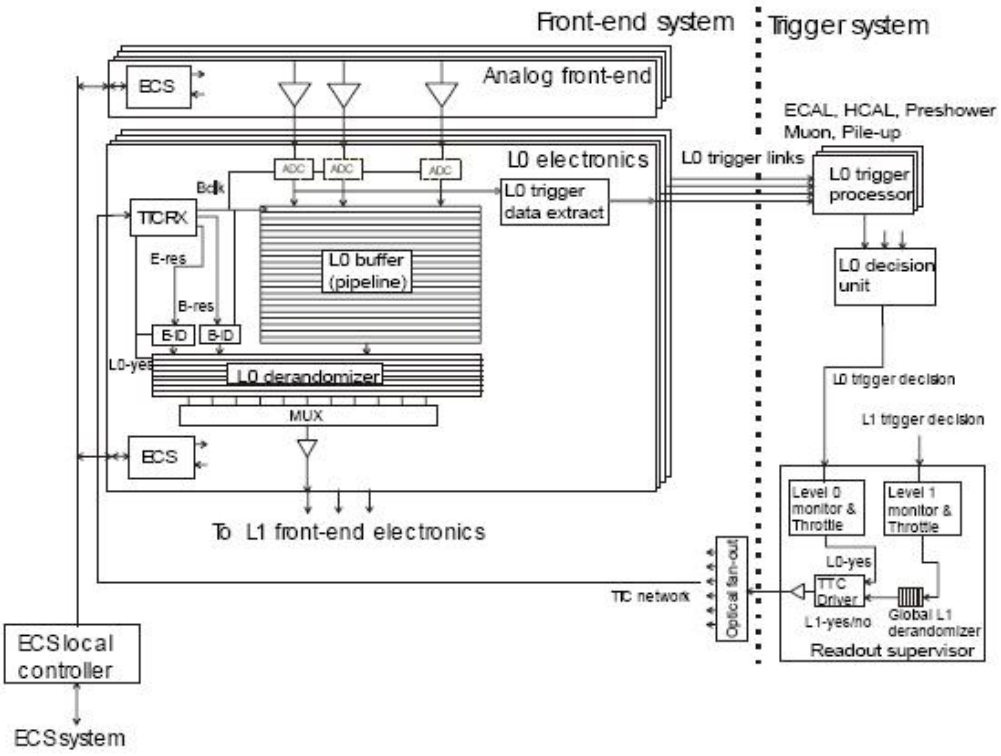

Figure 2.9: The L0 Front-End Electronics architecture.

Level-0. If the decision is positive, data is written to a *L0 derandomizer*. Finally, the data is sent to the Readout Boards (*TELL1 / UKL1*) which perform a hardware processing of the data. Data is transferred at a maximum average frequency of 1 MHz and then finally transferred through the readout network to the processing farm. The TFC system ensures that the maximum average frequency of event tranmission never exceeds the available bandwidth. A second level of trigger, *High Level Trigger, HLT* [10] selects events and reduces the output rate of the readout chain from 1 MHz to about 2 kHz. It is based on C++ applications which run on thousands of computing nodes.

The whole readout system uses a very simple dataflow protocol on the readout network: the so-called *push protocol with pull mechanism*. Data is transferred to the next stage when new data is available. There is no synchronisation or communication between components of neither of the same level nor between components of different levels. Any processing node just declares his availability in receiving events to the TFC system, which then sends trigger commands and destination broadcasts to the Front-End electronics. Event fragments from several successive events are packed into a so-called Multi-Event Packet (MEP) and when the packet is completed, it is pushed through the readout network to reach the HLT farm.

The MEP distribution scheme allows reducing the transfer rate stage after stage from 40 MHz to 2 kHz globally by reducing the overload of a network packet.

A central scheme for the control [16] of the MEP distribution was implemented. This assignes the same IP destination to a MEP containing a certain number of events belonging to the same type of trigger (i.e. calibration, physics, timing). The destinations are broadcasted to the TELL1/UKL1 Readout Boards over the CERN TTC system. The scheme has the advantage that it imposes a certain level of concurrency in the Front-End electronics and that it allows rapid update of the MEP destination table in case of local breakdowns in the processing farm. Basically the scheme is structured as follow: farm nodes declare themselves as available to receive MEPs when the local event queue contains less than a certain number of events by sending *MEP Requests* to the TFC system. The TFC system thus assigns the destinations of the MEPs dynamically according to the availability of the farm nodes.

The key characteristics of the readout system are as follow [11]:

- the connectivity between sources and destinations is provided by a large switching network.
- rate reduction is achieved by packing several events into one Ethernet frame, so-called Multi Event Package (MEP).
- flow control is implemented centrally by disabling/enabling the trigger via TFC system.
- HLT runs over farm processing units.
- every processing units receives an event to be processed only when they declare themselves available to do so.

Hence, the TFC system is the heartbeat of the entire readout chain, since it manages the clock, the timing alignment as well as the synchronous and asynchronous control information to the front-end electronics. Moreover, the TFC architecture allows to support a fully partitionable system, that is the possibility of running autonomously one or any ensemble of sub-systems in a special running mode independently of all the others. Partitioning is vital in the LHCb experiment since it allows to run tests, perform time alignment, and upgrade each sub-detector autonomously.

The TFC system will be described in detail in the next sections since it plays a central role in the work presented in the thesis.

2.3.3 The Timing and Fast Control system

The Timing and Fast Control System is responsible for controlling and distributing timing, trigger, synchronous, and asynchronous commands to the LHCb Front-End

electronics [13]. Figure 2.10 shows the complete TFC architecture.

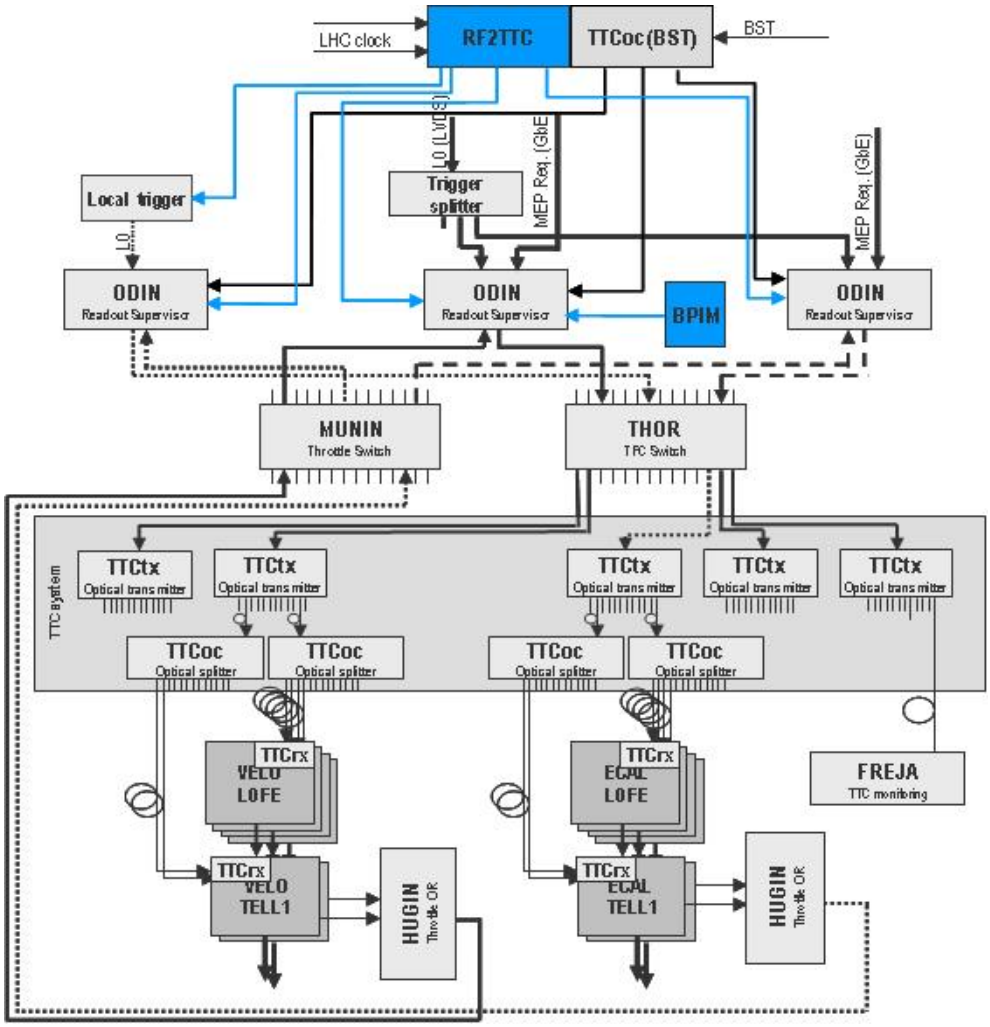

Figure 2.10: Overview of the TFC system.

The TFC mastership has been centralized in the Readout Supervisor, called *ODIN* [15]. In order to support a fully partitionable system, the architecture contains a pool of Readout Supervisors, one of which is used for data acquisition during physics run and which receives the Level-0 Trigger decision. For separate local runs of sub-systems a programmable TFC Switch, called *THOR*, is used. It allows associating sub-systems to the other Readout Supervisors and allows distributing in parallel the information to the Front-End Electronics of each sub-systems. The information trasmitted by the Readout Supervisor are:

- the LHC reference clock at 40 MHz, that is the Master clock of all the electronics;

- the Level-0 trigger decisions;
- commands to control processing in Readout Boards;
- commands like resetting counters in the FEE and resetting the FEE in order to prepare it for data taking;
- calibration commands;
- IP addresses for MEP destination.

If the physics trigger rate gets abnormally high or data congestion occurs in the event building network, there is a potential risk of overflow in the buffers of the Front-End electronics. In order to prevent this, the Readout Supervisor controls the trigger rates according to the status of the buffer. Whereas the status of the fast buffers can only be known by emulating them centrally in ODIN, slower buffers are monitored locally. The Throttle Switch feeds back the buffer overflow warning signals from the slower buffers in the readout to the appropriate Readout Supervisor according to the current partition configuration. The Throttle ORs work as concentrators of buffer overflow warning signals from the subsets of Readout Boards and make a logical OR of the signal within the same sub-system.

In Figure 2.10, the BPIM and the RF2TTC modules are highlighted in blue. These modules are responsible for the timing of the whole TFC system and therefore the LHCb experiment. The Beam Phase and Intensity Monitor is a crucial system to measure and monitor bunch-by-bunch the phase and the intensity of the beams with respect to the main clock edge. The RF2TTC receives and adjusts the clock from the LHC distribution system and send it to the TFC system. Thus, the time alignment of the entire LHCb may be perfomed centrally. These modules and systems are described extensively in the next chapters.

The modules of the backbone of the TFC distribution system are all standard components of the CERN TTC system [14].

Summarizing, the TFC is responsible for a list of main tasks:

- *Readout control*: control of the entire readout system is done by one of the ODINs in the pool. The control of the readout implies controlling the trigger rate, balancing the load of events at the Event Filer Farm, balancing the load of buffers in the electronics. The TFC system can auto-generate internal triggers for calibration purposes.
- *Event description*: an event bank description is appended to each event with vital information on the type of trigger of the event, the bunch identifier of the event, the destination of the event and the timestamp of the event.
- *Partitioning*: implemented via the TFC Switch with the aim of easing parallel activities.

- *Slow Control*: done by the Throttle Switch together with the Throttle OR in order to give back-pressure to maintain the readout speed below the throughput limit of the Data AcQuisition system (DAQ).
- *Coarse and fine time alignment*: through the RF2TTC and BPIM systems, it is possible to time align the whole LHCb experiment in a way that each sub-detector can produce a precise signal at the optimal point and that this signal is stable.
- *Luminosity*: a combination of physics event types is selected by the TFC system in order to allow absolute luminosity measurements.
- *Run statistics*: information about the trigger rates, run deadtime, number of events accepted, types of events accepted, bunch currents, luminosity and load of buffers are stored in a Database to allow retrieving run statistics and information per run or per LHC fill.

A detailed description of the various components of the TFC system is given in Appendix A.

Summary

This Chapter introduced the work presented in the next chapters within the LHCb experiment and CERN. The LHC and the LHCb experiment were described, outlining the various instruments composing the LHCb detector. Briefly, the physics goals of the LHCb experiment were touched. The LHCb readout system and the Timing and Fast Control system were described in detail. The concept of having a centrally managed and intelligent LHCb timing, trigger and readout control system was highlighted as it is a strong characteristics of the work described in the thesis. It allows for a high level of integration and interconnection with the other systems which are described later.

Chapter 3

LHCb experimental aspects at the LHC and motivations for the work presented in the thesis

In this Chapter, some of the most important experimental aspects related to the LHCb experiment will be reviewed. It was already mentioned that the LHCb experiment has some particularities with respect to the general purpose Detectors ATLAS and CMS. The structure of the LHCb interaction region, which is near the injection line of beam 2, plays an important role in the operation of the experiment. The most important LHC elements, which have an impact on the LHCb experiment are described in this Chapter. Sources of background and types of machine background are described. A section in this Chapter is reserved to the various phases of an LHC physics fill, from the point of view of the LHCb experiment. The LHCb global timing reception and distribution system is reviewed as this is of fundamental importance for the efficiency of the detector.

All of these aspects taken together contribute to the complexity of the LHCb experimental conditions. Their impact on the operation of the LHCb detector are the main driving force for developing a complete system for beam, background and luminosity monitoring and optimization of global operation of the experiment. The motivations for such a system are given in this Chapter.

3.1 LHCb interaction region and sources of background

The LHCb detector is a forward single-arm spectrometer, located near the injection line of beam 2 and equipped with very sensitive and precise sub-detectors. One of these, the VELO, is a movable device which is located around the interaction point and therefore highly exposed to dangerous beam conditions. These particularities expose the LHCb detector to possible extremely harsh background conditions.

Eventually they have an impact on detector operation with direct consequences on trigger efficiencies, data quality and accumulated radiation dose.

Figure 3.1 shows the location of the LHC magnets around the interaction region of LHCb (IP8). The fact that LHCb is located behind an injection line is the reason for which the LHCb Long Straight Section is different with respect to the one of ATLAS and CMS.

The LHCb Long Straight Section is about 600 m long. It is surrounded by dispersion suppression regions and arcs where the beams are bent in their circular paths around the machine. Left of LHCb - about 3 km away in IP7 - there is the LHC betatron cleaning region where the beam is cleaned in the vertical and horizontal phase space. LHCb is built in the direction of the clockwise beam (beam 1) and therefore mostly sensitive to background induced by beam 1 directly due to the fact that LHCb is time-aligned along beam 1 or by inefficiencies in betatron cleaning which happens just before the LHCb site. Particles originating from proton beam interactions with the gas in the vacuum chamber or with the aperture material of the accelerator on either side of the interaction point constitute the *Machine Induced Background*, or MIB. These particles usually reach the experimental areas from the machine tunnel. The rate of this type of background is generally proportional to the machine beam current and depends on a given operating condition. Sources of MIB can then be listed as follow:

- Inelastic and elastic interactions of the beam with residual gas nuclei in the Long Straight Section close to LHCb. This source is local to LHCb and gives a *direct* background to the experiment. For simplicity this type of background is called *beam-gas*.
- Elastic and diffractive beam-gas interactions in the whole LHC.
- Betatron cleaning inefficiency at IR7 which results in beam halo protons out-scattered and not absorbed in the collimation system in this region.
- Momentum cleaning inefficiency at IR3, where an off-momentum beam halo is produced.
- Collisions in the ATLAS experiment (IP1), where a fraction of elastic and diffractive interactions may reach LHCb.

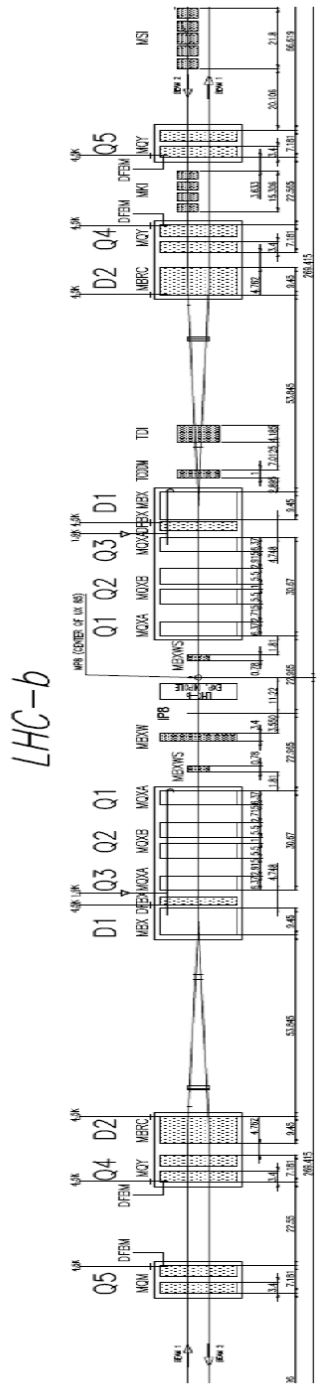

Figure 3.1: Drawing of the LHCb Long Straight Section (LSS).

About 70-120 m away from the interaction point a series of collimators are installed to protect mainly the superconducting elements in the machine to avoid quenching. The role of these collimators is to remove *beam halo*. The beam halo is mostly composed by particles in the beam slowly drifting outwards to higher transversal amplitudes. This halo is removed with a three level collimation system [19] and the tertiary collimators (TCTs) are the third layer. Showers originating from any of the sources listed above (apart the first one) and hitting the TCTs around LHCb will give an *indirect* background to the experiment. For simplicity this type of background is called *tertiary halo* or *quartiary halo* if it comes from the very last level of collimators. A complete simulation framework [20] regarding Machine Induced Background in the LHCb experiment has been developed and gives estimation of rates and fluxes for each of the background sources listed above. Figure 3.2 shows how these MIB sources contribute to background in LHCb and how the collimator hierarchy is developed in the LHCb LSS.

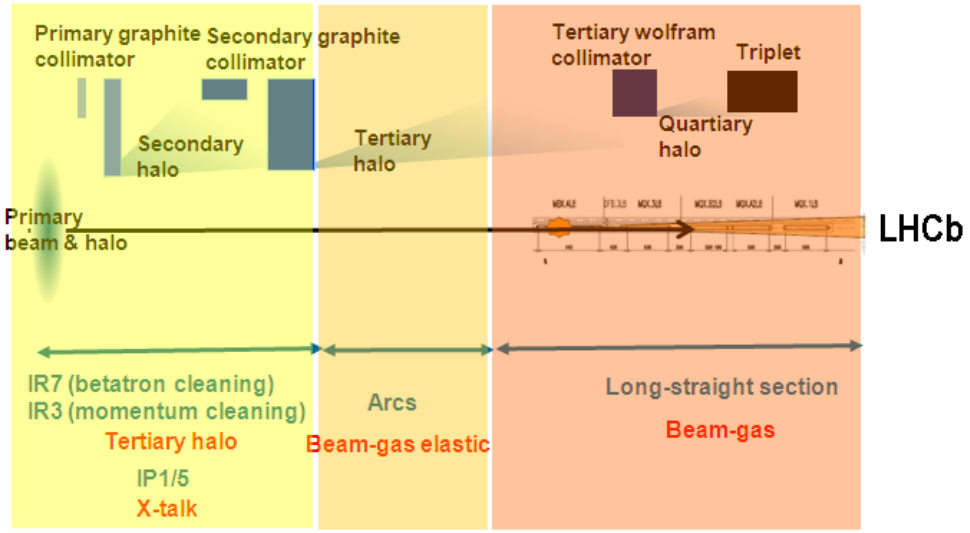

Figure 3.2: Graphical representation of MIB sources around the LHCb interaction region. The primary halo of the beam is cleaned in IR7 and IR3 where betatron and momentum cleaning are performed. Losses from the primary cleaning are then absorbed by secondary collimators and then tertiary collimators generating tertiary halo based mostly on elastic and diffractive effects. The cleaned beam interacts with the gas in the long straight section of the experiment generating direct background or beam gas.

Other LHC elements are installed near the LHCb experimental region in order to allow injecting beam 2 in the machine. These elements can be seen in Figure 3.1 and are called TDI and MKI. The TDI is a 4 m long hexagonal Boron Nitride absorber coated with Titanium. Its purpose is to protect the LHC magnet dipoles and the LHCb experiment from possible accidents or hardware failures during the injection procedure. The TDI is a movable device and its two jaws are set accordingly to

the operation procedures. The MKI is a beam kicker and its purpose is to deflect the beam from the injection line to the beam line in the vertical plane.

Other important LHC elements are compensator magnets (MBXW and MBXWS) whose aim is to correct the trajectory of the beams around the LHCb spectrometer, whose field is highly asymmetric. They produce local orbit bumps which allow for collisions at the LHCb interaction point. The LHCb spectrometer dipole in fact is located about 5 m to the right of IP8 and is designed to give a deflection of 181 μ rad at the top energy of 7 TeV. The field is located in the vertical plane, and hence the magnet gives a horizontal deflection. The LHCb spectrometer is about 1.9 m long and the integrated field is about 4.2 T. The spectrometer field polarity can be swapped in order to study asymmetries in physics signals and to reduce systematic errors in physics analyses. The strong effect of the magnet is compensated by three compensators which, when acting with the experimental dipole magnet, give a closed asymmetrical bump across the IP. The bump gives a residual IP crossing angle of 135 μ rad. An additional crossing angle is imposed on LHCb in the horizontal plane to reduce parasitic bunch collisions, and a vertical plane parallel separation bump for injection is imposed. Figure 3.3 shows the horizontal and vertical bumps around the LHCb interaction region.

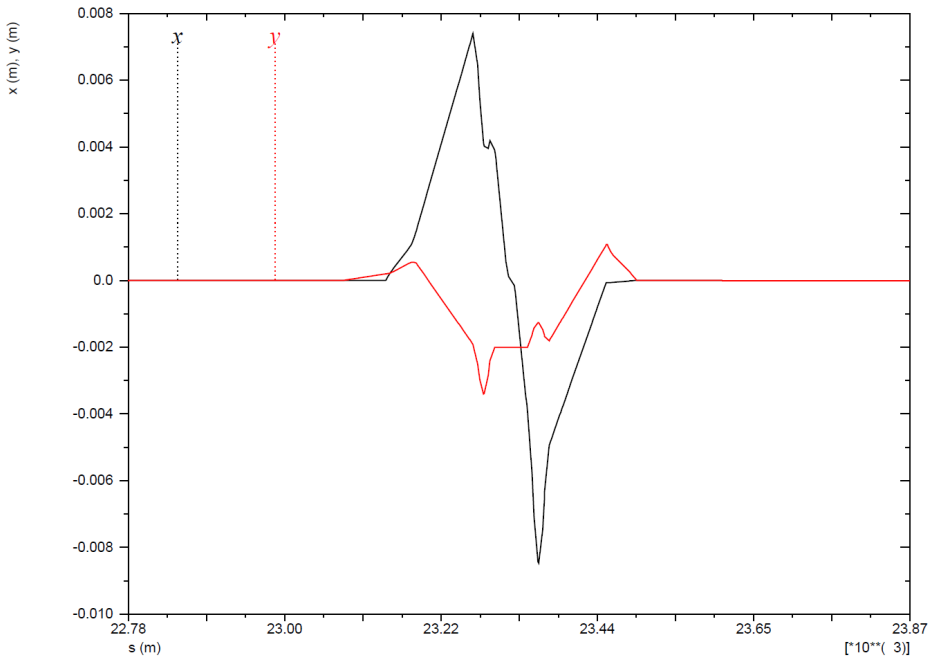

Figure 3.3: Horizontal and vertical bumps across LHCb. The crossing angle in LHCb is in the horizontal plane.

In the case of a failure of any of these machine elements, the risk of damage in LHCb is very high. A high level of protection and the presence of a large number

of interlocks to the machine is necessary to try minimize the risk. However, even though failures do not occur, possible wrong settings of these elements can result in high background, beam degradation, high rates of beam gas, high radiation doses and bad data quality. A close monitoring and analysis of the beam characteristics and experimental conditions is therefore essential to improve machine performance and experimental operating conditions. A tight collaboration with the LHC machine experts allowed calibrating every element in the machine thoroughly in order to find the optimal settings.

3.2 LHC physics fill at LHCb

In this section a brief description of the various steps of an LHC physics fill is given as seen from the LHCb experiment point of view. The various modes of operation within a physics fill are described graphically in Figure 3.4 where magnet currents and total beams intensity are represented as a function of time. These modes are the driving forces for the operation of the LHCb experiment, which are brought forward by two shifters in the LHCb control room. A shifter is a person which controls, monitors and operates the LHCb experiment during the days of operations and physics data taking.

Whenever the beams are dumped a new physics fill starts. A new Fill Number is transmitted to the LHC experiments, defining the beginning of a new LHC fill. It actually starts with a *PRECYCLE*, where all the magnets in the accelerator are ramped down to reach the current for the energy at 450 GeV. This energy is the injection energy, matching the energy of the SPS. During this short period, there is no beam in the machine and the LHCb experiment sets up the configuration of all the electronics and the voltages in the injection mode.

After the *PRECYCLE*, the injection phase starts. According to a well defined set of safety measures, the injection procedure is initiated by an *handshake* between the LHC machine and the four experiments. The machine-experiments handshake is transmitted via software and its main purpose is to inform about a possible injection. As a consequence, each experiment put the detectors and the eletronics in a safe state. When the injection is allowed by the experiments, the handshake is terminated and beams can be injected in the machine. One single low intensity bunch is injected in the *INJPROBE* mode, if high intensity bunches with more than 10^{11} protons-per-bunch are foreseen to be injected in the machine. This bunch is called *pilot bunch* and it is injected in the first available bucket of each beam. The high intensity bunches are usually injected in trains and often several trains are injected. A train of bunches is defined as a set of bunches which are separated in time and space by a fixed amount.

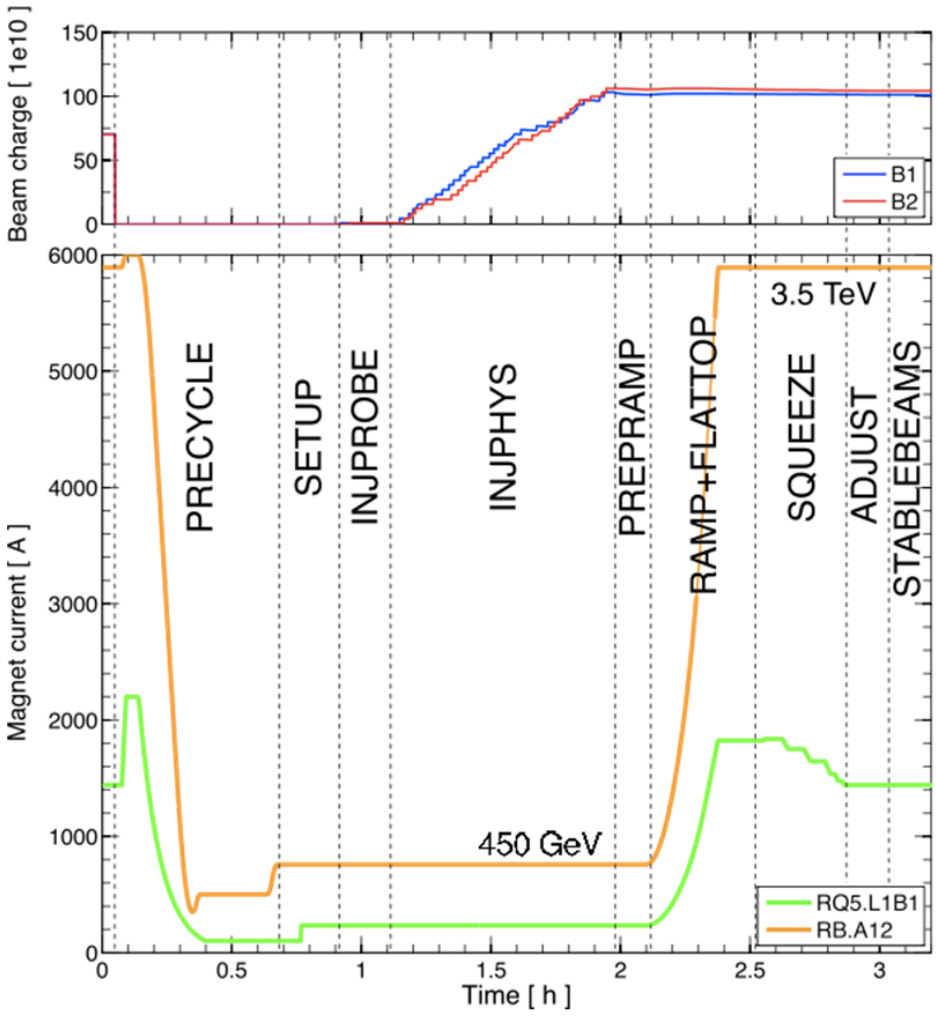

Figure 3.4: Schematic drawing of the LHC filling cycle. At the bottom, the various Beam Modes are highlighted in a plot of magnet currents (green and yellow) as a function of time. At the top, the total intensity of each beams is shown as a function of time, blue is the clockwise beam (beam 1) and red is the anticlockwise beam (beam 2). *Courtesy of S. Redaelli, BE department.*

The *LHC filling scheme* defines precisely where the bunches should be, their spacing, the number of bunches per train and the total number of bunches. The transfer of high intensity bunches happens in the *INJPHYS* mode. During this mode, trains of bunches are transferred from the SPS to the LHC accelerator via injection lines. This is made possible by the presence of particular magnets and deflectors in the injection line which are able to bend the particles to direct them into the LHC beam pipe. In Figure 3.4, the injection process can be seen in the top plot where the intensity of each beam increases each time an injection of a train of bunches happened.

The LHC machine enters the *RAMP* mode, after the injection is successfully terminated. The magnets are ramped up at a speed of 10 A/s to the nominal current for high energy beams. During 2010, the maximum energy achieved by the LHC was 3.5 TeV per beams, giving a centre-of-mass energy of 7 TeV. During this mode, the frequency of the beams changes slightly due to the accelerated beams and this can create abnormal beam behaviour and possible beam losses. In this phase, the LHCb experiment has still most of the high-voltges off in order to protect the detectors and the electronics from possible beam accidents.

The *FLAT TOP* mode is reached when the target current is reached, the beams are at their target energy of 3.5 TeV. In this mode, certain LHC collimators are set for high energy beams and the procedure for squeezing the beams starts (*SQUEEZE*). In this phase, the beams are squeezed at the interaction points following a β^* function which basically shrinks the beams transversally. Hence, beams are more focused and a higher luminosity can be reached. During 2010, $\beta^* = 3.5\,\mathrm{m}$.

When the beams are squeezed, they are put into collisions in the *ADJUST* phase. Local bumps at the interaction points are collapsed and the LHCb experiment ramps up all the high voltages to their settings for physics data taking. Crossing angles are applied at the interaction points. The direction along which each beam travels through LHCb is *tilted* in order to avoid having parasitic collisions. The crossing angle is applied in the horizontal plane at the LHCb interaction point. The concept of crossing angle and β^* function will be described in detail in Chapter 7.

Via the use of *optimization scans* in the vertical and horizontal plane, the best settings for the beams to collide at the maximum luminosity is found for each of the experiment. As soon as the procedure is finished, the *STABLE BEAMS* mode is declared. This is the mode where the experiment records physics data. The LHCb experiment can therefore move the Vertex Locator towards the centre of the beam and record physics events with all the subdetector involved. During the *STABLE BEAMS* period, another handshake can be performed with the machine to move back to the *ADJUST* mode. This is done in case some optimization tests has to be done or if some settings have to be applied. In this case, the VELO retracts its halves for safety reasons.

The LHC fill is kept stable and the experiments take data until the beams

are dumped. This can be a programmed dump, after another handshake between the machine and the experiments. It can be an unprogrammed dump due to bad beam characteristics producing fast or slow losses around the LHC ring. In the Beam Loss Monitors (BLM), only those above a well defined set of thresholds can trigger a beam dump. Another case of beam dump is the *asynchronous beam dump*. This can happen for different causes, for example when the RF system switches off because of a powercut or a rapid frequency changed occurred. No single spontaneous asynchronous beam dump was observed during 2010 operation.

3.3 LHCb global timing reception and distribution

In the LHC accelerator, particles are accelerated in Radio-Frequency cavities where a time-varying electrical field is applied. This variation is synchronous to a 400.79 MHz radio frequency clock (RF) which defines 35640 buckets along the LHC accelerator. A bucket is defined as a time interval where a bunch of particles. Each bucket has a length of 2.5 ns. The injection of bunches of protons (or ions) is described by the filling scheme of the LHC. The minimum time interval between two consecutive bunches is defined as 24.95 ns allowing 3564 defined locations, while the maximum number of bunches of protons (or ions) allowed in the machine is 2808 per beam due to the gaps associated with the rise time of the PS/SPS/LHC injection kickers and the LHC dump kicker.

A division (1:10) of the RF frequency is defined as the *Bunch Clock*, while a pulse at every RF bucket 1 is defined as the *Orbit Clock* or Revolution frequency [14]. The clocks are re-phased to the beams in order to provide two separate and independent Bunch Clocks (*BC1* and *BC2*) as well as two separate and independent Orbit Pulses (*ORB1* and *ORB2*). The beams are coarsely *cogged* together already at injection to force the appropriate collision schemes at the experiment interaction points, and a fine adjustment is applied during the ramp for the interaction region to be at the optimal position for the experiments.

The LHC clocks physically reach the location of the LHCb experiment via 14.1 km of fibres buried up to 1m underground. A Timing Receiver Crate, developed by the PH-ESS group with the participation of the experiments [14], receives the clock, converts it, cleans it with narrow band quartz-based PLL circuits and fans it out to the whole LHCb Timing and Fast Control system. The Timing Receiver Crate is a standard 6U VME64x compatible crate. As shown in Figure 3.5, it contains two RFRx modules which convert the optical signals of the three Bunch and the two Orbit clocks coming from the SR4/CCC into electrical signals. A RF2TTC module converts the clocks into ECL signals and allows performing various adjustments on each signal before making them available to the experiment timing system. The RF2TTC can produce an internal set of clocks to drive the electronics of the experiment independently of the state of the RF system at Point 4 while there is no beam. The RF2TTC allows selecting the source for the Main

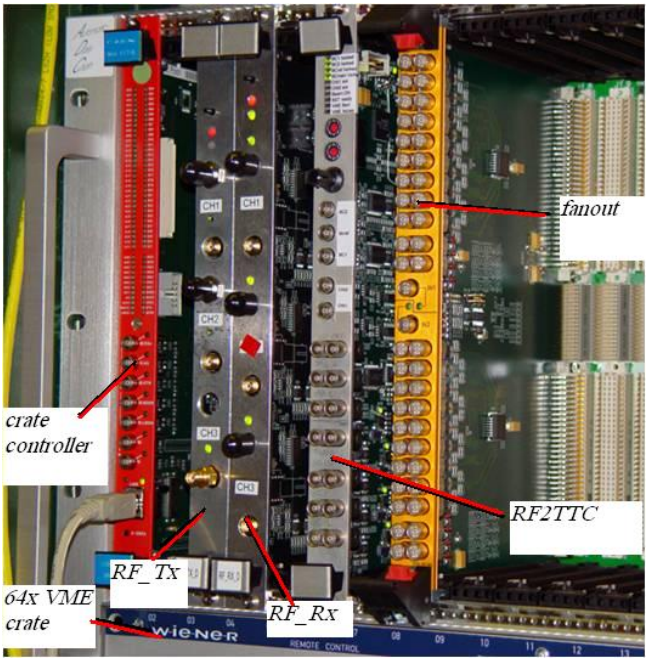

Figure 3.5: Picture of the Timing Crate.

Bunch Clock and the Main Orbit Clock outputs.

Finally, the two Main Clocks are fed into two dual 1:18 ECL Fan-Out modules, the first of which provides each LHCb Readout Supervisor (ODIN) with the Bunch Clock and the Orbit Clock in order to perform the readout control of the entire readout chain and the event management. As shown in Figure 3.6, the second fan-out feeds directly the Bunch Clock to the so called TTCex boards which perform the encoding of the experiment clock together with the two channels for trigger and readout control commands. The TTCex converts the multiplexed signal to optical and transmits it to the Front-End electronics and the Readout Boards. Configurable high-resolution delays in two TFC Switches allow adjusting the data channels for optimal sampling by the TTCex boards. The timing distribution scheme as described here is an upgrade of the TFC system as described in Chapter 2.3.3 to accomodate more stringent requirements on the jitter of the clock edge distributed to the entire LHCb readout system. Details of the motivation of the upgrade are given at the end of this section 3.3.1.

A reset of the clocks and a resynchronization of the SPS and the LHC is performed at each fill before the SPS-LHC transfer of bunches, with the consequence that the clocks disappear for about 1 ms. As the reset is made in the SETUP Beam Mode, LHCb switches from the internal clock to the machine clocks when the injection phase starts. There are other cases in which the clocks are resynchronized. A precise list of the modes and the states in which the LHC machine/RF group

provides stable clocks has been specified.

The phase of the clocks distributed to the experiments is fixed with respect to the RF clock at the *RF installation* at point 4.

However, during the acceleration of the protons from the injection energy at 450 GeV to the collision energy, a slow frequency change of the clock is expected. At 7 TeV the change in the 40 MHz frequency amounts to about 86.8 Hz. The jitter of the Bunch Clocks can be as large as up to 300 ps during the ramp due to the adjustments made in order to track the rising magnetic field. If the jitter of the Bunch Clocks is too large, this can have consequences on the operation of the experiment. In fact, many electronics devices equipped with Phase-Locked-Loops (PLL) can lose synchronization to the main clock. If this happens during data taking, a full reset is needed which affects the efficiency of the experiment. A large jitter of the RF frequency can influence the quality of the beam. If the jitter is too high, that can produce an effect called *de-bunching*, were part of the bunch of protons move to a neighbour bucket due to lenghtening of the bunch longitudinally. A close monitoring of this effect is extremely important, because it can produce ghosts bunches and influence the quality of the physics data and the luminosity normalization.

In addition, a drift of the clock phase is expected due to the exposure of the fibres to outdoor temperature variations. For LHCb, the expected typical drift is about 352 ps/degree of temperature, corresponding to 24.96 ps/(degree of temperature*km). This implies a typical day-night drift of about 140 ps and a seasonal drift of about 7 ns considering a typical variation of 20 °C. In order for the LHCb sub-detectors to operate optimally with no impact on the track efficiencies and energy calibration, the phase must be maintained within a range of ± 0.5 ns.

Consequently, the timing of the clocks and the bunch arrival times are continuously monitored, in order to display timing trends and raise alarms in the LHCb control room in case of possible malfunctions. It implies being able to fully and reliably control the timing reception in order to reconfigure the system for different purposes. It allows re-optimizing rapidly the global phase of LHCb and to feed back timing status information to the LHC control room. The system to monitor and control the timing of the LHCb experiment is described in Chapter 4.3.

3.3.1 Upgrade of the timing distribution system

The timing distribution system was upgraded with respect to the original system because the requirements on clock jitter became more stringest during the commissioning phase of the LHCb detector in 2008-2009.

The system was initially designed as shown in Figure 3.7. The main difference with respect to the upgraded system is the presence of a single Clock Fanout, a single TFC Switch and the use of the module TTCtx. This module is used to

distribute the clock together with the two channels for trigger and readout control commands to the Front-End electronics and the Readout Boards of each LHCb sub-detector.

In this configuration, the single Clock Fanout feeds the main Bunch Clock and main Orbit Clock to the pool of Readout Supervisors for global readout control. The TFC Switch then feeds the data channels to the TTCtx boards corresponding to the associated partition. Finally, the TTCtx boards convert the data channels from electrical to optical. This is done whenever a logical transition of the input signal is detected. There is no clock fed to the TTCtx, hence the jitter of the transmitted clock depends on the quality of the data channel signals at the input of the TTCtx boards.

It was noted that the quality of the signals from the TFC Switches to the TTCtx boards was not good enough to assure a transmission of the clock without desynchronization at the Front-End electronics. After detailed studies, it was discovered that the rising time and falling time of the signals generated in the TFC Switch were consistently different. This phenomena had a big effect on the final jitter of the clock. Comparing the signals from the old system to the new upgraded system can help highlighting this effect. This can be done comparing the top and bottom of Figure 3.8. Both Figures represent screenshots taken from a very fast oscilloscope. The various signals under observation are highlightened and referred to: C2 is the clock at the output of the Clock Fanout and C3 is the data channel signals at the input of the TTCtx. C1 is the reconstructed clock from the data channel pattern on a receiver board. In LHCb, the Readout Boards are equipped with the receiver CERN TTCrq chip, therefore the reconstructed clock is measured directly onboard at the output of this chip. The pink histogram (F2) represents the distribution of the measured periods of C2 and the green histogram (F4) represents the distribution of the measured skew between C2 and C1. The idea of these screenshots is to demonstrate how the upgrade of the timing distribution system in LHCb reduced the jitter of the reconstructed clock, independently from the quality of the input clock. In fact, the quality of the reconstructed clock simply depends on the rising and falling time of the transmitted data channels.

The jitter of the input clock is about 30 ps, with a gaussian distribution in both cases. The jitter of the reconstructed clock is instead different in the case of the old and the new system. In the old system, the distribution is not gaussian (F4) and the skew between the clock edge and the reconstructed signal reaches the value of about 200 ps. In the new system, the distribution is gaussian and the skew reaches the value of about 40 ps, improving considerably the quality of the transmitted signals and reconstructed clock.

This upgraded system was implemented during the commissioning phase of the LHCb detector in 2008-2009 and can be considered as a first upgrade of the TFC system.

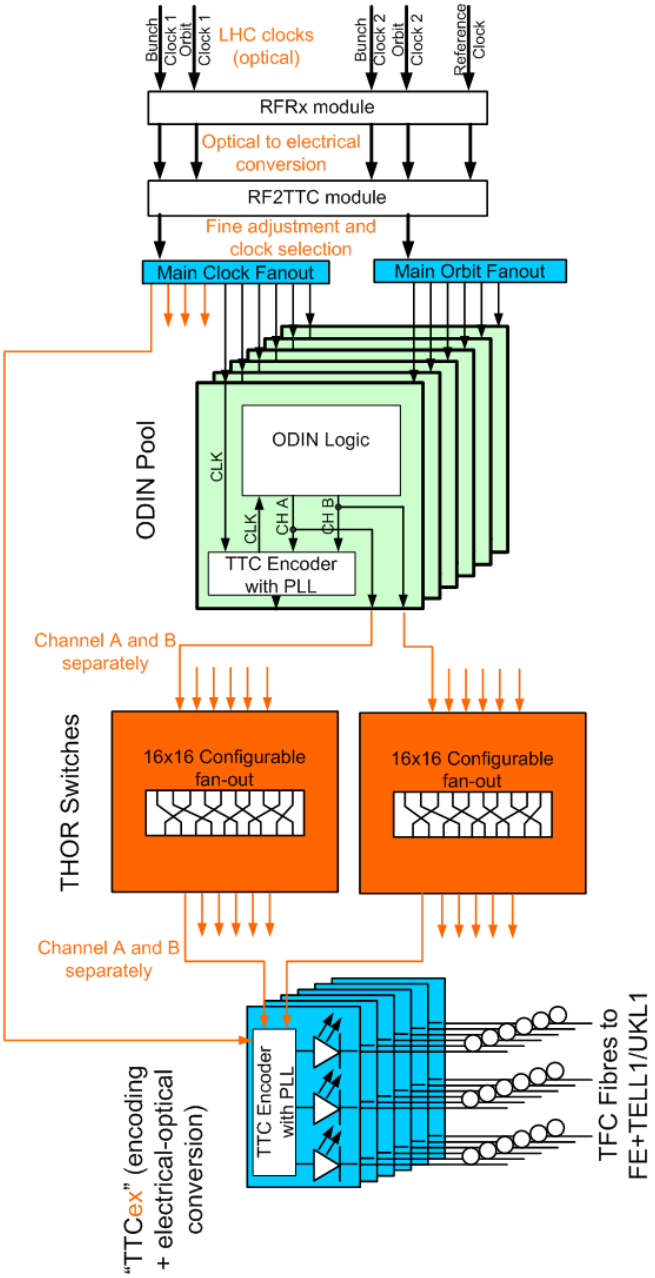

Figure 3.6: Layout of the distribution of timing, trigger and the readout control commands to the Front-End electronics and the Readout Boards by the LHCb Timing and Fast Control system.

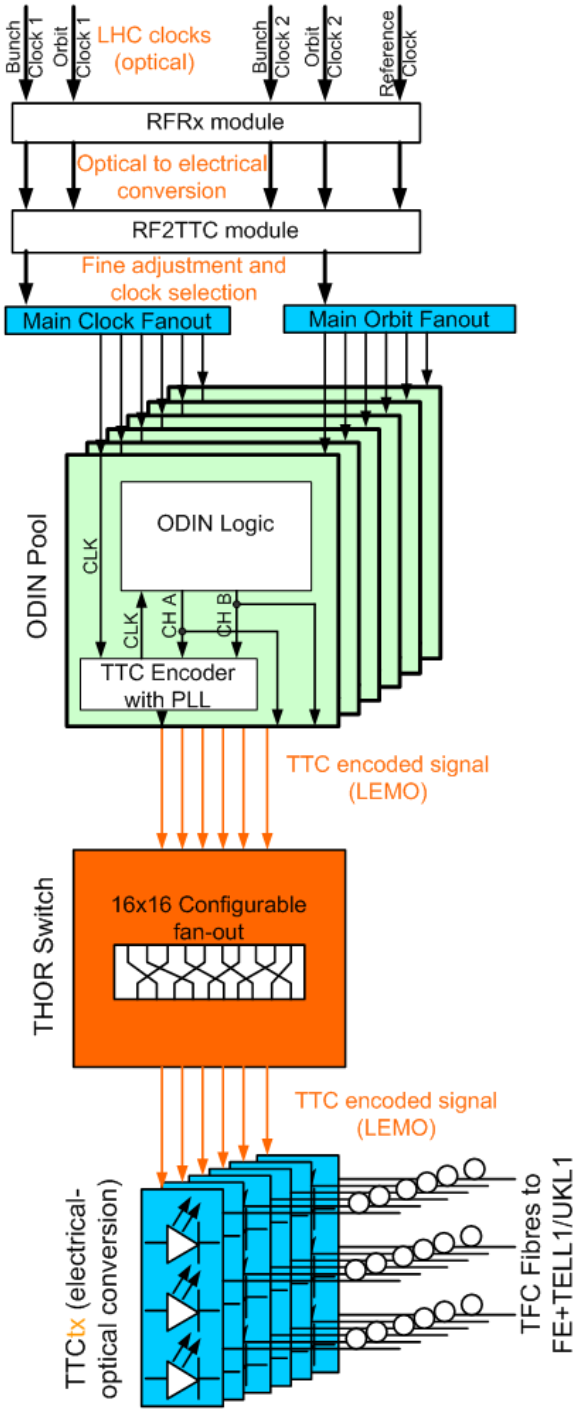

Figure 3.7: Layout of the old distribution system of timing, trigger and the readout control commands to the Front-End electronics and the Readout Boards by the LHCb Timing and Fast Control system.

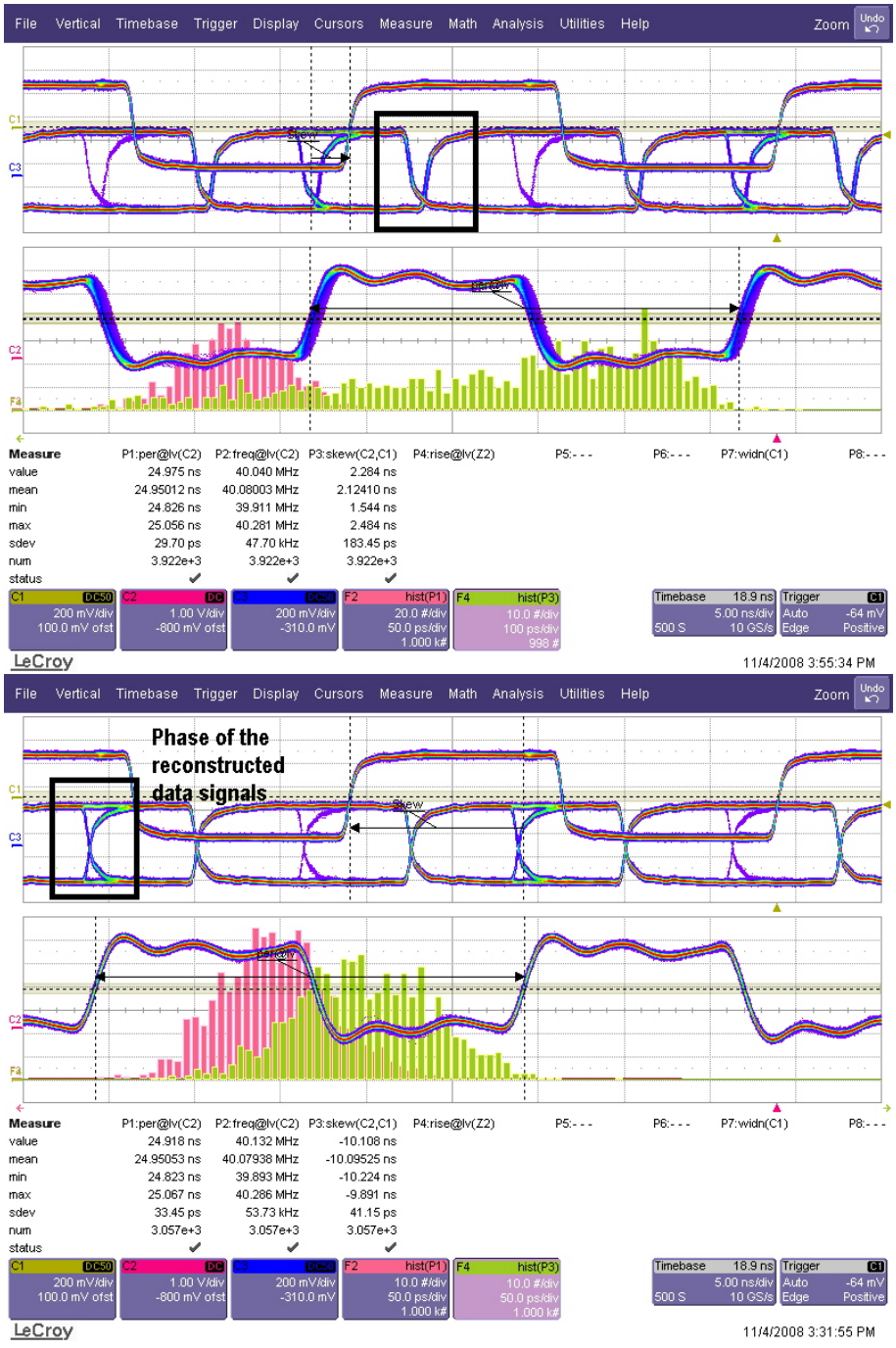

Figure 3.8: Oscilloscope screenshot for the input clock signal and the transmitted signal in the old timing distribution system (top) and new distribution system (bottom). The rising and falling time (in black box) of the transmitted signals are different and this has an effect on the jitter and quality of the transmitted signal. This effect disappeared after the upgrade.

3.4 Requirements for the work presented in the thesis

The success of the particular LHCb physics programme at the LHC is tightly connected to its operation performance and experimental conditions as they directly affect the amount of data that is recorded and its quality. The understanding of the running conditions and the machine operation has proven to be important during the first year of collisions at the LHC.

In fact, the background conditions in which the LHCb experiment has to operate can be difficult and may directly affect the trigger performance, operation efficiency as well as physics data quality. A complete beam, background and online luminosity framework comprising hardware and software system is then required to understand every aspect of the experimental conditions in LHCb. Different systems covering different levels of safety with different levels of processing speed are necessary. An online framework to control and interconnect these different sub-systems and operate them globally accordingly with the LHC operation is required. This framework has to ensure a tight connection with the LHC operation for machine protection and data exchange during beam operation at the LHC. This is of fundamental importance in order to minimize the risk of accidents and damage to the detector and at the same time maximize the experiment efficiency. A tight exchange of information between the various LHC experiments and the LHC machine is therefore essential to understand the beam characteristics and the various experimental conditions.

Finally, the possibility of an upgrade of the LHCb detector in the near future must be covered by the proposal of a new timing, trigger and readout control system.

During my work as a PhD at CERN, I was responsible for the development, calibration, analysis and operation of the Beam Loss Scintillators and the Beam Phase and Intensity Monitors systems. In the following sections, the Beam Loss Scintillators system will be extensively described. The usage of the system within LHCb will be strongly stressed as it plays a central role in the beam, background and luminosity monitoring framework. In section 4.2, the Beam Phase and Intensity Monitors system will be addressed as it is vital for the global timing of the LHCb experiment and as I was responsible for the LHCb global timing control. I was also involved in the development of a complete online framework for machine protection and global operation of the LHCb experiment, in particular developing the software tools needed to retrieve and analyze data in a fast way. Finally, I was involved in the first discussions about a possible upgraded readout architecture for the upgrade of the LHCb experiment. A first proposal for a new timing, trigger and readout control system was made and will be described in the next sections.

Here a list of the main requirements for the topics just presented is given. These requirements are the driving motivations for the work presented in this thesis and are strongly connected to the LHCb experimental aspects described in the previous

section.

Beam losses and beam halo. Fast beam losses can affect the performance of each detector in LHCb and can affect the physics data quality. These can be sudden events, often related to an hardware malfunction or wrong settings. Also, beam characteristics can evolve during a physics fill. Exploring the reasons for such evolution, estimating the time scales and predicting possible developments are vital over a longer term. Often these behaviours are unknown and therefore the system should be flexible enough to include new developments to study new phenomena. For these purposes, fast response in the order of ns and flexibility are the main requirements.

Online luminosity monitors. The amount of data that is recorded by the LHCb experiment and delivered by the LHC machine can be estimated via online luminosity monitors. LHCb dedicated luminosity monitors and methods should be put in place in order to measure such quantities.

LHCb global timing. The LHCb experiment needs to be precisely time aligned with the passage of the beam. This has to be done globally since the global LHC clocks are received via single fibres at the LHCb site and the clock must be transmitted with a very high reliability and low jitter. A system that monitors the LHCb timing with respect to the passage of each bunch in the beam is therefore needed. High precision in the order of ps and reliability are the main requirements for this system.

LHCb global operation and machine protection. A tight link between the LHC machine and the LHCb experiment must be in place as an underlying software framework for the LHCb Experiment Control System. This is required in order to coordinate the operation of the experiment with the operation of the machine. Beam accidents and malfunctions can occur during beam operation, so alarms should be issued in case of malfunctions and configurations should be loaded according to the states of operation. In this last case, hardware connection ensures the fastest response possible and reliability, while a software implementation ensures completeness and flexibility.

LHCb software tools for online analysis of experimental conditions. The number of experimental conditions involved in the operation of the LHCb experiment is so large that software tools to retrieve, visualize and store these information in a quick, flexible and reliable way are essential. A series of software tools for analysis and online operation are hence required.

The upgrade of the timing, trigger and readout control system for an LHCb Upgrade. The idea of running the LHCb experiment at a higher luminosity of about $10^{33}\,\mathrm{cm}^{-2}\,\mathrm{s}^{-1}$ was put on the table in order to collect more data that it was foreseen initially [44]. This would require a new timing, trigger and readout control system to comply with an upgraded electronics architecture of the newly developed sub-detectors in the scenario of an upgraded LHCb experiment.

3.4.1 State of the art

The LHC accelerator is a completely new machine as well as the LHCb experiment. Effects or beam and background behaviour needs tools, methods and systems which are already developed and ready to be used or ready to be commissioned with first beams and first collisions. In this thesis, the systems developed to comply with the aformentioned requirements are described in detail and the results of the newly implemented system are provided in the last Chapter.

The common denominator of all the systems is the operation of the LHCb experiment at the LHC. This is true for all the other experiments at the LHC, which have to face with new detectors and new systems in new environments and conditions. The requirements are therefore common for the other LHC experiments as well, but the implementation were different. An effort to confront these systems is continuously ongoing in order to find common solutions according to the different needs.

A first example in this case is the development of the global timing monitoring system. Each experiment at the LHC receives the clock directly via fibres. A common development at CERN allowed having the same reception system at each experiment site. However, the distribution of the clocks is done differently as well as the monitoring systems. The ATLAS and CMS experiments developed a common system based on oscilloscopes to monitor the global timing of their experiment [31]. The main advantage of such a system is the simplicity and reliability. However, the implementation of the same system with electronics boards gives a much higher flexiblity, readout speed and can be integrated in the global readout system of an experiment. This was the solution chosen by LHCb and it is advocated in this thesis. ALICE as well chose to use the developed LHCb system for its flexibility and speed. The timing monitoring system is also used in the trigger chain of ALICE to validate a physics trigger with respect to the type of collision.

The same electronics board complies with an LHCb scintillator system for beam, background and online luminosity monitoring. This system will be described in detail in Chapter 4.1.1. The concept of using a scintillating system was revealed to be an extremely powerful one. It was already used in other experiment like Belle and Tevatron, but LHCb was at the forefront of developing such instrumentation. This system helped heavily the operation of the LHCb experiment by providing measurements on beam losses, beam halo, beam gas rates, complete 25 ns structure of the beams and also providing a luminosity measurement which was independent from the main LHCb luminosity measurement. The initial concept was taken by other experiments. ALICE is installing a very similar system to the one for LHCb reusing the LHCb general purpose readout boards [32]. ATLAS also developed a completely independent experiment (ALFA) based on scintillating fibres for an absolute luminosity measurement for ATLAS. The LHC machine is also developing scintillating systems for beam monitoring. Coupling a scintillating system with a very fast and very flexible FPGA-equipped readout electronics allowed imple-

menting new functionalities as they were needed. In this thesis, the solutions for a scintillator system at the LHC are described and highlighted.

The requirements mentioned that a tight connection between experiments and the LHC machine is needed. Machine protection, global operation and experiments efficiencies are extremely important topics at the LHC. A complete framework for data exchange, information exchange and global interactions between experiments and machine was in fact planned and put in place within a CERN-wide common framework. The LHCb implementation is described in this thesis, giving particular attention to the implementations and the methods used. Being able to retrieve information and process them quickly was as important as running an experiment. This was in fact the topic of a related development work where each experiment and the machine developed their own software tools to analyse offline the information about experimental conditions. The machine developed the software TIMBER within the LHC Logging Project [33]. This software is widely used to gather machine conditions, settings and beam characteristics in a quick and flexible way. A lot of ideas behind the functionalities of the software where actually driven by the experiment themselves. Hence, common functionalities were envisaged. The LHCb experiment developed its own tools to analyse experimental conditions and generate summaries of the most critical experimental conditions per physics fill. This system proved to be extremely useful to research and study possible observed anomalies.

Finally, an upgrade of the LHC accelerator is being envisaged at the time of publication of the thesis. The LHCb experiment is expressing interest in upgrading the detector to collect more data to improve the sensitivity to signals and possibly expand the LHCb physics programme. Also in this case, all experiments are planning upgrades for their detectors and readout systems. In this thesis the proposal for an upgrade of the timing, trigger and readout control system is given. New technologies, implementation and methods are described. The upgrade of the readout system of the LHCb upgrade has just started and numerous solutions has been screened to satisfy the requirements of a complex system like the readout system of an LHC experiment. The system proposed here has been widely accepted by the LHCb upgrade collaboration and validations of the concepts are planned to be accomplished soon.

Summary

In this Chapter, the motivation for the work presented in this thesis is outlined. These motivations are strictly connected to the LHCb experimental conditions at the LHC. These conditions are dependent on the location of the LHCb experiment within the LHC accelerator, on its background sources, on the operation of the LHC machine and on the LHCb global timing reception and distribution system. An upgrade of the timing distribution system was implemented in order to cope with tighter requirements on the jitter of the clock. The various requirements for

the complete system described in this thesis are listed with a brief overview of the state of the art of the system and a comparison to other CERN-wide related projects.

Chapter 4

LHCb beam, background and luminosity monitoring

A framework for beam, background and luminosity monitoring has been developed within LHCb in order to satisfy the requirements presented in the previous Chapter. This framework includes many instruments whose aim is to monitor the experimental conditions as a function of the beam characteristics and machine settings. Understanding the behaviour of these conditions and their evolution with time allows improving the machine performance and the efficiency of the experiment at the same time. Coverage of different processing speeds and data acquisition rates are required in order to obtain a broad picture of beam and background conditions at LHCb.

Protection against beam incidents or wrong settings is vital to avoid instantaneous damages to the detector. This requires a response time in the order of microseconds and hardware interlocks which can dump the beams. It may also forbid the injection of the beams in presence of a problem. Slowly damaging background effects, like beam scraping against a collimator, abnormally high level of beam halo or interactions with gas don't require a high level of safety, but a response time at the level of few nanoseconds is needed. These effects can have a big impact on trigger rates and the quality of data as well. The correlation between the information given by an online Data Quality monitoring, which monitors the quality of the recorded data, and the beam and background monitoring can help understand the source of the problems. Slower background effects can be the cause of detector trips. In fact, during the injection process many LHCb sub-detector keep their High Voltages off in order to protect themselves, but as soon as the physics fill approaches the *stable beams* condition, the voltages will reach their optimal value. In case of abnormally high concentration of particles or abnormally high rate in a region of a sub-detector, voltages can spontaneously switch off due to high currents flowing or high concentration of charge. Slower background can have an effect on the electronics installed on the detector to read out the signals. Single

Event Upsets, which is the corruption of the recorded data at the Front-End side, are one example. Accumulated dose due to radiation are of high interest since many of the LHCb sub-detectors have a limited lifetime. In fact, the LHCb experiments and its detectors are designed to work for 10 years at an average instantaneous luminosity of $2 \times 10^{32}\,\mathrm{cm}^{-2}\,\mathrm{s}^{-1}$. The more luminosity will be accumulated, the more the sub-detectors will suffer from ageing effects. This means that each LHCb sub-detector will start having a reduced efficiency when certain level of radiation dose will be accumulated. They could suffer from long-term damage if the radiation dose was too high or too concentrated in a period of time. This effect gives even more importance to the implementation of a monitoring framework which can help maximize the ratio between luminosity recorded and signal background and maintain ageing effects at an acceptable level. Such monitoring framework allows the detector to be more efficient and the amount of useful physics data recorded with respect to the amount of machine delivered physics data is maximized.

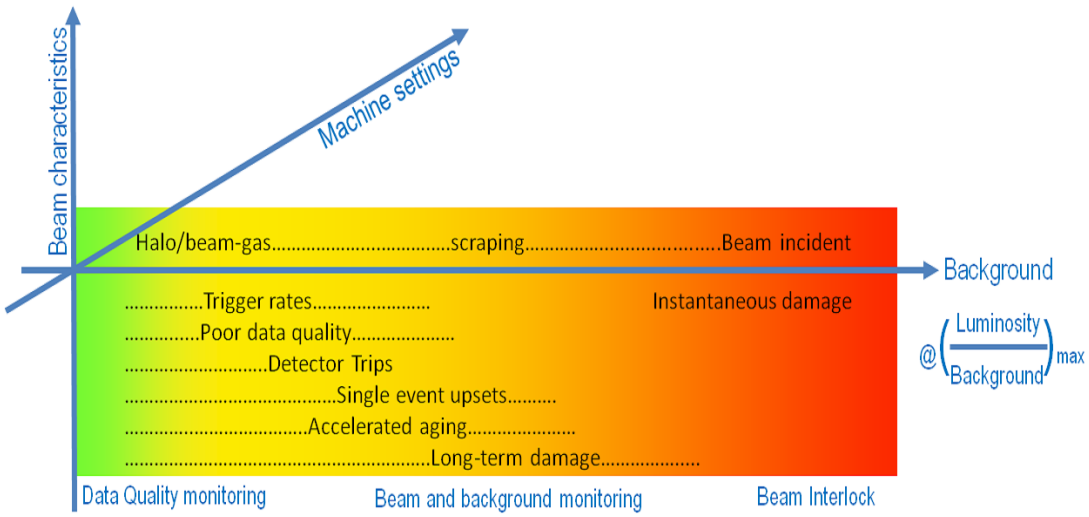

Figure 4.1: The LHCb experiment conditions in terms of background is effectively a complex function of the machine settings and the beam parameters. Depending on the amount and time structure of the background it has different consequences for the experiment.

Figure 4.1 frames graphically the concepts described previously in the background phase space. It is here introduced the idea of monitoring and studying the experimental conditions as a function of the beam characteristics and the machine settings at the LHC.

Figure 4.2 shows the various sub-systems involved in the LHCb beam, background and luminosity monitoring framework. Here a brief description of each sub-system will be given:

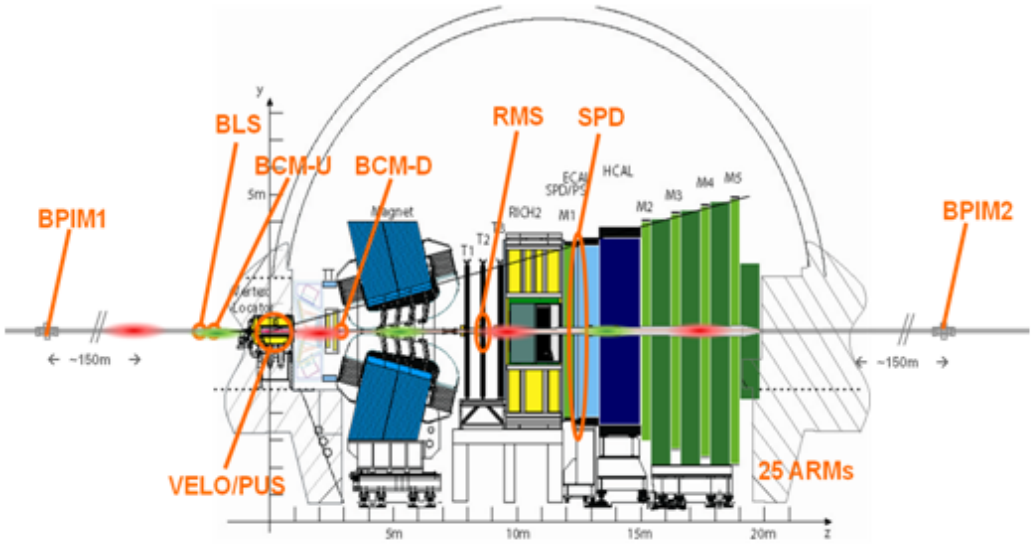

Figure 4.2: An overview of the beam and background monitors and their locations around the LHCb experiment.

- Beam Condition Monitors (BCM) [21] are two Chemical Vapor Deposition (CVD) diamonds-based detectors composed of eight sensors each. These sensors are installed around the beam pipe in a circular fashion. The main aim of the BCMs is to protect the LHCb experiment against adverse beam conditions. In fact, the diamond detectors measure the flux of particles every $40\,\mu$s and *dump* the beams if the flux is above any of a set of predefined threshold levels. The hardware connection to the LHC Beam Interlock System (BIS) assures the highest level of automation and speed, so that the beam can be dumped in less than three complete turns. Another important use of the BCM is to observe the spatial distribution of beam losses. Whenever high losses are measured, it is possible to have a clue about the direction of the losses by identifying which sensor around the beam pipe measured the highest loss. This is of extreme importance, because a correlation with other background instruments can help identifying possible malfunction or wrong settings. The BCM measurements are published to the LHC control room under the *BCKG1* and *BCKG3* numbers.

- Beam Loss Scintillators (BLS) system [22] is composed of two small scintillators located in the horizontal plane 12 cm away from the beam pipe. The main aim of the system is to detect fast beam losses from the beam, both during the injection phase and during circulating beams. Its fast readout allows measuring losses at a frequency as high as 40 MHz. Moreover, the BLS system is close to the interaction point and therefore it is sensitive to bunch interactions. It can be used as a source of relative luminosity measurement

independent from the LHCb detector.

- Beam Phase and Intensity Monitors (BPIM) [23] is a system entirely dedicated to the timing and the monitoring of the bunch structure. Two dedicated LHC beam pickups are sensitive to the passage of each beam. An LHCb custom-made readout board measures the phase and the intensity of each bunch in each beam continuosly at 40 MHz. This system is used to monitor continuously the phase of the global LHCb clock. The global timing of LHCb is shifted in order to maintain a constant clock phase with respect to the passage of the beams at the LHCb interaction point.

- Radiation Monitoring System (RMS) [24] is composed of four metal foils covering a spacial region around the beam pipe. Its surface covers the Inner Tracker detector. Each of the foil consists of seven sensors. Each of them is connected to a charge integrator followed by a voltage-to-frequency converter. The higher the charge is detected, the higher the frequency is. This sytem tracks losses at the milliseconds level. The distribution of the sensors around the beam pipe allows studying the spatial distribution of the losses.

- VELO/PileUp System (PUS) [25] is part of the VELO detector. Four sensors are used to trigger on beam-gas interactions to measure the *PileUp* of an event. The PileUp of an event is defined as the number of proton-proton interactions per crossing.

- Scintillating Pad Detector (SPD) [26] is part of the Calorimeter detectors and it is composed of many scintillating pads. Its main scope is to measure the *Multiplicity* of an event. The Multiplicity of an event can be defined as the number of scintillating pads in which particles produce scintillation. As the Multiplicity of an event is proportional to the number of tracks, this information can be used in the first-level trigger in order to select events.

- Active Radiation Monitors system (ARMs) measure the accumulated radiation dose around the LHCb cavern. The 25 ARM sensors are distributed around the LHCb detector. A continuous monitoring system provides in real-time the accumulated doses.

Each of these systems covers an aspect in the background phase space as described in Fig. 4.1. The BCM is the system with the highest level of safety as it is meant to protect the LHCb experiment and it can dump the beam. Each time that the beam is lost via an unprogrammed dump, the BCM records the measurements for the previous few seconds and stores them for offline processing. The BLS is the fastest online detector as it can analyse beam losses at 40 MHz. The BLS is therefore mostly used to study fast losses, beam halo, beam-gas rates and it is used for luminosity estimation. The BPIMs are entirely dedicated to the global timing of the LHCb experiment giving information regarding the phase of the beams and their intensities. The RMS is a radiation monitoring system for the

Silicon Tracker. It is mostly used to measure the integrated radiation dose. The PUS and the SPD are read out by the LHCb data acquisition system and they provide useful information about beam-gas rates. PUS is mostly used for beam-gas originating from beam 2 while SPD from beam 1. The ARMs are mostly dedicated to measure accumulated doses for radiation monitoring purposes and they have an integration time of minutes.

In the following sections, the LHCb scintillator system (BLS) and the Beam Phase and Intensity Monitoring system (BPIM) for beam, background and luminosity monitoring are described in detail. Their implementation and functionalities are highlighted and in Chapter 8 some analyses with 3.5 TeV proton beams are presented.

4.1 An LHCb scintillator system for beam, background and luminosity monitoring

The system is commonly referred to the Beam Loss Scintillator system (BLS). Its initial scope was to look at injection problems. However, the opportunities of using such scintillators as a detector for beam, background and online luminosity were exploited and treated in this thesis. Its functionalities have been gradually implemented during the running of the LHCb experiment thanks to its flexibility.

4.1.1 The LHCb scintillator detector

The LHCb scintillator system comprises two cubic plastic scintillators of 48 cm^3 installed few cm away from the beam pipe in the horizontal plane. They are located on the wall in front of the VELO. Each scintillator is inserted into a photo multiplier tube (PMT): an HAMAMATSU multi-mesh R2490-05 for the BLS C-side and an EMI pan-type 9839A of about 2 inches of diameter for the BLS A-side. As a convention, C-side is towards the centre of the ring, while A-side is towards the outside of the ring. The cathode of each PMT is 40 mm diameter with a LED fast driver aside for calibration. Each scintillator itself is shielded against stray magnetic field with a μ-metal tube inserted in a steel tube. A TYVEK envelope is wrapped around each of the cubic scintillator in order to collect light. Figure 4.3 shows the position of the scintillators on the wall between the VELO detector and the accelerator tunnel.

The pulse generated from the PMT is then processed by the LeCroy 612AM module which limits the pulse between +0.2 and -5 V regardless of the input signal which can be as high as to -200 V. In addition, the limiter has two outputs that allow having the signal observed through an oscilloscope and a hardware readout system at the same time. The installation of the system was carried on by Rustem Dzhelyadin and more detail can be found in [27].

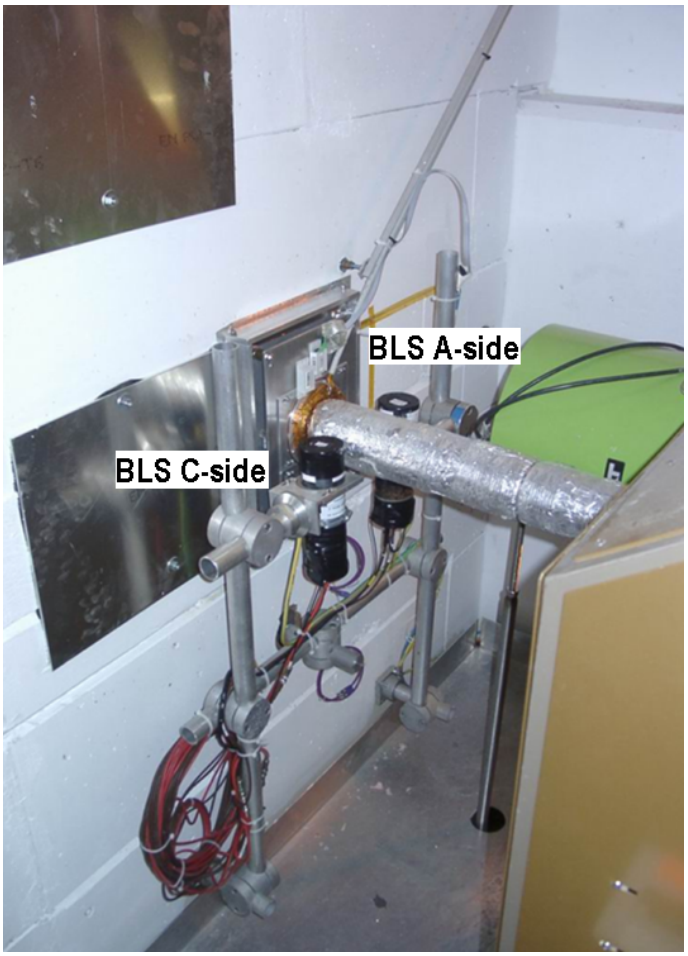

Figure 4.3: Picture of the LHCb scintillator system installed in the LHCb experimental cavern close to the beam pipe one meter before the VELO detector.

4.1.2 The readout of the LHCb scintillator detector

The general purpose readout boards for the global LHCb timing monitoring system were chosen as the readout boards for the scintillator system. These boards are commonly referred to as Beam Phase and Intensity Monitors (BPIM) and were initially developed to monitor the bunch-by-bunch phase and intensity of each LHC beams. The BPIM readout boards were already produced, tested and installed within LHCb and, thanks to their flexibility, the hardware copes with the scintillator system requirements.

In addition, a PVSS-based [36] control interface integrated in the global LHCb Experiment Control System allows monitoring the status of the system and display online accidental losses of the beam. The boards are remotely controlled and configured via expert PVSS panels. A more general panel is used by the LHCb

shifters in order to collect first information on the status of the beam and possibly correlate information with other background tools. The processed data is transmitted to the LHC machine for online feedback during physics fill. This is done via the LHCb online framework for machine protection and global operation described in the next sections.

An LHCb general purpose acquisition board

The BPIM electronics board is a custom-made board originally developed by the LHCb Online group to read out the signal generated from the beam pick-ups dedicated to LHCb. Its main purpose is to measure the intensity of the beam and the phase of the beam at 40 MHz with respect to the LHC clock, on a bunch-by-bunch basis.

The BPIM is a 6U VME standard board running at 40 MHz equipped with: an analogue signal processing to integrate the input pulse; an ADC to digitize the analogue integration value; an FPGA to process information and to perform online data analysis. Two FIFOs 32k deep will ensure an online storage of data to be retrieved by a server running on a Credit Card PC [29] mounted on the board. The board has separate Bunch Clock input and Orbit Pulse input, two general purpose ECL outputs, one general TTL input/output and one general purpose 8-bit LVDS output. The latter can be connected to the LHCb Readout Supervisor. Finally a TDC is used to measure the phase difference between bunches and the Bunch Clock with a precision of < 30 ps. A programmable delay chip allows shifting the phase of the clock with a precision of 10 ps.

The BPIM has been developed and installed in the LHCb pit during 2008. It was successfully tested at the SPS after the prodcution of the first prototype [8], and during the commissioning of the LHC with real beam. The ALICE experiment has profited from the board for their first-level trigger.

The Analogue signal processing

The analogue signal processing is based on amplifiers, buffers and an integrator in order to reach the highest bandwidth and fastest integration achievable. A first buffer is used to re-drive the input pulse in order to minimize reflection effects and noise distortion. The buffer is followed by another compensated buffer and a linear rectifier whose aim is to cancel possible overshoots. Finally, the obtained negative pulse reaches the integrator, which continuously integrates the pulse over a 25 ns interval. A reset pulse brings the integrator to its baseline, ready to integrate another pulse in the neighbour 25 ns interval. The reset pulse makes the integrator inefficient for about 3 ns over 25 ns, corresponding to about 90% of efficiency.

The entire analogue chain has a 1:1 gain which keeps the original pulse shape unchanged up to the integrator. Therefore, the only calibration needed for the ana-

logue signal processing is to find a constant ratio between the input pulse area and the integrated peak. However, the input stage is equipped with a programmable attenuator which can attenuate the input pulse by a desired and well known factor.

The Digital signal processing

The digital signal processing is based on three major chips: an ADC, an FPGA and a FIFO. The integrated analogue pulse is directly fed into an ADC which samples and digitizes it every 25 ns and sends it to an FPGA as a 12-bit word. It is necessary to precise that the ADC samples the input pulse continuously, every 25 ns. Therefore, the processing of the data is entirely delegated to the FPGA, while the storage of the data is delegated to two 16k $\times$ 16-bit FIFOs. Up to 65000 16-bit words can be stored and then retrieved by the Control System. The FPGA is the real heart of the board. It is able to process data up to 120 MHz inside the FPGA and to control all the parameters of the board. Moreover, the possibility to re-program the FPGA via JTAG as much as necessary ensures enough flexibility to cope with possible upgrades of the system. Firmware version can be loaded at start-up from an EEPROM.

Two types of processing have been identified: triggering on injection; continuous readout during circulating beams.

Triggering on Injection

In order to trigger on the injection of an SPS batch of bunches in the LHC, a hardware signal associated with the SPS extraction system must be used. This signal is transmitted over the clock transmitting network, and commonly referred to as *injection pre-pulse*. It comes few microseconds before the actual extraction/injection of bunches and can be thus used as a trigger to start acquisition of data from the BLS in injection mode. The pulse is received by the main LHCb global timing receiver board, which fans the pulse out through a NIM/ECL output converter. Via this board, it is possible to adjust the timing of the pulse in order to align it with respect to the passage of the beams in LHCb. The pulse is converted to TTL signal via a simple CAEN signal converter. Taking advantage of the fact that the BPIM has two clock dedicated inputs and one TTL general purpose input/output, it is possible to use the injection pre-pulse to start the readout of the BLS and place each measured loss into a precise Bunch Crossing ID (BXID).

When the readout is triggered, the BPIM is stores data for 10 to 20 full LHC turns, bunch-by-bunch. However, to increase the number of turns per injection to be exploited, the FPGA can process intelligent running sums, in order to analyse just the most recent injected bunches. It is in fact likely that fast losses are mostly due to the most recent injection since it was shown that losses at injection have a higher flux than losses during circulating beams. Hence, it is possible to collect

data around the injected BXID for a programmable number of crossings and repeat the same measurement for up to 5000 consecutive orbits.

Continuous Readout

Once the beam is fully injected, the BLSs monitors continuously background induced by circulating beams. A BLS can just wait for an input pulse to be higher than a programmable threshold value and start running sums around the identified BXID. This first threshold is set in order to be sensitive to losses of many particles. Thanks to the flexibility of the FPGA, the length of running sums is programmable. For the first operation at the LHC it was chosen to be of a length of 10 BXID, but most likely the length will be chosen according to the LHC filling scheme and according to the scope of the measurement. It can be short in order to observe many fast losses for consecutive bunches or it can be long in order to observe long tailed background. The latter case is the most preferred one during multi-bunch operation, where many bunch will be injected in the same train.

Moreover, a second threshold is implemented in the FPGA code so that it is more sensitive to low angle scattered particles from proton-proton collisions. In this way, the system can be used as a luminosity counter for LHCb. In this configuration, each signal is gated with the type of crossing from the LHC filling scheme and if a signal happens in a collision crossing that is counted as a luminosity trigger.

4.1.3 Functionalities of the scintillator system

The LHCb scintillator system acquired many new functionalities during the first year of running at the LHC. In fact, as already mentioned before, the BLS was initially intended to only observe losses at injection. However, the choice of using the LHCb general purpose readout board equipped with an ADC and an FPGA allowed exploiting many more functionalities. Here a list of functionalities are presented together with their role in the LHCb beam and background monitoring framework.

Study of injection dynamics

When the system is working in the *Triggering on injection* mode, it is synchronized to the injection of a bunch or train of bunches from the SPS to the LHC. The BLS is able to observe the 25 ns structure of these losses, identifying the BXID for the worse loss and indentifying all possible anomalies associated to the injectio of beam in the machine. An example of the use of this functionality is described in Chapter 8.1.

Continuous monitoring of beam losses and beam halo

In the more general framework of a background study at the LHC, background protection and beam analysis, the LHCb experiment publishes a series of background numbers which correspond to different measurements of beam losses around the interaction point 8, where LHCb is located. In short:

- BCKG1 gives a measurement of normalized losses in the inner region of the detector;
- BCKG2 gives a measurement of normalized beam halo;
- BCKG3 gives the fraction of measured losses compared to the experiment abort threshold (so-called Dump threshold);

In LHCb, BCKG1 and BCKG3 are constantly provided by the BCM and are the normalized measurements of beam losses respectively over $80\,\mu$s and $1280\,\mu$s of integration time and averaged over the BCM Upstream and Downstream stations. BCKG2 is instead provided by the scintillator system and the measurement is normalized to a scale of 1-100. In practice, BCKG2 corresponds to the worst measured beam loss during the period of each update which is typically 5 s.

Beam gas rates monitoring

The system is used to monitor the trend of beam gas rates as these depend strictly on the beam characteristics and the quality of the vacuum. An example is given in Chapter 8.2.

Online luminosity monitoring

The BLS is also used as a source of online luminosity independent from the main LHCb luminosity source. More details are given in Chapter 7.

Abort gap monitoring

Before each first bunch in each beam (BXID = 1), there should be a $3\,\mu$s gap without particles in order to allow for rise time of the dump kicker pulse. This gap is called *abort-gap*. For LHCb purposes, the abort gap monitoring is useful in order to monitor possible de-bunched beam due to RF synchronization failures or to monitor particles captured in this gap by the momentum cleaning. From the LHCb point of view, this should not happen because the LHCb Front-End Electronics perform synchronization checks and resets during the abort-gap and no trigger shall be received during this interval. However, because of the asymmetry of the position of LHCb with respect to ATLAS and CMS, the abort gap in LHCb is not

the same as in ATLAS and CMS and depends on the LHC filling scheme used. Two programmable registers are then used to monitor the abort gap as calculated from the filling scheme.

4.1.4 An upgraded scintillator system for the 2011/2012 physics run

The first scintillator system at LHCb has proven great performance and flexibility even though the system was built with spares parts. All around the LHC experiments, scintillator systems similar to the LHCb one are being commissioned and will be used for the 2011/2012 physics run.

An upgraded scintillator system was proposed at the end of the 2010 physics data taking period. The main reasons for an upgrade are the following:

- Ageing: the BLS C-side scintillator was starting to show signs of ageing due to non-equalized voltages at the dynodes. Moreover, the BLS C-side scintillator had an HAMAMATSU PMT with a borosilicate glass, which tends to age under radiation.
- Position: the BLSs cover only a very small acceptance. In fact, it is calculated in the chapter dedicated to analysis that the scintillator system acceptance was only 16% of the LHCb total acceptance. Moreover, the two scintillators were installed only in the horizontal plane, hence not providing any information for losses in the vertical plane.
- Quantity: only two small scintillators were installed. Having the possibility to at least duplicate the number of scintillators would allow increasing the acceptance of the detector and enriching the beam background information.

An entirely new scintillator system was installed during the 2010/2011 technical stop by R. Dzhelyadin and L. Roy. Details on the installation of the new system are given in reference [28]. Here only a brief description of the new system is given.

Figure 4.4 shows the new scintillator system installed in the LHCb cavern. It comprises six scintillators, divided in three different group according to their shape and sizes:

- BLS07 and BLS08 replaced the old BLS01 and BLS02. The shape and sizes remained the same (cube of $48\,\mathrm{cm}^3$). The plastic scintillators were changed, the two PMTs are the same EMI9839A type with the base modified to draw a current of 1.1mA at 1.1kV. They are located in the horizontal plane, about 12 cm away from the beam pipe.
- BLS03 and BLS04 were installed in the vertical plane, about 28 cm away from the beam pipe. These new scintillators have a rectangular shape, $14 \times 14\,\mathrm{cm}^2$

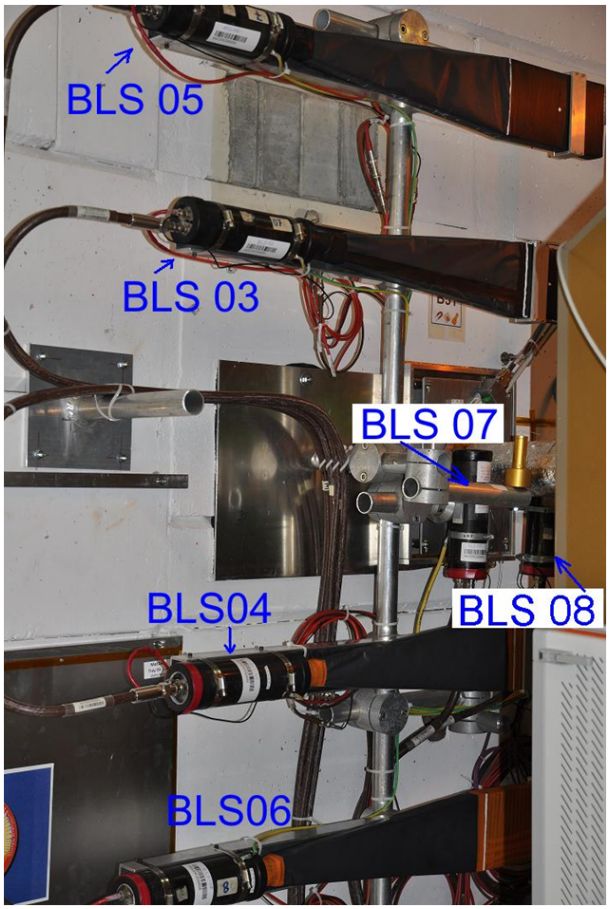

Figure 4.4: Picture of the upgraded LHCb scintillator system installed in the LHCb experimental cavern.

with 3 cm of depth. A light guide was needed in order to collect the light from the scintillator to the PMT.

- BLS05 and BLS06 were also installed in the vertical plane, about 61 cm away from the beam pipe. The dimensions of these two scintillators are bigger as they have a rectangular shape of $14 \times 28\,\mathrm{cm}^2$ with a depth of 3 cm.

All the PMTs are the same, EMI9839A, with the base modified to draw a current of 1.1mA at 1.1kV. In Figure 4.5 the schematic layout of the new LHCb scintillator system is depicted.

The good performance of the system and the important role within the LHCb beam, background and luminosity monitoring required an upgrade of the system in order to allow for more precision of measurements and even more flexibility. The upgraded system will contribute heavily to the 2011-2012 physics run providing useful information on beam characteristics, beam injection quality, machine back-

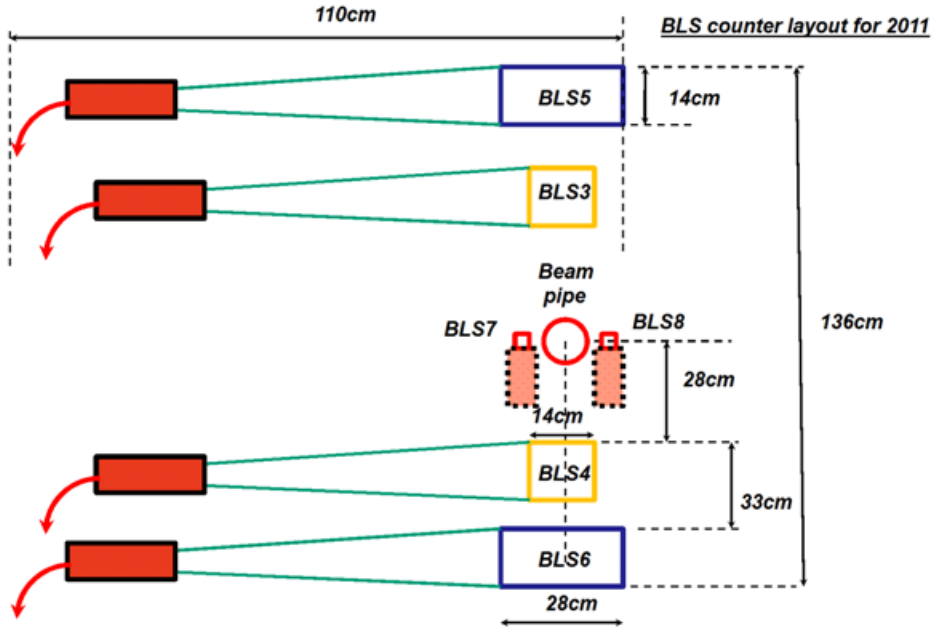

Figure 4.5: Schematic layout of the new LHCb scintillator system.

ground and luminosity. The LHCb scintillator system provides data at 40 MHz, on a bunch-by-bunch basis thanks to its fast readout and flexibility.

4.2 Beam intensity monitoring and monitoring of the LHC filling scheme

In order to perform a precise monitoring of the LHC bunch structure called *filling scheme*, and the intensitiy of each bunch, a machine-independent system based on beam pickups has been developed. It monitors at high-speed and high-precision the intensity of each bunch of the two LHC beams and compare its measured filling scheme with the expected one. Various operational problems during the preparation of the physics fills may lead to wrong LHC filling schemes. Ghosts or satellite bunches with offset collisions may affect data quality and luminosity counting. Satellite bunches are usually the result of unwanted bunches coming from the SPS. Ghosts are usually bunches which originally came from the beam injected in the machine and were produced due to de-bunching effects. It is therefore vital to monitor the intensity of each beam, the intensity of each bunch in each beam and the LHC filling scheme.

4.2.1 LHC Beam pick-ups

LHCb has two dedicated beam pick-ups shown in Figure 4.6, which are part of the LHC accelerator complex and are referred to as BPTX.5L8.B1 and BPTX.5R8.B2.

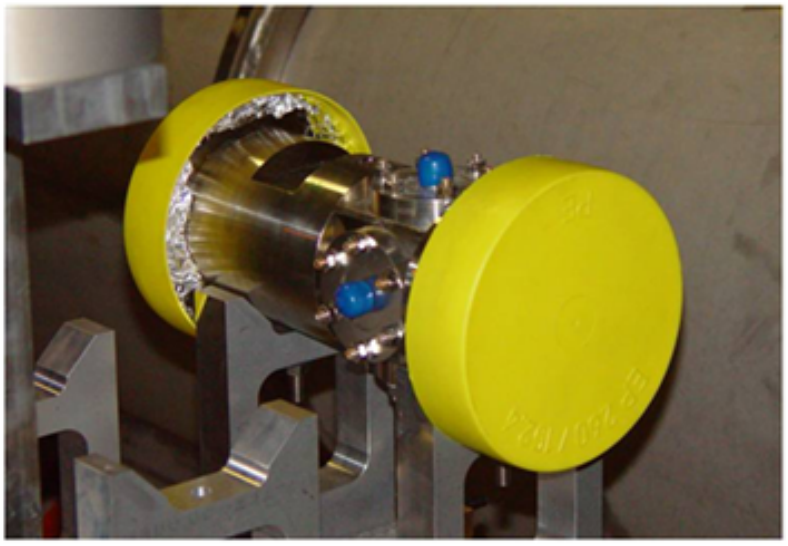

Figure 4.6: Picture of one of the two LHCb beam pick-ups.

The pick-ups are installed about 150 m away from the LHCb interaction point on each of the incoming beams. They are based on button electrodes with a capacitive pick-up graphically described in Figure 4.7.

As shown in Figure 4.8, they produce a bipolar pulse which is a direct measurement of the phase and the intensity for each bunch. The functioning of such buttons is well described in [30] and [31]. At the passage of a bunch, the positive charges cause the free-moving electrons of the metallic beam pipe to form a mirror charge on its surface. This mirror follows the bunch around the accelerator giving rise to an image current, with equal magnitude but opposite sign compared to the bunch current. The image current will travel over the circular electrode surface of the button pick-up and give rise to a signal. Since the energy of the signal captured by the pick-ups is negligible compared to the energy of the beam, this set-up can be used to monitor the beam without influencing it. Figure 4.8 shows a simulation of the expected pulse shape from a single button at different intensities and Figure 4.9 shows the expected pulse shape for different bunch lengths for the same bunch intensity. In practice each BPM station consists of four button pick-ups symmetrically mounted around the beam pipe. To first order, the sum of the pulse from all four buttons is independent of the transverse position of the beam and proportional to the intensity of each bunch. However, as shown in Figure 4.9, the energy and length of the pulse is strongly dependent on the bunch length introducing a level of complication in the readout of the input pulse.

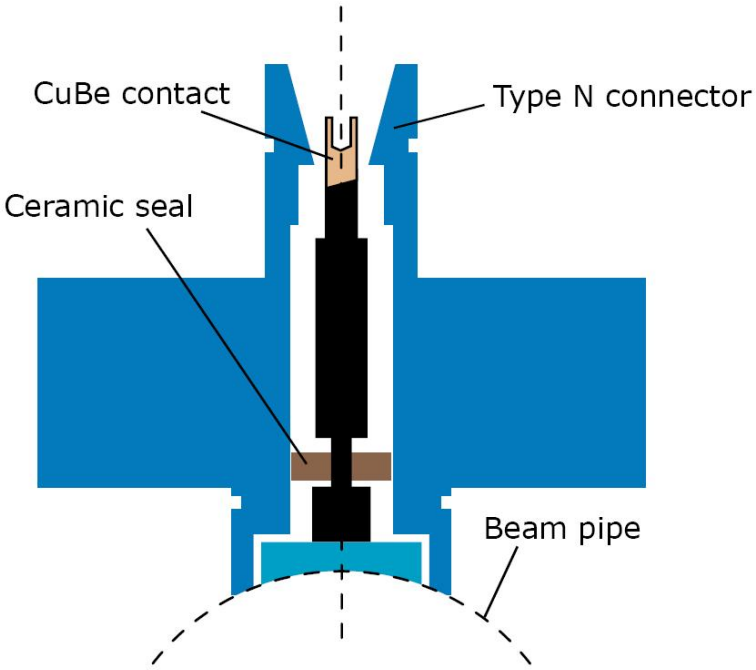

Figure 4.7: Picture of one of the four button electrodes which form the LHCb beam pick-ups

The bipolar pulse is fed via about 280 m of Nexan CMA50 coaxial cables, with a 2 dB of attenuation ratio at 80 MHz per 100 m and a very low signal-to-noise ratio, to the BPIM readout electronics board which measures the intensity and the phase of the beams bunch-by-bunch.

4.2.2 LHCb Beam Intensity Measurement

Figure 4.8 shows that the input bipolar pulse generated by the beam pick-ups is a very sharp pulse with a width of about 1.5/1.8 ns and an amplitude of about 20 V peak-to-peak. In order to measure the current contained in one bunch, an integration of the area of the bipolar pulse is necessary. This is achieved by a rectifier stage in the BPIM which inverts the positive part of the bipolar pulse, sums it up to the negative part and then integrates the pulse analogically. Very fast current amplifiers (4.58 V/ns slew rate and 1.7 GHz bandwidth) are used for this analogue stage. The integrated pulse is then fed to an Analogue-to-Digital Converter (AD9432BST from Analog Devices, 105 MHz MSPS max, pipelined) which outputs a 12-bit value at 40 MHz to the main FPGA onboard for processing. The integrator is then reset every 25 ns in order to be ready to integrate the next bunch and introduces a dead-time of about 3 ns. This allows reading out the

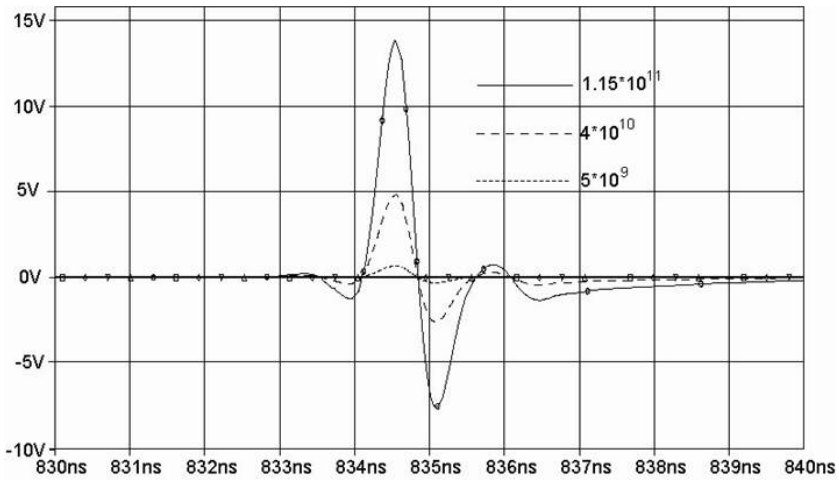

Figure 4.8: The pulse shape from simulation for different bunch intensities from a single button electrode.

bunches intensity measurements as a function of the BXID for a full turn. The intensity data is output continuously through an 8-bit general purpose output which is interfaced with the LHCb Readout Supervisor ODIN. The 8-bit word is added to the ODIN data bank for each crossing and appended to the main LHCb recorded event. The intensity measurement is very similar to the measurement performed for the beam losses with the BLS. The main difference is that while in the BLS system the input pulse has a width of two to three clock cycles, the input pulse from the BPTX pick-ups has a width of few nanosseconds. Via programmable onboard delays, the input pulse is aligned in time to allow the board to sample the ADC value at the optimal sampling point. This in practice means that the ADC value is sampled whenever the integrator has finished to integrate the few nanoseconds wide input pulse. The efficiency of the BPIM system is therefore 100%: a full input bipolar pulse coming from the BPTX is integrated, converted to 12-bit digital word at 40 MHz and stored for data processing, graphical presentation and data mining on archive.

The input bipolar pulses for beam 1 and beam 2 are read out for a full LHC orbit. The outcome is then compared to the expected LHC filling scheme. If some inconsistencies are found, an alarm and a flag are raised and transmitted to the LHC and the LHCb control rooms. This is part of the online framework optimizing the LHCb experimental conditions. Its implementation will be described in detail in the next Chapter.

The same system was installed in the ALICE experiments with the same LHCb readout boards. The very high efficiency and reliability of the board allowed the system to be implemented in the trigger architecture by providing a validation pulse at 40 MHz to the ALICE Central Trigger Processor. This pulse is used to

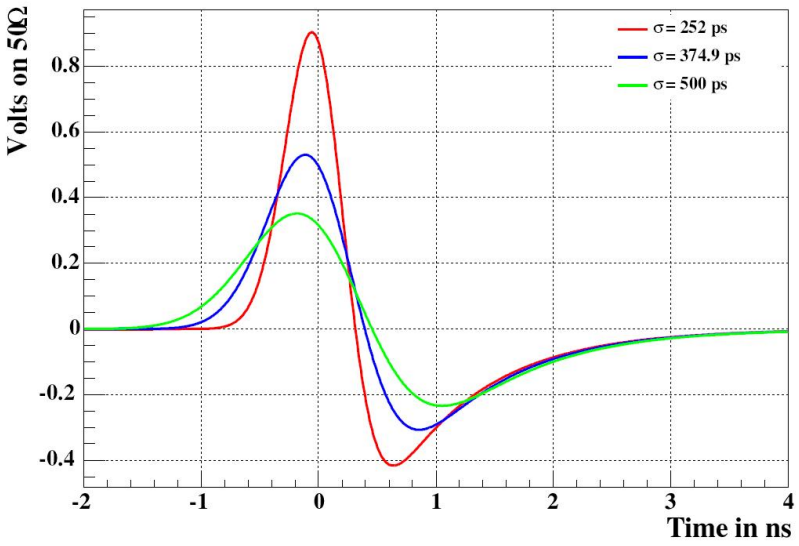

Figure 4.9: The pulse shape from simulation for different bunch lengths.

distinguish between crossing types and it is used in conjunction with the trigger coming from other ALICE sub-detectors.

An analysis of the calibration of the beam intensity measured by LHCb and the beam intensity measured by the machine is described in the section 8.3.

4.3 LHCb global timing monitoring and control

The LHCb global timing monitoring is performed using the same BPIM card used for the intensity and LHC filling scheme monitoring. Its main aim is to obtain a measurement that represents the phase of each bunch sampled by the BPIMs with respect to the LHCb global Bunch Clock. This measurement on the two beams allows monitoring the difference in bunch arrival time of beam 1 and beam 2 in order to guarantee the proper fine-cogging of LHC and thus well-positioned bunch crossings longitudinally at the IPs. This quantity is usually referred to as ΔT.

As shown in Figure 4.9, ideally, a threshold corresponding to a fraction of the input pulse corresponds to the stable sampling point for the phase measurement. However, due to the extreme pulse characteristics a simplified adjustable *constant-level crossing* method is used. For this purpose, the timing measurement employs two Digital-to-Analogue Converters to define two threshold levels for a comparator:

1. A threshold which defines the presence of a pulse associated to real beam and allows noise suppression.

2. A constant-level threshold that defines the sampling point on the falling edge of the positive half of the bipolar pulse.

The two thresholds are fed to a high performance comparator (MAX9601EUP, dual ECS/PECL 500 ps, Ultra-High-Speed Comparator by Maxim) which compares the level of the input pulse with the threshold level. A validation pulse is then produced using Flip-Flops and is fed to the Time-to-Digital Converter (TDC) together with the pulse generated from the clock edge which is used to restart the internal TDC counter. The TDC used is the ultra performing TDC-GPX produced by ACAM [34]. The datasheet specifies a TDC resolution of about 27 ps with a 28-bit time counter corresponding to a time range of 40 μs.

The control of the global timing was already described in Chapter 3.3 and it is performed via the RF2TTC card. The monitoring of the timing is performed continuously. The measurement is used to shift the global timing whenever necessary, in order to keep the global LHCb clock phase within ± 0.5 ns with respect to the passage of the beams at the LHCb IP.

The commissioning of the timing monitoring system with first 3.5 TeV colliding beams is described in section 8.4. Measurements and analysis of the observed clock phase drift are shown in section 8.5.

Summary

In this Chapter, a description of the BLS and BPIM systems was given. They are two central systems in the LHCb beam, background and luminosity monitoring framework. An introduction of the functionalities and instruments which are part of the framework was given to frame the systems within LHCb and the LHC. The excellent good performance of these systems and their flexibility allowed them to heavily contribute to the 2010 physics runs by providing vital data about beam characteristics, background conditions, luminosity evolutions and global timing measurements.

Chapter 5

Optimization of experimental operation in LHCb

The complexity of the LHC and its extreme running conditions have demanded an unprecedented dialog between the accelerator and the experiments. LHCb has been at the forefront of developing a hardware and software framework [35] which are connected to all of the LHC communication interfaces. They are related to timing, control and monitoring of the machine and beam parameters. The framework handles the local systems for beam, background and luminosity monitoring described in the previous Chapter with the ultimate goal to protect the LHCb experiment. It improves the LHCb global operation performance and includes failsafe connectivity with the beam interlock system.

The framework drives the global operation of the detector and it is integrated into the readout control. It provides the shifters with the guidelines to take fast decisions to run the LHCb experiment safely and efficiently. In particular, it has allowed the detector to be operated with only two shifters already during the LHC pilot run in 2009. The requirements are reliability and clarity for the shifters, and the possibility to retrieve the past conditions for offline analysis. All essential parameters are archived. An interactive analysis tool has been developed providing overviews of the experimental performance and allowing a post-analysis of any anomaly in the operation.

In this Chapter, the architecture and the functions of the LHCb framework for machine protection and global operation are described, including the basis of the automation of the LHCb operational procedure and detector controls. The information exchange between LHCb and the LHC as well as the shifter and expert software tools are covered. Finally the control system for the electronics boards and the integration of the software framework within the global LHCb Experiment Control System are presented.

5.1 An online software framework for machine protection and LHCb global operation

In order to satisfy the requirements for machine protection and optimization of the experimental conditions, a very large interconnectivity is needed between the LHC machine and the LHCb experiment as well as between systems within LHCb. Figure 5.1 shows an overview of the data flow in the framework architecture.

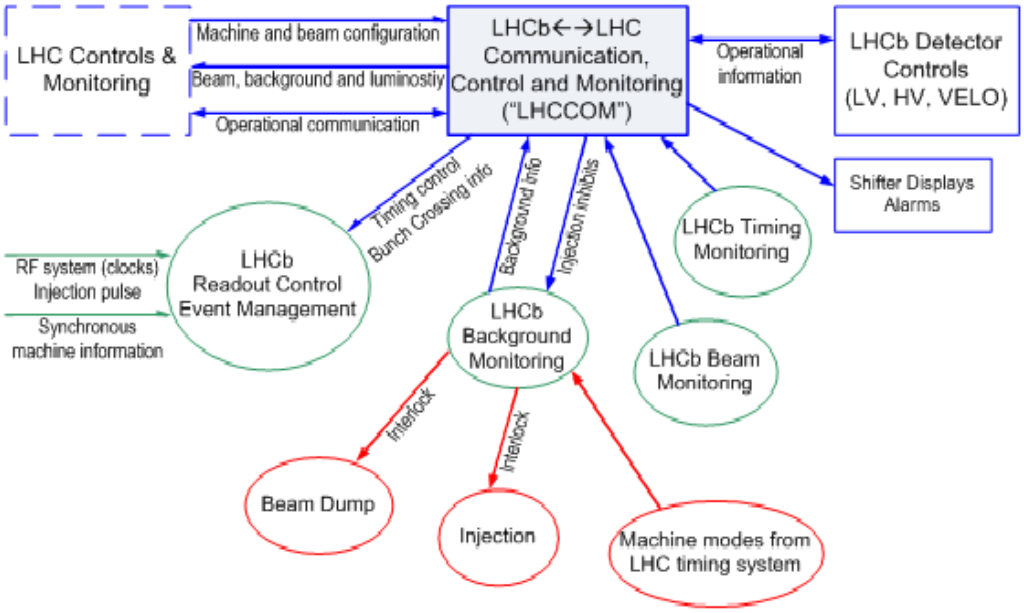

Figure 5.1: Overview of the LHCb online framework for experiment protection and operational control and monitoring. Blue colour illustrates software components and network links. Green colour illustrates hardware systems with essential functions and redundancy. Red colour illustrates critical hardware systems and connection with failsafe and redundant logic.

The framework merges software and hardware systems and their interconnectivity. It contains a series of units to:

- protect the experiment during fast beam extraction;
- automate and secure the operational procedures;
- control the readout and manage the events for physics, luminosity and calibrations;
- monitor, diagnose, and provide feedback in real time to the LHC and the LHCb control rooms;

- archive all machine, beam, and detector parameters for offline analyses.

The core of the framework consists of a control system developed using the PVSS SCADA tool from ETM [36]. It performs the readout of the hardware, the global data exchange between the various sub-components, and runs the control logic. The system, called *LHCCOM*, runs on a power redundant Linux machine and has shown that it can cope with the required high load of data. In the following sections, the framework's functionalities and their implementation are described.

5.1.1 Experiment protection and safety

The LHCb experiment can inhibit injection of both beams via a failsafe hardware interlock. This is used in order to assure that the proton injection can only take place when LHCb is in the proper safe state. The injection inhibit is used to prevent further beam transfers between SPS and LHC during the preparation of the fill, since the powering of the detector begins immediately after the injection phase. The injection inhibit is associated with the background monitors in a way that it can pause the injection without dumping the circulating beam if the injections are abnormal. An injection quality summary is transmitted automatically via software after each beam transfer to inform the LHC control room on the quality of the injected beams.

As the ultimate protection, the LHCb experiment has several failsafe links to the Beam Interlock System (BIS) which allows dumping the beams within three turns in case excessive beam losses or malfunctioning are detected. These losses are too fast to be corrected, therefore the beams are dumped. The main input from LHCb comes from the two LHCb Beam Condition Monitors which are installed on the beam pipe inside the LHCb detector. The dump logic is based on a set of running sums with thresholds estimated from simulation and experience with beam. Due to the failsafe implementation of the BCM readout electronics, it functions as the driver of the injection interlock. The whole system is supervised by the LHCCOM which monitors the status of the BCM and acts on the injection inhibit depending on the information from the detector control system.
The LHCb VELO detector may only move to its data taking position once the physics conditions have been established and the beams are stable and colliding. A *Movable Device Allowed* flag and a *Stable Beam* flag are transmitted via the *General Machine Timing* system (GMT [37]) directly to the LHCCOM system, and to the VELO interlock logic and motion control. If all conditions are fulfilled, the global detector control system will initiate the VELO closure, or inversely automatic opening. Hence, the status of the VELO is an input to the BIS. If the VELO is not in the open position (*garage position*) and the beams are not declared stable, then the beams are dumped because the safety conditions for the VELO are not met anymore. The status of the LHCb spectrometer is part of the BIS. This is because particles around the LHCb interaction region follow a precise path which

is defined by the field of the spectrometer and the three compensator magnets around LHCb. If one of these magnets fails or switches off, the risk to damage the detector or the accelerator elements is too high and therefore the beams are dumped.

Figure 5.2 shows graphically the scheme for experiment protection and safety.

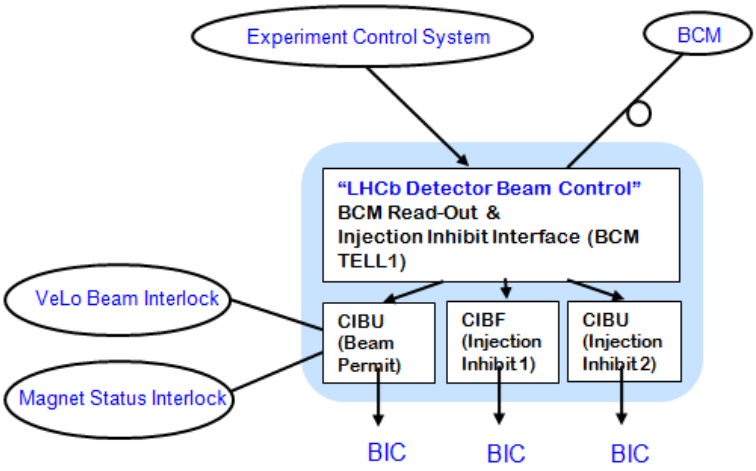

Figure 5.2: The BCM readout electronics continuously runs the dump logic comparing a set of running sums with thresholds estimated from simulation. The experimental control system acts on the BCM readout electronics via software in order to inhibit or allow injections depending on the state of the LHCb detector. Only if all the conditions are positive, the injection inihibit per beam is lifted and the machine can inject the beams and bring them to collision.

5.1.2 LHCb global operational procedures

The operation of the experiment is strictly connected to the LHC machine operation. The LHC machine operational phases are defined via so called *Beam Modes* and *Machine Modes*. In order to simplify the operation of the LHCb experiment, the 18 main LHC beam modes have been mapped onto eight LHCb states in which the configuration of the LHCb detector is different as shown in Figure 5.3.

In this way, the sub-detector voltages, beam, background and luminosity monitoring systems are controlled as a function of the LHC modes. Similarly, the configuration and control of the LHCb readout and trigger relies on the LHC machine mode and the sub-detector states. There are two situations in which the LHC moves from a safe situation to an unsafe situation for the experiments. From no-beam mode to the *Injection* mode and from *Stable beam* mode to an *Adjust* mode in which the machine manipulates the beams for machine development purposes. In order to make these transitions safe for the experiments, they are preceded by a software handshake via the data exchange network. The handshake consists of a

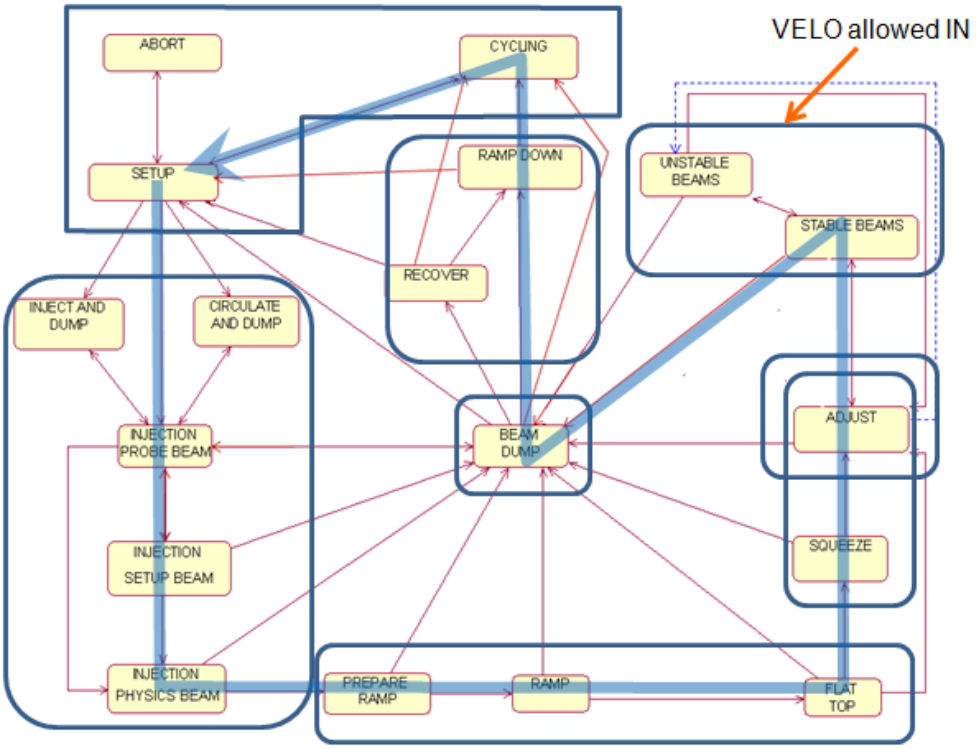

Figure 5.3: The 18 main LHC modes (yellow boxes), which have been regrouped in the eight LHCb modes (blue circles). The arrow shows the path that the global detector control system follows during an LHC Fill. Only two LHC modes allow the VELO to close.

warning issued by the machine followed by the declaration of a *ready* by the experiments, once each experiment has been configured for the unsafe mode. Lifting the injection inhibit is associated with the injection handshake. All of this forms the basis of the automation in the overall LHCb Experiment Control System. This automated implementation ensures a high reliability, shifter friendliness and reduces the action of the shifters to monitoring and confirming actions.

5.1.3 Information and data exchange

A large fraction of the logic above, as well as the displays and tools used by the accelerator operators and LHCb shifters require a massive exchange of data between the accelerator and the experiments.

For all non-critical information, this is performed by common data exchange software [38] which is integrated into the LHCCOM system. In total, the LHCCOM system receives as input more than 20000 parameters, including LHCb experiment

conditions, LHC machine settings and safety conditions. The data exchange allows the experiment to follow closely the operation of the machine and to take actions accordingly. Alarms are associated to particular conditions which require immediate action from the shifters. Inversely, it allows the machine operators to know the states of the experiments and to improve the beam parameters. Information is shown live on web pages and can be accessed from anywhere. The information is in many cases used in feedback systems. For example, the machine control software for the luminosity optimization scans is semi-automatic and receives directly the online luminosity parameters and the profiles of the luminous region from LHCb via the LHCCOM system. Another example is the Van der Meer scans for luminosity calibration. The LHCb readout control receives real-time the scan step information via the LHCCOM system and insert the information directly in the event data bank.

For 2011, LHCb will need luminosity levelling in order to keep the instantaneous luminosity constant throughout an entire LHC fill. This will be implemented by driving machine control software for the beam separation at the LHCb interaction point based on the transmission of the current luminosity and the desired luminosity.

5.1.4 Software tools for analysis of experiment conditions

The gathering and exchange of information play an extremely important role in the framework. The data are analyzed online, processed and displayed in the LHCb control room via dedicated screens. However, in order to understand the sources of inefficiencies and to improve the beam characteristics, it is necessary to analyse the information both online and offline. Thus, data are recorded in an Experiment Conditions Archive and can be interactively analyzed offline via a dedicated Analysis Tool. Its aim is to provide graphical representations of the data and correlations. The analysis framework produces automatically the LHCb Run Summary and updates the LHCb operation web pages with luminosity and performance plots (Figure 5.4). The system generates automatically a set of files for the LHC Programme Coordinator. These files are used to correlate information between the experiments and the machine and to increase the running efficiency. A large fraction of the data is stored in the LHC Logging Database for offline analysis.

Here the developed software tools and their implementation within the Online framework for global operation and control of the LHCb experiment are briefly described.

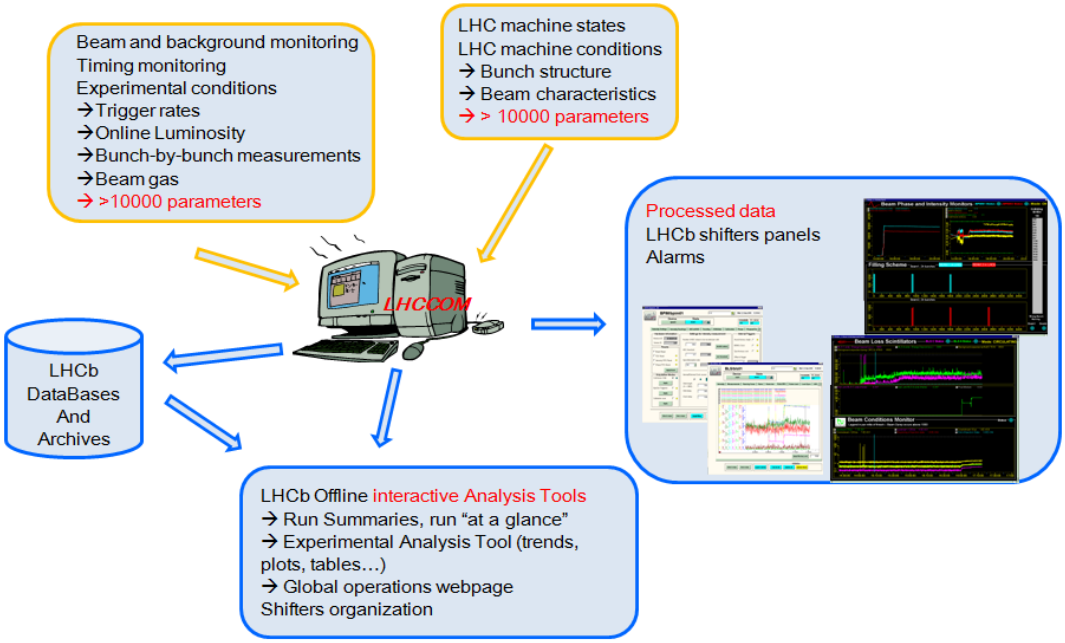

Figure 5.4: The software-based LHCCOM system is responsible to process the data coming from the LHC and the LHCb experiment. In total, more than 20000 parameters are analyzed, processed and stored. PVSS-based graphical user interface panels are used to show the process data *live* in the LHCb control room via dedicated screens. Alarms are associated in case malfunctions or bad settings are identfied. The stored data can be accessed offline via a series of dedicated software tools which are able to trend, plot and export to file the data. Also summaries per LHC fill regarding the most important experiment conditions are automatically produced.

LHCb Experimental Analysis Tool

It was mentioned before that the gathering and exchange of data play a vital role in the global operation of an experiment at the LHC. However, tools to analyze experimental conditions in a fast, reliable and flexible way are as important. It is in fact necessary to understand the source of problems or anomalies quickly and precisely. These tools are ultimately used to optimize luminosity and background. They can be used both online or offline. They should be made available for experts, but for shifters, in order to gather information quickly, and to communicate problems clearly and without ambiguities.

Within the online framework, an Experimental Analysis Tool was developed. Its a PVSS-based software tool, interfaced with the LHCb Experiment Conditions Archive. The ideas behind the development of this software tool are common to all experiments and independent from the technology used. The choice of developing

this software in PVSS was only driven by the fact that PVSS is the main technology used for the global LHCb Experiment Control System.

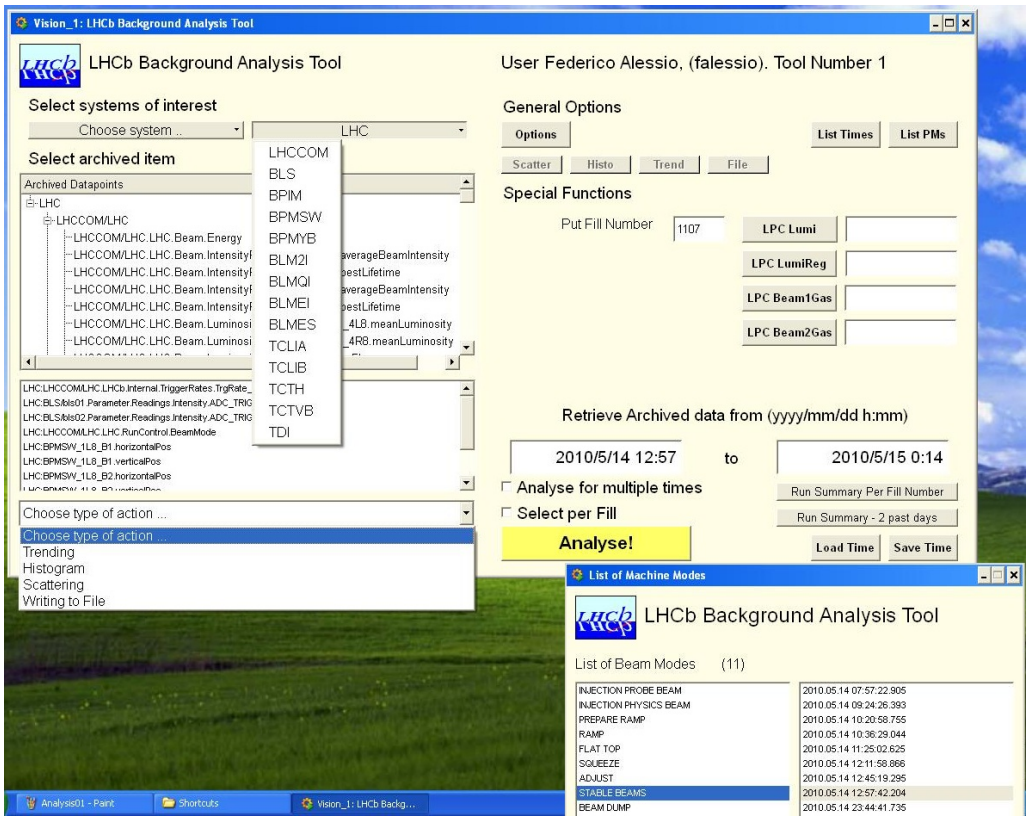

Figure 5.5: Screenshot of the LHCb Experimental Analysis Tool top panel.

Here a list of the functionalities of the developed software tool is given:

- navigate through the Archive and select what is of interest for a particular case;
- apply cuts on data and select values outside the nominal level;
- monitor particular time period, for example around an unprogrammed beam dump;
- visualize the data in trends, histograms, scatter plots or tables;
- dump data to file for offline processing, allow for print/screenshots;
- process the data and perform some preliminary statistics analysis on data, i.e. average, RMS, correlation, possibly fit;
- allow for preconfiguration for regular analysis, i.e. save and load a particular configuration for fast and quick analysis;

- reach the highest automatization by launching predefined analyses which can be applied to any set of data in order to search for anomalies or other effets.

The software was developed in few months at the beginning of 2010. The tools was extremely useful to correlate, observe, search for particular phenomena and anomalies which were reported. It has been heavily used throughout the whole 2010 data taking period and it actively helped increasing the performance of the LHCb experiment.

Figure 5.5 shows the top panel of the Analysis Tool. The interesting archived conditions can be chosen, a time interval can be specified or select according to an LHC fill number or beam mode. Each experimental conditions can be trended, put in an histogram, plotted against another condition or written to file to be exported. Expert modes menu are available, in particular the Analysis Tool is used to generate the official LHCb summary files for the LHC Programme Coordinator and the LHCb Run Summary.

LHCb Run Summary

The LHCb Experimental Analysis Tool is used to generate a complete Run Summary per LHC Fill. The idea behind a Run Summary is to gather all the most important experimental conditions and observe their variations throughout an entire LHC Fill.

The Run Summary is generated automatically by selecting an option in the LHCb Experimental Analysis Tool. The tool automatically retrieves a set of conditions from the archive during the period of a selected fill. The conditions are then organized in separate PVSS panels according to the type of condition: beam, background, luminosity, efficiency and trigger rates. These conditions are then plotted over time and they can be interactively examined by shifters or experts. Moreover, a simple dashboard table with the most important experimental conditions is automatically generated. Having all the most important information *at a glance* allows highlighting possible anomalies that can be investigated further.

Screenshots of the luminosity panel, beam panel, background panel and efficiency panel as well as the dashboard table as an output of the LHCb Run Summary software are shown in Figures 5.6 to 5.10. A recent Fill 1755 was chosen as this was a 6-hours fill where LHCb recorded data at its nominal luminosity constantly throughout the whole fill.

Figure 5.6 shows the trend of the most important parameters connected to the luminosity in LHCb. The integrated delivered and recorded luminosity are provided. Figure 5.7 shows the trend of the most important characteristics of the beam as measured by LHCb: the phase of the clock with respect to the passage of the beam, the centroids of the luminous region and the size of the luminous region are here provided. Figure 5.8 shows the most important background figures

of merit in LHCb: these are the background estimated by the BLS and BCM systems. The intensities of the beams are also shown for completeness. Figure 5.9 shows the global time and luminosity efficiencies and their breakdown according to the sources of inefficiency. In LHCb, there are four source of inefficiency: the powering of the HV, the VELO safety, the configuration of the DAQ and the deadtime. Finally, Figure 5.10 shows the simple dashboard with the most important experimental conditions per LHC fill as automatically generated by the LHCb Run Summary software.

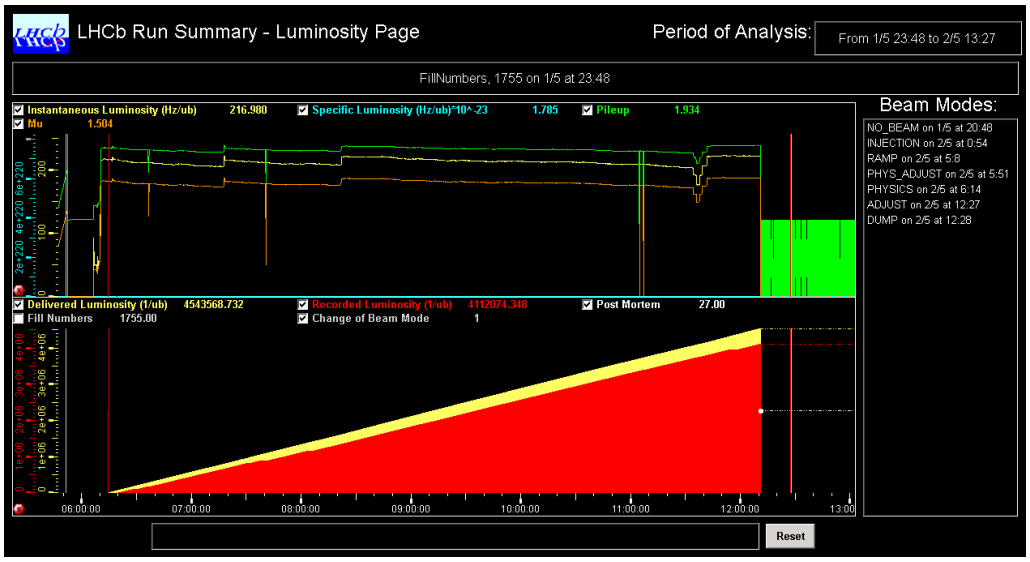

Figure 5.6: The LHCb luminosity Run Summary panel.

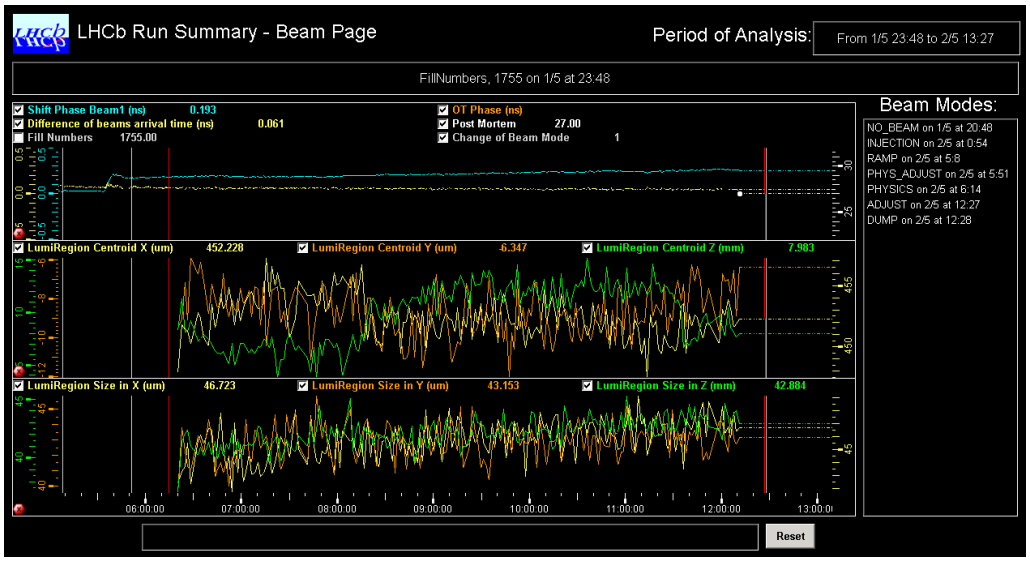

Figure 5.7: The LHCb beam Run Summary panel.

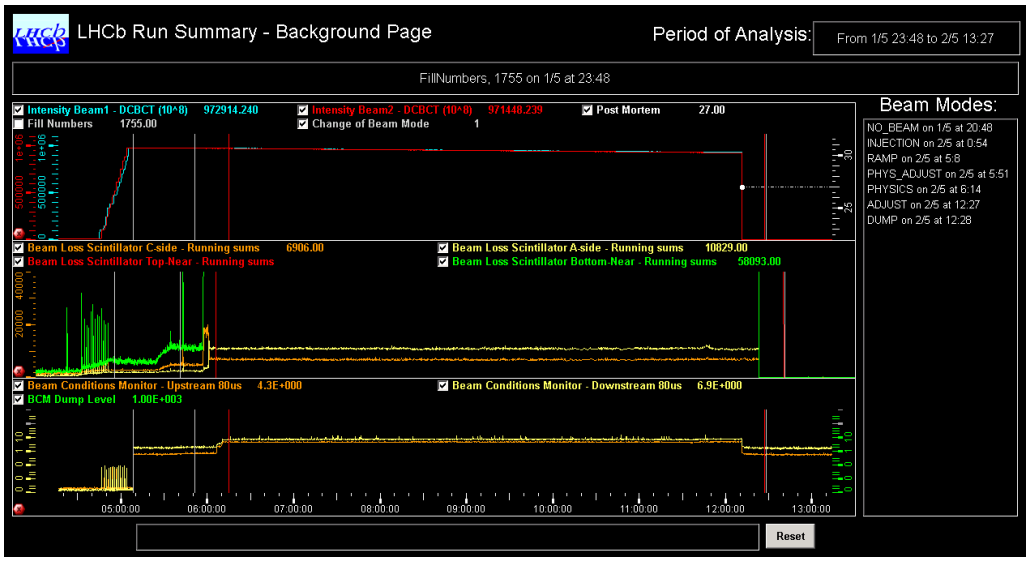

Figure 5.8: The LHCb background Run Summary panel.

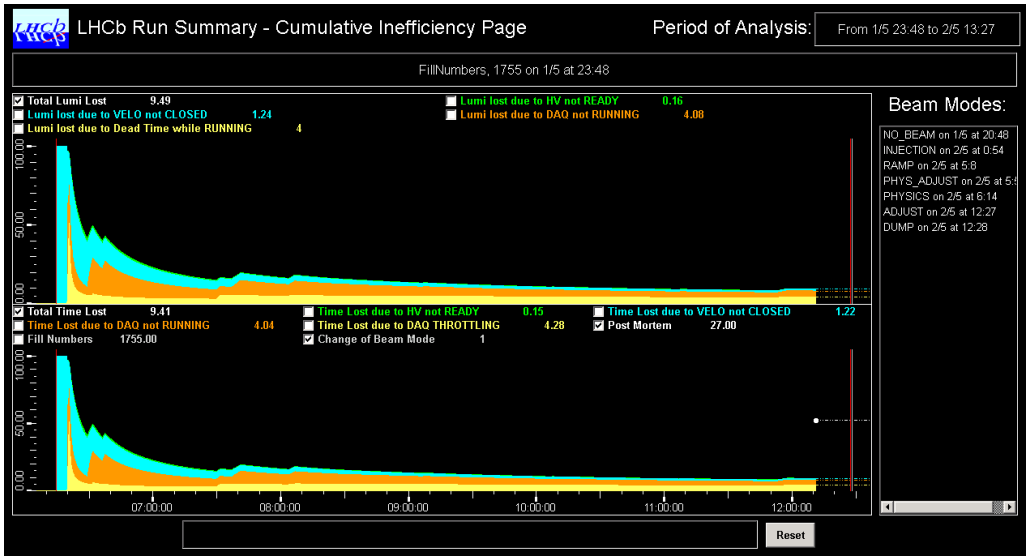

Figure 5.9: The LHCb efficiency Run Summary panel.

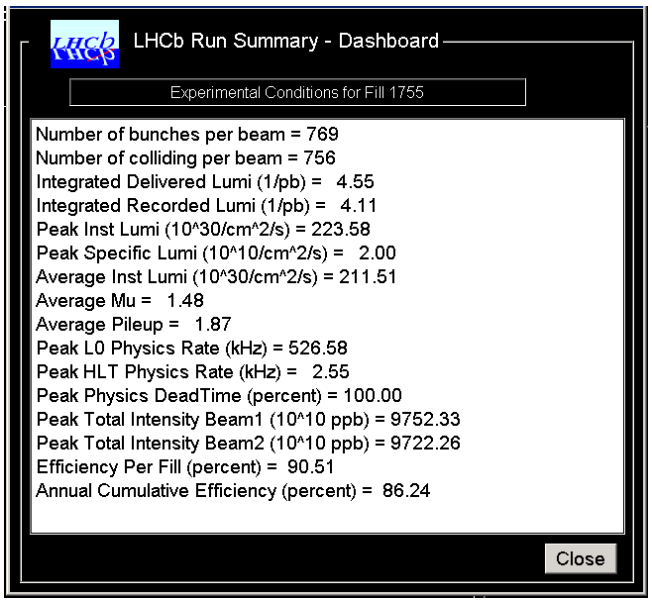

Figure 5.10: The LHCb dashboard Run Summary panel.

LPC Summary Files

At the end of each LHC Fill a set of summary files are generated and made available to the LHC Programme Coordinator. These files are used to correlate information between the experiments and the machine and ultimately increase the performace of both the machine and the detectors. The final aim is to improve the quality of the colliding beams and physics data, maximizing the integrated luminosity.

These files contains information about:

- instantaneous luminosity and specific luminosity throughout the whole fill. Statistical errors are associated to the measurement.
- luminous region centroids and sizes of the colliding beams as measured by the VELO detector. These files contain the unfolded resolution of the VELO luminous region.
- beam gas luminous region centroids and sizes of beam 1 and beam 2 as measured by the VELO detector.

These files are automatically generated via PVSS at the end of an LHC Fill. The values are retrieved from the Experiment Conditions Archive and organized in files. Automatic copy and storage of the files is performed.

Operation Webpage

The same files which are made available to the LPC are used to automatically generate plots which contain the most important experimental conditions per LHC Fill. Other conditions are automatically retrieved from the Experiment Conditions Archive and plotted:

- Average number of interactions per crossing per LHC Fill;
- Total beams intensities;
- Integrated delivered and recorded luminosity;
- Global LHCb efficiency and its breakdown;
- Bunch-by-bunch instantaneous and specific luminosity;
- Bunch-by-bunch intensity per bunch.

These plots are generated automatically via a ROOT macro at the end of an LHC Fill and made available on the web at:

https://lbweb.cern.ch/groups/online/OperationsPlots/index.htm.

These plots are shown in Chapter 5.1.2, where the global operation and efficiency of the LHCb detector are reviewed.

5.2 Integration of the software framework and boards control system in the global LHCb ECS

The online framework for machine protection, global operation and optimization of the running conditions as well as the control systems for the electronics boards for beam, background and luminosity monitoring are an integral part of the global LHCb Experiment Control System. In this section, the integration of these systems within the LHCb ECS is described.

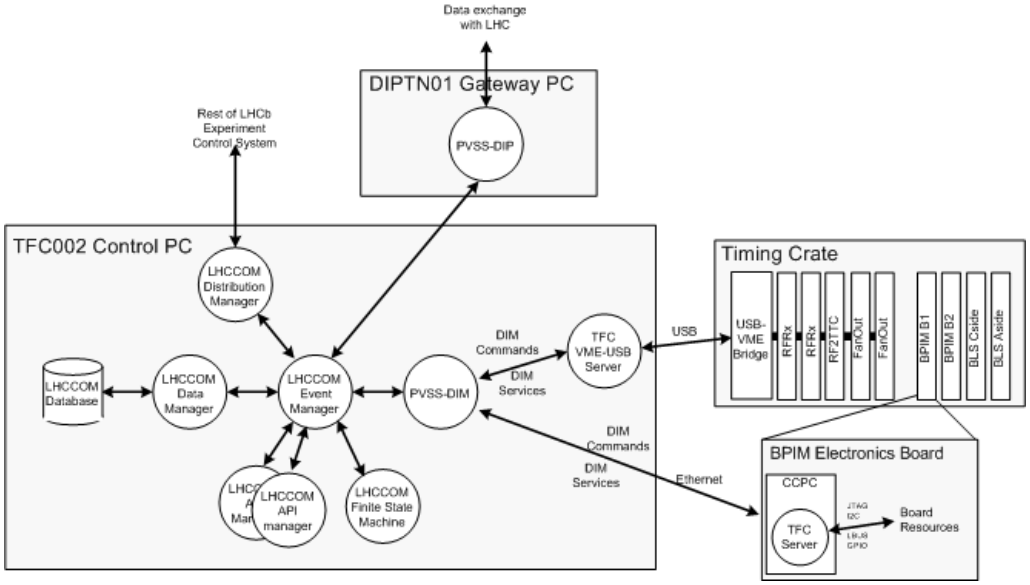

Figure 5.11: Architecture of the control system for the timing reception, the timing monitoring and the BLS readout system. The architecture shows the connection to the LHCb Experiment Control System and the data exchange servers in order to communicate with the LHC machine.

The control and monitoring of the Timing Reception electronics is performed via the VME bus by a crate controller based on the CAEN V1718 VME-USB bridge [39]. A VME/USB server written in C performs the hardware accesses to the electronics and communicates with the PVSS system using the Distributed Information Management system (DIM) [40]. This system is a communication system for distributed environments. It provides a network transparent inter-process communication layer.

The control interface of the general purpose readout boards is based on a Credit Card-sized PC [29] with Ethernet. It runs a strip-down version of Linux and performs the access to the board resources via native busses by glue logic [41]. A server based on DIM allows the PVSS system to configure and monitor the electronics. The general software architecture and communication protocol of this system is the same as that for the LHCb Timing and Fast Control and is described

in detail in [42]. The system allows generic subscription to monitoring information for continuous archiving and permanent display in the control room.

The control system LHCCOM is responsible for exchanging data with the LHC machine. This is performed via dedicated servers based on the Data Interchange Protocol (DIP) [38]. DIP is a system which allows relatively small amounts of soft real-time data to be exchanged between very loosely coupled heterogeneous systems. The LHCCOM event manager processes real-time the information from the electronics boards and from the analysis software. It archives them, transmits them to the LHC via DIP and displays them in the control rooms on dedicated fixed displays.

The LHCCOM system is part of the LHCb Finite State Machine framework allowing easy control and transmission of states and alarms to the overall LHCb Control System and to the LHCb Alarm screen. In fact, the LHCb Experiment Control System incorporates a state machine in which every device is described by a logical unit. The latter receives commands and assumes the state of the device based on a well defined set of associations. A device or a group of similar devices are controlled by a logical control unit that determines their state. This state is the reflection of the global state of all the devices below this control unit. Each control unit is part of a hierarchy of control units and ultimately receives commands from the top node either automatically or by human intervention. It is possible to exclude units corresponding to a device. In that case, the command will not reach the excluded unit, but only the included units below the top node. The association of a unit to a device allows controlling any kind of device, hardware or software.

All important monitoring parameters are logged in an online Experiment Conditions Archive together with all other running conditions. Here a list of the most important parameters which are archived and logged is given:

- LHC Machine Modes, LHC Beam Modes and LHCb State. Fill Numbers, Safe Beams Flags and Movable Devices Flags.
- LHC filling schemes, expected and measured by the BPIM system. Together with it, a computation of the number of bunches, number of colliding bunches and their spacing is performed and values are archived.
- Total beams intensity and intensities per bunch as measured by the DCBCT, FBCTs and BPIM system.
- Instantaneous delivered and recorded luminosity. Integrated delivered and recorded luminosity. Luminosity per bunch as measured by the LHCb scintillator system (BLS).
- Clock phase with respect to the passage of the beams at IP8 as measured by the BPIM system.

- Background estimation numbers as measured by the BCM and BLS sytem and transmitted to the LHC control room (namely BCKG1, BCKG2, BCKG3).
- VELO position, status of HV, status of the data taking run, status of the trigger and efficiencies (global and breakdown per system).
- run statistics: trigger rates, deadtime, throttle information, trigger configuration, load on farm nodes and on the readout network.

Summary

The availability of the listed parameters is of vital importance for the efficiency of the LHCb experiment. It was acknowledged during the 2010 physics run that the framework described in this Chapter played a central role in optimizing the LHCb experimental conditions for physics data taking, helping operating the detector with high quality and with a very high efficiency. Moreover, the processing of the exchanged data and its integration in the global LHCb Experiment Control System allows controlling a massive set of procedures and automated actions and configurations. Also the safety of the experiments depends on many of these information as explained in the previous sections.

Chapter 6

LHCb centralized readout control and its upgrade

In order to cope with the very high interaction rate of about 1 MHz, the large event size of about 60 kB/event, and the very complex detector and trigger, a centralized and highly reliable synchronous real-time readout control and event management are required [42]. The centralized readout control is performed by the LHCb Readout Supervisor, which is the heart of the Timing and Fast Control system.

The LHCb Readout Supervisor (ODIN) is interfaced with many sub-systems as graphically explained in Figure 6.1. It is interfaced to:

- the L0 Trigger from which it receives the L0 decision for each crossing. It monitors the trigger counters from the sub-detectors which participate in the first-level trigger decision;

- the Front-End electronics to which it sends synchronous and asynchronous commands, timing, clock and trigger decisions;

- the Readout Boards, to which it sends the farm destination of an event, and from which it receives a throttle trigger which is meant to pause the readout in order to cope with high processing time in the Readout Boards or high pressure on the network;

- the Event Filter Farm, via a MEP Requests mechanism. In addition, ODIN compiles and transmits to the Event Filter Farm a data bank which contains information about the identity of the event, such as the UTC timestamp, run number, event number, orbit number, crossing number, LHC crossing type, event type, trigger information etc. The data bank is appended to each event during the event building;

The Readout Supervisor produces all the special non-biased triggers in order to analyze and determine the luminosity offline, the necessary commands and triggers to monitor the long-term detector stability and ageing due to radiations.

The Readout Supervisor is directly connected to the LHC accelerator via several interfaces to receive the LHC clocks, machine timing, and the various LHC parameters. It is interfaced with the LHCb beam monitors to receive the beam current measurements per crossing. Its central position allow the system to produce efficiently and reliably the run statistics, data taking performance parameters, and the online luminosity. All these parameters can then be archived for offline analyses.

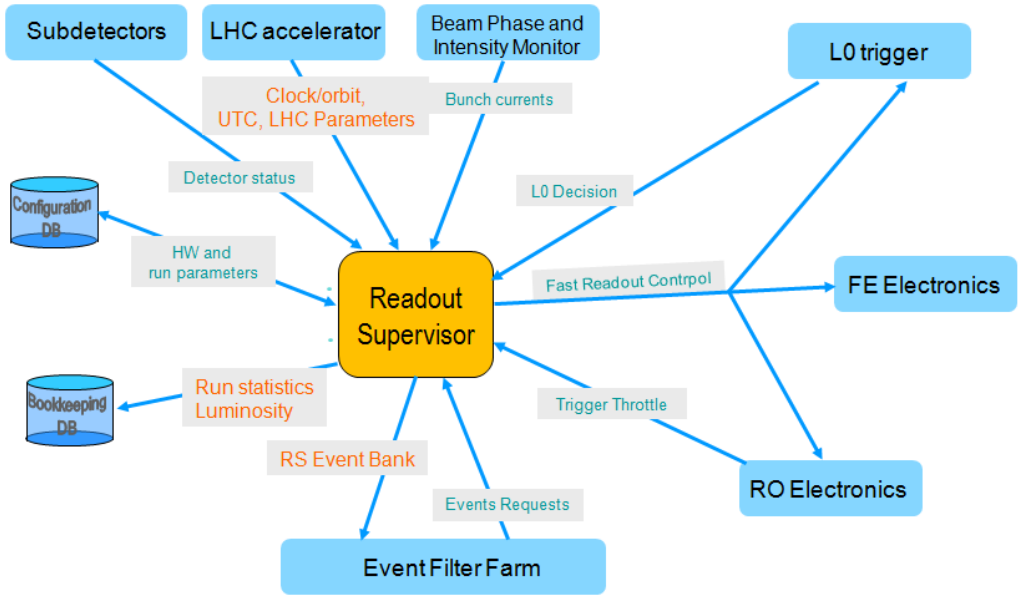

Figure 6.1: The LHCb Readout Supervisor plays a central role in the LHCb readout control. It is responsible for a multitude of functionalities such as the distribution of the timing, trigger, event destination assignment and synchronous and asynchronous commands to Front-End electronics and Readout Boards. It is interfaced to databases and the LHC accelerator to monitor the experimental conditions and to produce run statistics and online luminosity.

In this Chapter, we describe the reasons for an upgrade of the Timing and Fast Control system into the more general upgrade plan for the LHCb experiment. The new TFC system architecture is described in detail and the new electronics boards envisaged to fulfill the upgraded requirements are highlighted. Finally, a brief description of a first simulation work on the new TFC architecture will be given. It aims at showing that the system is compatible with the upgrade scenario.

6.1 An upgraded LHCb detector and readout electronics

The LHCb detector is designed to perform precise flavour physics measurements at the LHC. The first goals of LHCb can be achived by collecting about $5\,\text{fb}^{-1}$ of integrated luminosity in about five years of data taking at an average instantaneous luminosity of $2 \times 10^{32}\,\text{cm}^{-2}\,\text{s}^{-1}$. To go beyond an upgrade of the detector is required. The upgrade will allow the detector to operate at a higher average instantaneous luminosity, having a fully flexible trigger architecture. The aim is to collect about $50\,\text{fb}^{-1}$ after ten years of operation.

In reference [43] and [44], the LHCb Collaboration presented a first proposal for a possible upgrade in a shutdown period in 2017. The target luminosity is $10^{33}\,\text{cm}^{-2}\,\text{s}^{-1}$, which is five times the original design specifications. In practice, the LHCb experiment is considering an upgrade towards a *trigger-free 40 MHz complete event readout* in which the event selection will only be performed on a processing farm by a high-level software trigger with access to all detector information. A first draft of the readout electronics specifications of the upgraded LHCb experiment was published in [45].

The main reason for choosing a trigger-less architecture is due to the current trigger architecture which enriches the sample of dimuons events, but has a low efficiency for fully hadronic channels. This is because the selection of events is based on the transverse energy deposition of several GeV particles in the Calorimeter sub-detector. Any increase in luminosity would require applying harder cut reducing even more the efficiency of the hadron channels. The most efficienct way to overcome this limitation is to have the full event available at a software level. If considerable changes in the detector performance are achieved by having the full event information available, then the LHCb experiment can profit from an increase in luminosity exploiting the higher-pileup events.

Figure 6.2 shows the upgraded LHCb readout architecture as compared to the current LHCb readout architecture of Figure 2.8. The Front-End electronics will record and transmit data continuously at 40 MHz. The non-zero suppressed event size would result in a very large number of links between the Front-End and the new Readout Boards. It has been already shown that almost a factor of ten could be gained by sending zero-suppressed data. The zero-suppression would thus have to be performed in radiation-hard Front-End chips. The consequence is that the data will be transmitted asynchronously to the Readout Boards. Therefore, the data frames must include an event identifier in order to realign the event fragments in the Readout Boards. Figure 6.3 shows a logical scheme for the proposed Front-End Electronics.

Optical links based on the CERN GigaBit Transceiver (GBT [46]) are being considered for the readout between the Front-End electronics and Readout Boards. The Readout Boards will mostly act as interfaces to the event-building 16 Terabit/s

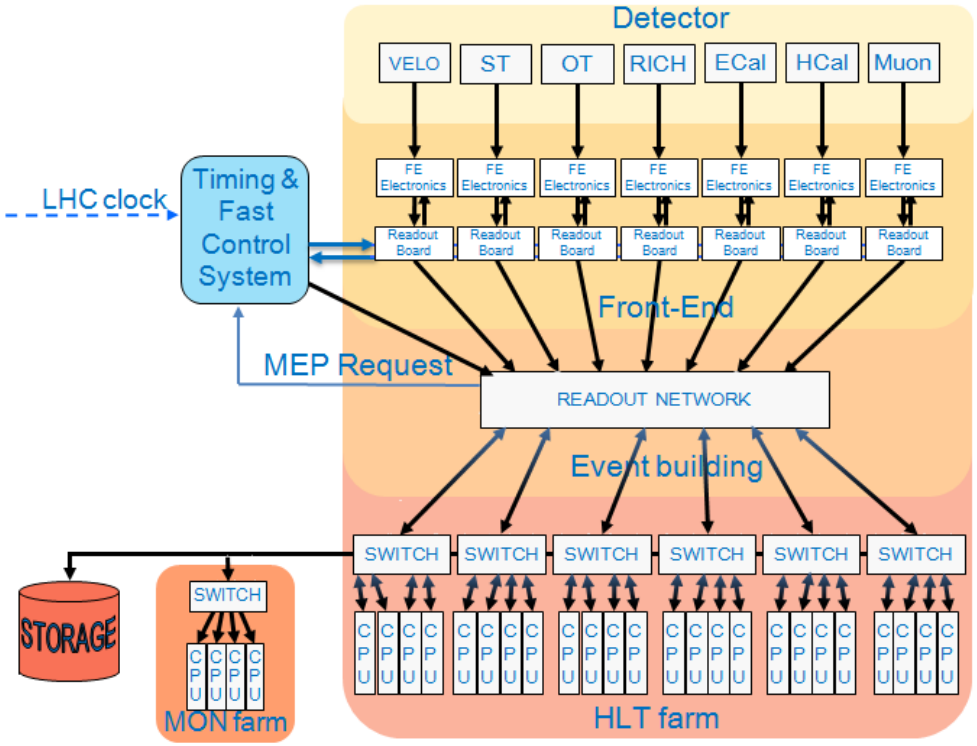

Figure 6.2: The upgraded LHCb Readout system architecture.

network based on IP-Over-InfiniBand. Events will be packed in Multi-Event Packets in order to reduce the total overhead of the event packets. The Event Filter Farm is to be based on commercial multi-cores. The only exception in the replacement is the current first-level trigger electronics which already operates at 40 MHz and which may be used to either maintain the readout rate at the current maximum of 1.1 MHz during the time the new readout electronics is being installed or at a rate between 1.1 MHz and 40 MHz if the installation of the Data Acquisition network and Farm is staged. The use of the current L0 Trigger system implies that the new TFC system will have to support the current distribution system based on the CERN TTC development [14].

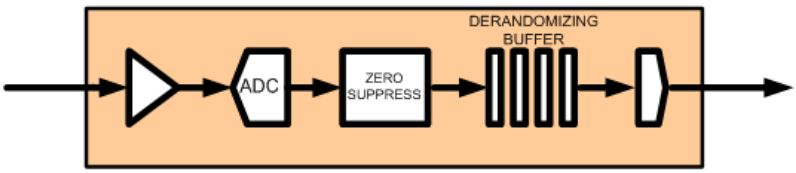

Figure 6.3: A simple drawing of a single Front-End chip architecture.

A throttle mechanism based on buffers monitoring must be envisaged. This

type of rate control is used to protect the output bandwidth of the new Readout Boards if data truncation is not desired. A throttle signal from the new Readout Boards will be sent to the new TFC system which will take care of controlling the trigger rate.

The fast timing, trigger and commands and slow configuration of the Front-End boards will be done via a Front-End interface board which will act as the unidirectional interface between the Front-End and the TFC system, and as the bidirectional interface between the Front-End and the Experiment Control System (ECS).

The experience with the current TFC system allows a critical review and inheriting features which have evolved and matured over already ten years. In the following sections, a new TFC architecture based on entirely new technologies together with an outline of the major TTC functions and their implementations are described.

6.2 Functionalities of the upgraded TFC system

In the upgraded architecture, the control will be performed by a TFC Master which on one hand will have a direct link from the LHC systems and on the other hand will distribute the LHC beam-synchronous clocks together with synchronous commands. It will transmits a rate-controlled trigger to the Front-End (here FE) and readout electronics, here Back-End or BE. The clock reception will provide means of aligning the global timing of the experiment. The TFC distribution network will transmit a clock to the readout electronics with a known and stable phase at the level of about 50 ps and very low jitter (< 10 ps). The latency of the distributed information will be fully controlled and maintaned constant. Local alignment at the FE and the BE of the individual TFC links and the synchronous reset commands together with Bunch Identifiers (BunchID) and Event Identifiers (EventID) checks will be required to assure synchronicity of the experiment.

The TFC communication network is to be bi-directional to collect input and output buffer status from the BE electronics in order to protect against overflows. The buffer information will allow controlling the rate at which events will be accepted in the BE modules.

The TFC architecture will still allow partitioning of LHCb sub-detectors. In practice this means that the system will contain a set of independent TFC Masters, each of which may be invoked for local sub-detector activities or used to run the whole of LHCb in a global data taking. The TFC Master will have interfaces to receive the *interaction triggers* for the CALO and the MUON sub-triggers. Trigger buffering will be required in order to absorb the different sub-trigger latencies, align the trigger information to the maximum latency, and perform the final trigger decision.

In addition to the dynamic rate control, the TFC Master will transmit a bunch crossing veto to the FE. This will be based on the LHC filling scheme and will allow the FE to only send event headers for crossings with no collisions in order to optimize the readout bandwidth. Exceptions to this veto will be generated by the TFC Master for calibration and monitoring purposes. The system will distribute synchronously the farm destination to the BE electronics for each crossing. This function will also include a request mechanism by which the Event Filter Farm nodes declare themselves ready to receive the next set of events for processing. The event transfer from the BE electronics will be thus a push scheme with a passive pull mechanism. The scheme avoids the risk of sending events to non-functional links or nodes, and produces a level of load balancing as well as an additional rate control in the intermediate upgrade phase with a staged farm. Ultimately this would rather be the only emergency control of the rate when the system has been fully upgraded to 40 MHz readout.

The TFC Master will have several mechanisms to generate forced trigger for calibration and detector monitoring purposes. This will include transmission of sychronous commands to generate calibration pulses, such as special data patterns, LED or laser pulses, etc. These triggers will override the collision scheme veto and the interaction trigger and may be transmitted to a special destination in the Event Filter Farm. In addition, since the proposed Front-End electronics will require performing zero-suppression by default, a scheme must be envisaged which will occasionally allow a non-zero suppressed readout for special purposes. As the bandwidth will not allow this at 40 MHz, the TFC Master intends to synchronize a sequence in which the readout of a non-zero suppressed event spans over several consecutive bunch crossings. The mechanism effectively will suppress the data of the other crossings by forcing pure header transfer via the same mechanism as the collision scheme veto.

A data bank containing information about the identity of an event (Run Number, Orbit Number, Event Number, Universal Time) and trigger source will still be transmitted by the TFC Master to the farm for each event as part of the event data. In order to save on the bandwidth out of the TFC Master, there may be a reduced bank for local sub-detector runs.

In order to replace the current readout electronics and commission the new electronics in steps, and make use of the L0 Trigger system which is already operating at 40 MHz, the new TFC system must support the old TTC system. The system must be conceived with robustness, flexibility, and with a large amount of logic resources in reserve. The system and its components must be built in a way that they can be used stand-alone in small test-benches and test-beams.

Figure 6.4 shows schematically the proposed new TFC architecture fulfilling the requirements of the upgraded LHCb Readout System. In the upgraded architecture, a pool of TFC Masters is instantiated in one single Super Readout Supervisor (*Super-ODIN*) based on a single large FPGA for all TFC functions. The link to

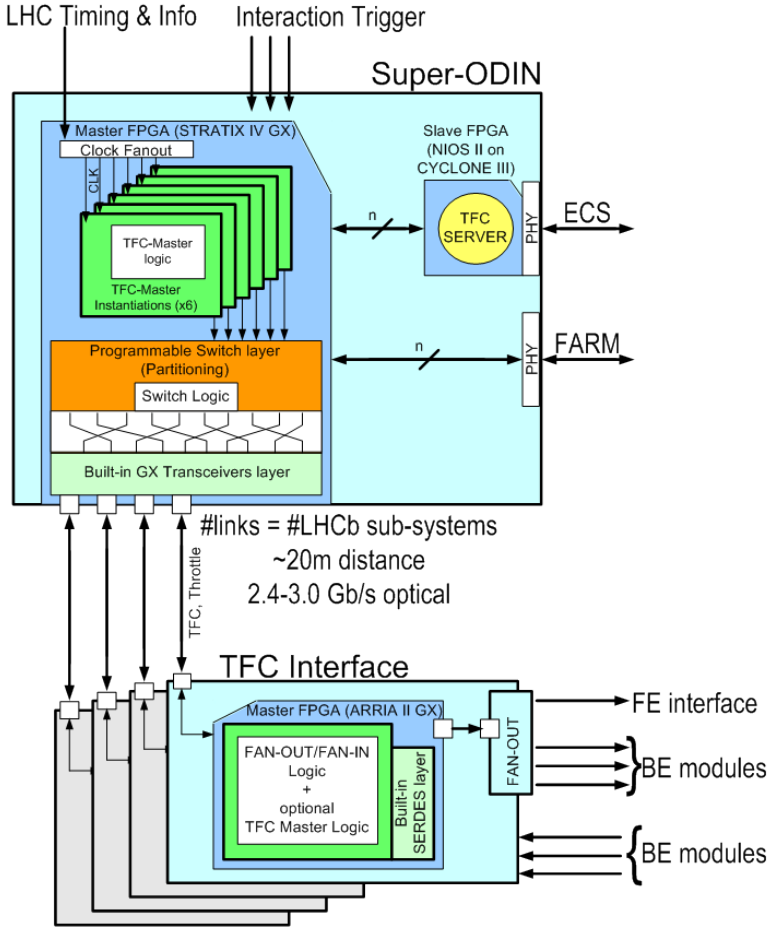

Figure 6.4: A schematic drawing of the upgraded TFC system.

the sub-detector readout electronics on the S-TFC Master consists of a set of high-speed transceivers. In order to operate the sub-detectors stand-alone in tests or calibrations, the instantiations are independent from one another, each of which contains the logic described in the requirements. A large FPGA incorporates the configurable switch fabric which allows associating any sets of sub-detectors to the different optional TFC Master Instantiations. The new S-ODIN is interfaced to the interaction trigger and the LHC interfaces.

In order to have a manageable set of transceivers on the S-ODIN, each BE crate contains a *TFC Interface* fan-out/fan-in module. Thus, each transceiver on the S-ODIN is connected via a bidirectional optical link to a TFC Interface board. Hence there are as many TFC Interfaces as there are BE crates and consequently

as many optical bidirectional TFC links and S-ODIN transceivers. As already mentioned, the FE electronics receive the ECS and the TFC information via their GBT interfaces from a dedicated interface board (FE Interface) in each BE crate. One of the outputs of the TFC Interface is dedicated to transmitting the TFC information to the FE via this interface. Thus, with 24 primary TFC links, the system would for instance support up to 24×19 BE modules. If more are required, the TFC Interface boards may be cascaded.

A TFC transceiver block in the TFC Interface Board and in the BE modules perform the clock recovery and decodes the TFC information. In the TFC Interface, the logical block relays a subset of the information onto the link dedicated to the FE electronics. In the BE modules, the TFC transceiver block transmits the throttle information over the TFC link back to the TFC Interface, which in turn builds a single frame for the entire crate to send back to the TFC Master belonging to the allocated partition.

6.2.1 Communication protocol for the upgraded TFC system

The new architecture requires defining the protocol on three internal types of links and two external seen by the sub-detectors:

1. The timing and synchronous control link between the S-ODIN and the TFC Interface.
2. The timing and synchronous control link between the TFC Interface and the FE Interface which is later transmitted together with ECS information on top of the GBT link.
3. The timing and synchronous control link between the TFC Interface and the BE Modules.
4. The throttle and trigger information link between the BE Modules and the TFC Interface.
5. The throttle and trigger information link between the TFC Interface and S-ODIN.

The following list of different types of synchronous control commands have been identified as necessary:

- Resets of bunch identifier and event number.
- Synchronous resets of readout logic.
- Bunch crossing veto to FE electronics.
- Trigger decision to BE electronics.

- Multi-Event Packet destination
- Calibration commands
- Synchronization commands for the non-zero suppressed readout mode.

The event packet destination is assumed to be communicated as the reduced set of bits out of the full destination identifier. In order to check the synchronicity, all TFC words will carry the bunch crossing identifier to which event it belongs.

It has been assumed that a word of 44 user bits per event is sufficient to encode all the synchronous control information listed above. Figure 6.5 shows a preliminary encoding of the complete TFC word transmitted by the S-ODIN to the TFC Interfaces. In order to increase the reliability, the protocol includes a scrambler to enforce DC balancing, a Reed-Solomon encoder, and bit interleaving, like the GBT protocol. The word transmission will thus be implemented in three progressive stages. The initial word is split in two words of 22 bits. The two words of 22 bits are treated in parallel. The first stage is composed of two 22-bits scramblers. The second stage is composed of one (60, 44)-Reed-Solomon encoder. The fully encoded 60-bits word is then passed through a third stage which interleaves the bits of the MSB- and the LSB-half of the word.

Encoding	43 .. 32	31 .. 16	15 ..12	11 .. 8
TFC Info	BID(11..0)	MEP Dest(15..0)	Trigger Type(3..0)	Calib Type(3..0)

7	6	5	4	3	2	1	0
Trigger	BX Veto	NZS	Data Force	BE reset	FE reset	EID reset	BID reset

Figure 6.5: Table with the preliminary encoding of a complete TFC word. This word contains the TFC information to the BE and FE electronics.

Therefore, the protocol for the synchronous control commands consists of 60-bits words per event meaning a TFC bandwidth requirement of 2.4 Gbit/s. In order to allow expansion, the design of the system will be qualified at up to 3 Gbit/s allowing user words of up to 55 bits. It should be noted that as a starting point, a single type of word is defined which encodes all the possible synchronous control information. If a packing factor (n) is defined for the transmission of the events from the BE boards to the Farm nodes, the event packet destination will only be transmitted every n events at most. In this case, the bandwidth may be exploited differently by defining several different types of words according to different future functionalities.

A link reset sequence will be defined and the latency and the phase are calibrated across the full chain. That is, all the way up to the Front-End electronics including the TFC transceiver blocks in the BE modules as well as in the FE Interface.

A decoding/encoding block in the TFC Interface is responsible to relay a subset of the synchronous control commands to the Front-End electronics, and separately to the BE modules. It should be noted that the TFC word per bunch crossing will be transmitted at a constant phase with respect to the actual crossing in such a way that the information is available at the proper time in the FE electronics. There are two consequences of this. Firstly, the information which is subsequently needed in the BE electronics must be buffered to account for the variable data processing time in the FE and the data transfer. Secondly, the interaction trigger will be transmitted together with the TFC information of a later bunch crossing at a constant offset corresponding to the maximum latency of the interaction trigger. The decoding and correction for this offset is handled by the TFC Interface.

The TFC information is merged with the ECS information in the FE Interface and transmitted via GBT links to the FE. A logical scheme on how the merging of the TFC information and the ECS information in the FE Interface should be done is described in Figure 6.6. The TFC information is packed into the GBT word at 40 MHz, while the ECS information is packed on best effort to fill up the ther 56 free bits in the GBT protocol. The ECS chain will have to implement a memory map with an internal address scheme for GBT addressing, GBT E-link addressing and bus type addressing.

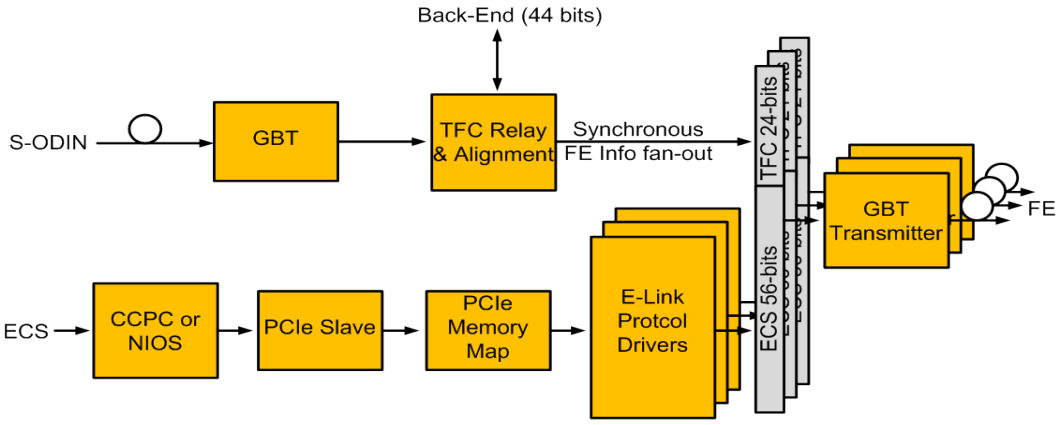

Figure 6.6: Logical scheme on how to merge the TFC information with the ECS information in the FE Interface. The ECS chain will contain a memory map to fulfill the requirements of the addressing scheme of the GBT transceiver.

A TFC word of 24 bits incorporated in the GBT protocol has been considered sufficient to encode the synchronous commands for the FE together with the bunch crossing identifier. Figure 6.7 shows the preliminary encoding of the TFC word to FE. Since the GBT protocol consists of 84 bits user words transmitted at 40 MHz, this leaves an ECS field of 60 bits towards the FE electronics which thus may be used asynchronously at a bandwidth of 2.4 Gbit/s. Four bits are dedicated to the GBT Slow Control, so the effective number of bits for ECS is 56.

The GBT chipset allows customizing the I/O buses and associating the user bits with different types of parallel and serial buses according to the needs in terms of bus width and bandwidth. The TFC word is likely to be output on three serial e-links in 8x-mode together with a constant-latency byte-alignment mechanism invoked at the TFC link reset. The e-links allow easy fan-out of the synchronous control commands to several front-end chips and simple decoding. It has to be evaluated if additional data protection is needed at this level.

Encoding	23 .. 12	11 .. 9	8 .. 5	4	3	2	1	0
TFC Info	BID(11..0)	Reserve	Calib Type(3..0)	BX Veto	NZS	Header Only	FE reset	BID reset

Figure 6.7: Table with the preliminary encoding of TFC word to be sent to the FE via the FE Interface.

Finally, the throttle and the trigger protocol basically consist of transmitting a local throttle bit together with the bunch crossing identifier of the last event. Since the system is asynchronous at this level, the bunch crossing identifier serves mainly for monitoring and additional checks. The protocol between the BE modules and the TFC Interfaces may thus be reduced to words of less than 20 user bits. Using the same encoding as described above means for instance words of 30 bits total length and thus a bandwidth of 1.2 Gbit/s allowing implementing these links with cheaper SER-DES interfaces. The task of the TFC Interfaces is to compile a single word with the trigger and throttle information from the BE modules and transmit it to the TFC Master. The transmission employs a protocol identical to that of the synchronous control commands.

6.2.2 A new TFC Master board

A single TFC Master logic block of the current TFC system is implemented in approximately 25k Altera Logical Elements divided in four FPGAs with a very high level of interconnectivity and uses in total about 2.4 MB of L2 cache-like memory for tables and intermediate data storage. About 400 functional parameters in about 100 32-bit control registers and 100 32-bit monitoring registers are accessed by the Experiment Control System. Today's technologies allow instantiating several full TFC Masters as cores of a bigger and faster FPGA. The fast built-in transceivers together with advanced data protection, DC-balancing, and clock and data recovery allow driving the TFC protocol directly from the FPGA. Based on the resource usage of the old TFC Master and the new FPGA available on the market in 2010, it has been verified that more than six TFC Masters could be instantiated together with the 24 transceivers performing the protocol described above and the bidirectional switch fabric layer between the instantiations and the transceivers to control the partitioning.

The LHC timing and the Beam Synchronous information will be directly decoded by the FPGA instead of via the current receiver ASIC (TTCrx) developed at CERN within the RD12 project. The use of the new FPGA allows adapting the new system to modifications due to future upgrades of the existing LHC distribution system.

6.2.3 A new TFC Interface board

The TFC Interface fans out the synchronous control information to a full crate of BE modules and one FE Interface, and will relay the trigger and throttle information back to S-ODIN. It thus requires a single full TFC GX transceiver for the connection with S-ODIN.

One or a few transceivers per TFC Interface would be used together with external high-speed link fan-outs rated at 3.125 Gbit/s. The throttle information will be received by the TFC Interface from each BE board via 1.6 Gbit/s links using simpler LVDS SER-DES interfaces in simplex mode. The TFC Interface will decode the information, assure the synchronicity and compile a single TFC word per event, which will be sent back to the S-ODIN.

Optionally, the TFC Interface will incorporate a single full TFC Master Instantiation identical to that of the one instantiated in the Super-ODIN. This will allow using the TFC Interface in stand-alone tests in any lab and test beam, and even at the installation of LHCb to operate the slice of a sub-system covered by a single BE crate.

6.2.4 Preliminary study on latency and phase control

It is crucial that the phase of the recovered clock and the latency of the serial data transmission are fully controllable and stable, and that they are completely reproducible each time the entire system is switched on/off. Whereas it was an obvious feature of custom-electronics developed for HEP applications, the issue is less obvious with commercial electronics. Here a proposed study which was conducted together with ALTERA [47] is presented. This study is only preliminary and will need validation on hardware.

In the upgraded scenario just described in the previous sections, the S-ODIN receives the LHC timing and distributes it to the entire readout chain. The TFC Interface recovers the clock from the serial data stream and fans-out the TFC information to the FE Interface and the BE modules. Both types of modules recover the clock from the serial data stream transmitted from the TFC Interface. The recovered clock and TFC commands must have a known phase and latency in the FE Interface in order to allow the FE to recover the clock and TFC commands via the CERN GBT chip with a known phase and latency as well.

Below follows an explanation of the investigated solution for the control of

phase and latency of the recovered clock with respect to the serial data stream with commercial electronics. At start-up, the receiver normally adjusts the bit clock automatically within the eye diagram of the bit stream, however with a certain window of uncertainty. The width of the window depends on the frequency of the bit clock and the jitter level. Considering the new TFC bit stream as 60 bits sent at a rate of 40 MHz with a very low jitter, the window interval is quantified as 200-250 ps around the centre of the eye diagram. Knowledge about the delay-step applied allows obtaining a constant fine adjustment of the bit clock. The process is illustrated in Figure 6.8.

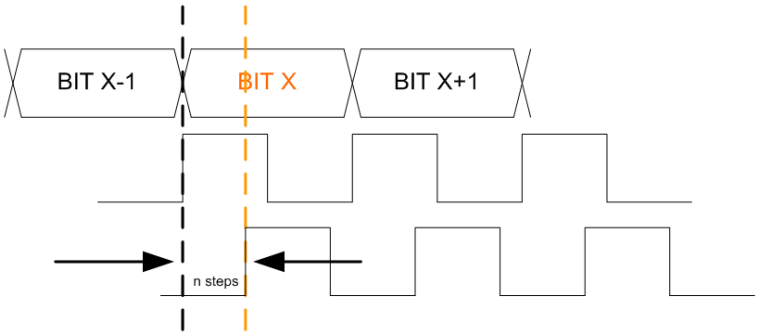

Figure 6.8: Initially the clock (middle signal) is aligned to the word data stream. However, to effectively align the clock edge to its best position with respect to the eye diagram of the data stream (top signal), the clock edge can be shifted in steps (bottom signal). Whenever the best setting is found, the number of steps (n steps) are the configurable parameter to maintain the phase constant.

The word clock is obtained by dividing the bit clock with the pre-configured word length. It will thus have the same fine phase as the bit clock. However, it will normally not be aligned with the actual word. Each Altera GX transceiver uses a Word Aligner (WA) in order to search for a particular pattern in the data stream. The WA effectively bit-slips the data stream with respect to the local word clock.

Once the data is aligned, the output clock from the receiver side is used to serialize the data in the re-transmitter side. The way to produce a constant latency and proper word clock phase is by applying a compensation mechanism on the data stream and the word clock based on the number of bit-slips. In fact, as shown in Figure 6.9, the output of the WA is used to bit-slip the data stream and the total number of bit-slips is used to shift the word clock using a built-in Enhanced Phase-Locked Loop. A FIFO is used to change clock domain for the de-serialized data.

6.2.5 Preliminary simulation work on the upgraded TFC system

A detailed simulation of the new TFC components was developed. It is fully configurable, synthesizable and it works at the clock-level. It includes an emulation

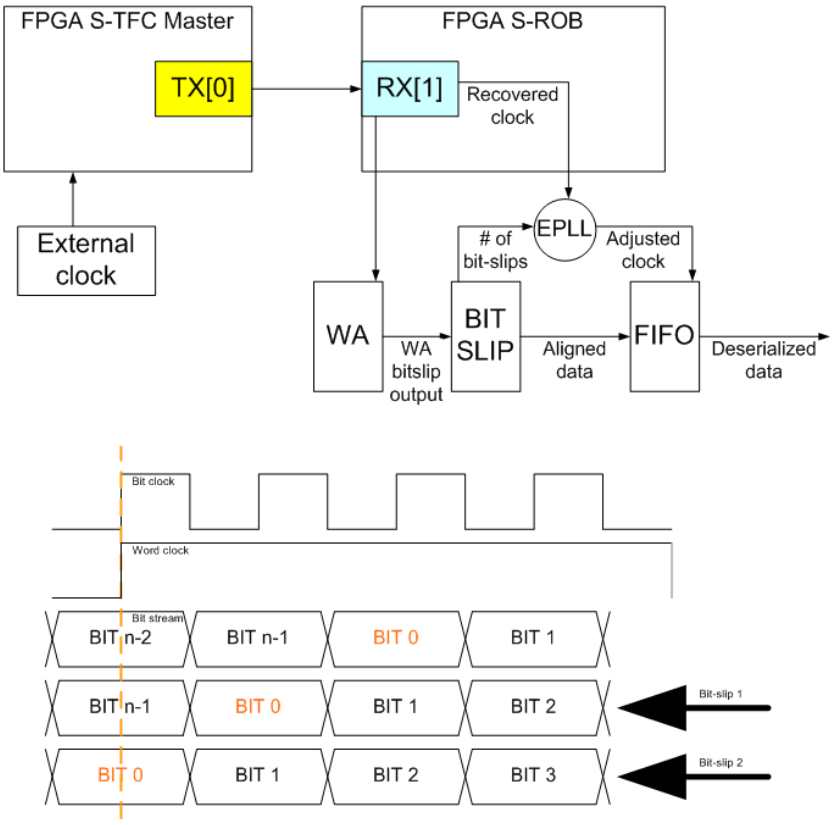

Figure 6.9: Scheme to maintain constant word latency and clock phase on a commercial optical link.

of the surrounding components such as the GBT links, the FE electronics and the BE boards. The test bench has already allowed defining the preliminary protocol for the new TFC information and has allowed developing the first version of the firmware for the S-TFC Master and the TFC Interface in their proper environment, estimating the resource usage, studying the latencies of the system, and defining the link reset sequence and timing alignment procedure.

Moreover, the development of a global common simulation framework is planned within the upgrade community of LHCb. This will allow studying and validating different sub-detector implementations of the FE electronics and eventually identifying common solutions for the FE electronics and BE. In this section, an example using the developed simulation framework is provided.

Figure 6.10 shows the single Readout slice of the upgraded system which was simulated. A single Readout slice comprises the new Readout Supervisor (S-TFC Master), a single BE and one FE board, outputting currently one GBT link. The starting point of the S-TFC Master logic is the TFC Readout Supervisor used in the current LHCb experiment. It includes modifications in the protocol, in the

reset sequence and in the links configuration. The implementation of the BE logic concentrates on the relay of the TFC commands onto the GBT link, via a S-TFC Decoder/Encoder block, and emulation of data congestion in the readout system in order to produce a trigger throttle signal.

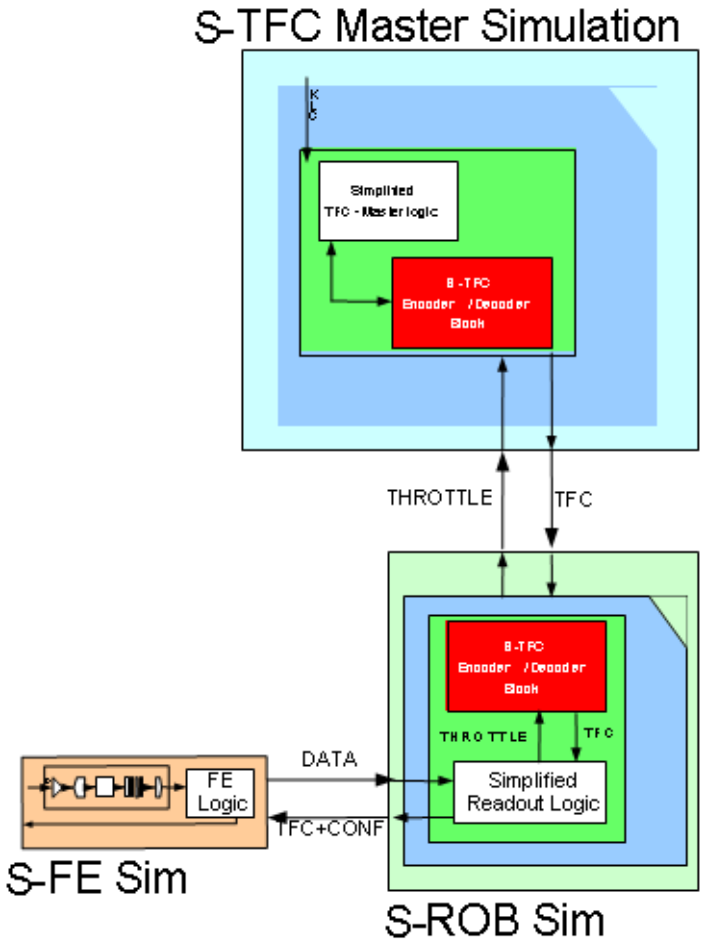

Figure 6.10: Schematic drawing of the single Readout slice as it was implemented in simulation. Each simulation block is highlighted in the drawing.

The Front-End block consists essentially of two parts. A *Data Generator* emulates the detector response, ADC and zero-suppression by producing data on a set of channels according to a Poisson distribution with a mean occupancy specific to the detector, and the LHC filling scheme. The second part implements the derandomization of the data, the packing of the data onto the GBT link, truncation handling, and emulation of the GBT link. The second part contains the decoding of the new TFC commands, and applies them to the processing of the events. Fig-

ure 6.11 shows a logical scheme of the Front-End channel as was developed for the simulation.

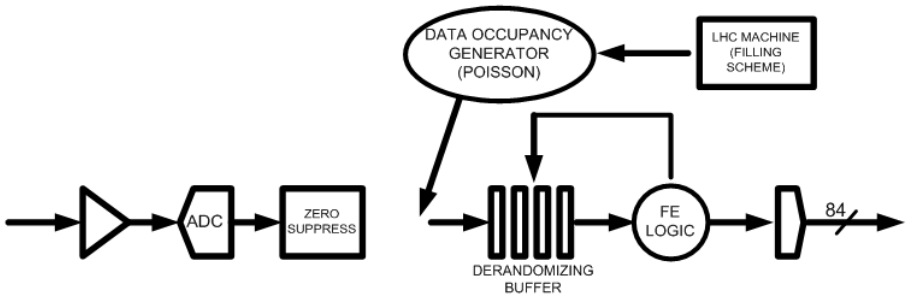

Figure 6.11: Schematic drawing of a single Front-End channel as implemented in simulation. A VHDL Poisson distribution generator generates zero-suppressed data. Data is buffered for processing and then packed onto the GBT link. The nominal LHC machine filling scheme is used in order to exploit the capability of the system during abort gaps and consecutive bunches.

The system can be customized by changing four main parameters:

- Detector mean occupancy for the data generation.
- Channel size in bits.
- Number of channels associated to a single FE board, i.e. one GBT link.
- Derandomizing buffer depth

The simulation is prepared in a way that the first part performing the data emulation may be replaced with a different data emulation and data compression to study the requirements of different sub-detectors.

In order to demonstrate the simulation Figure 6.12 shows the distribution of number of channel with zero-suppressed data generated from the Poisson distribution generator for a detector mean occupancy of 30% and 21 channels of 12-bits associated to a single GBT link. The bin of zero occupancy originates from gaps in the LHC filling scheme. Data is buffered in the 15-word deep Derandomizing buffer before being packed and sent over the link. Figure 6.12 shows the distribution of the Derandomizing buffer occupancy over almost 3 LHC turns. This particular configuration leads to a peak occupancy of 14 events implying that the truncation mechanism will strongly affect the performance of the system. The simulation shows that in this configuration, 10.5% of incoming events are truncated because of buffer overflow. With a word size of 80 bits, 80.4% of the bandwidth of the GBT link is exploited.

The link usage of the GBT link can be improved by optimizing the front-end parameters. In fact, configuring the Derandomizing buffer as 24 words-deep, sim-

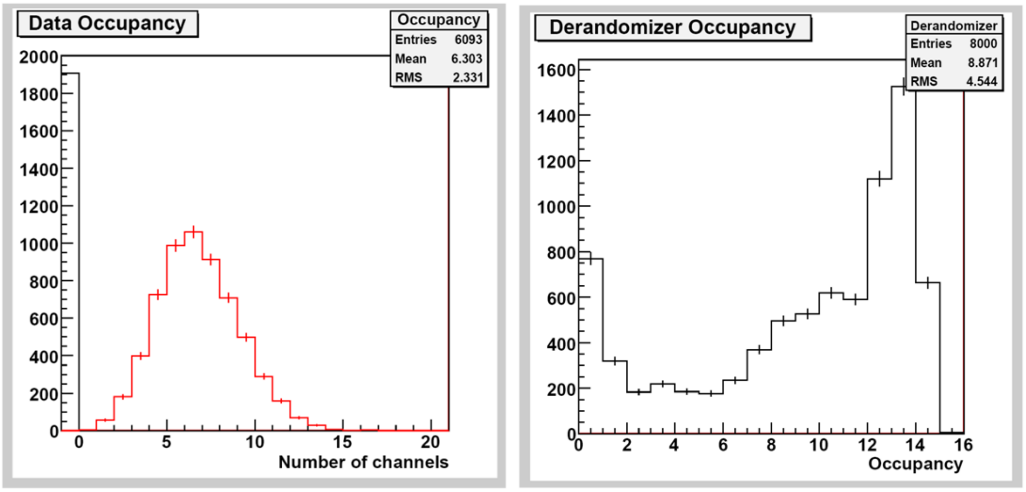

Figure 6.12: On the left, distribution of channels filled with zero-suppressed data in agreement with a Poisson distribution. On the right, distribution of the derandomizing buffer occupancy.

ulation shows that the system decreases the event loss by a factor 2, resulting in 5.4% of truncated events and a GBT link usage of 83.2%. Figure 6.13 shows the trend of the percentage of truncated events as a function of the Derandomizing buffer depth.

Summary

In this Chapter, the LHCb centralized timing, trigger and readout control system was outlined. Its connections to the other interfaces of the experiment and the accelerator were highlighted, underlining the connections to the systems described in the previous Chapters. It was shown that the advantage of having a centralized and intelligent readout control system allows for high flexibility and reliability. A proposal for an upgraded system in the framework of the upgrade of the LHCb experiment was put forward and here presented. The upgraded system relies heavily on large and modern FPGAs and serial transceiver and it is the result of the experience gained with the current working system. A first simulation attempt of the new system was shown, in order to validate the concept and frame it in the more general upgraded electronics readout system.

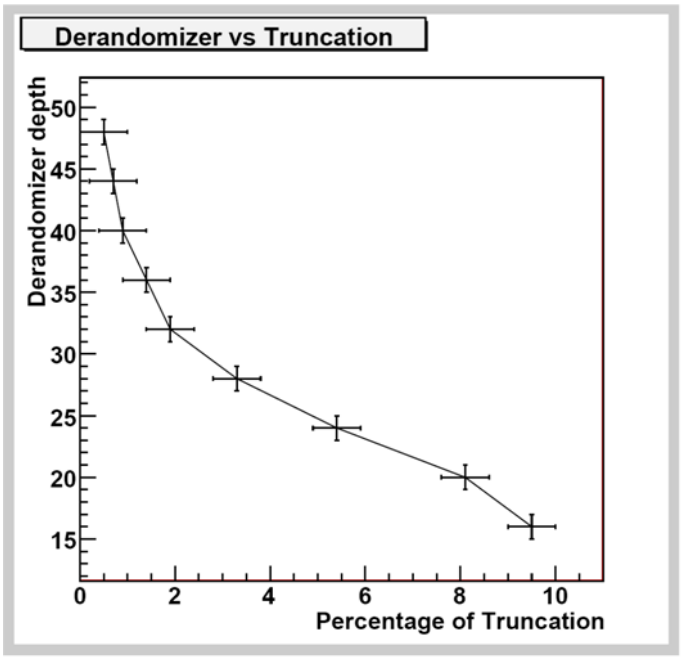

Figure 6.13: Percentage of truncated events as a function of the derandomizing buffer depth using the simulation framework.

Chapter 7

LHCb online luminosity monitors

The two main parameters characterizing the performance of a collider are its energy E and its luminosity L. During the 2010 proton-proton collision operation, the LHC accelerator operated at E = 3.5 TeV. The instantaneous luminosity L is related to the reaction rate R in Hz by the formula:

$$R\ [Hz] = L\ [cm^{-2}\, s^{-1}]\ \sigma_p\ [b] \tag{7.1}$$

where σ_p is defined as the cross-section of a particular process whose rate is defined by R. For more details, the concept of luminosity is extensively described in [48]. Here, only some of the aspects, which are required later on, are touched.

In the case of the LHC, each experiment need to measure the so called integrated luminosity, which is the integral of the instantaneous luminosity over a period of time:

$$L_{int} = \int_0^T L(t^{'})dt^{'} \tag{7.2}$$

The luminosity decays with time:

$$L(t) \rightarrow L_0 exp^{(-\frac{t}{\tau})} \tag{7.3}$$

where τ is the lifetime.

Contributions to this lifetime are from the decay of beam intensity with time, the growth of the transverse emittance and the increase of the transverse beam sizes. For simplicity reasons, the decay process of the luminosity is usually taken as an exponential behaviour. In this way, the contributions from different processes can be easily added.

The aim of the LHC is to maximize the *delivered* instantaneous and integrated luminosity by optimizing different parameters. In first instance, optimizing luminosity can be done by increasing its lifetime and by reaching the maximum

luminosity achievable with respect to the beam characteristics. However, many limitations can play a role in this regard. These limitations are strictly connected to the beam properties such as the beam size (σ_x, σ_y, σ_z), the crossing angle α, the separation between beams and various effects like beam-beam effects, tune shifts, hourglass effects and the chosen LHC filling scheme.

The mathematical combination of the mentioned effects results in the well-known expression for the luminosity of two approximated Gaussian beams colliding head-on:

$$L = \Sigma_{i=1}^{N_b} \frac{N_{i,1} N_{i,2} f_{rev}}{4\pi\sigma_x\sigma_y} \tag{7.4}$$

where $N_{i,1}$ and $N_{i,2}$ are the number of protons per colliding pair of bunches for beam 1 and beam 2 respectively, σ_x and σ_y are the beam sizes in x and y which can be defined as the standard deviations of the particles distributions over the x and y axis. The beam sizes can be defined as a function of the product of the normalized beam emittance ϵ_N and the squeezing β^*-function divided by the Lorentz factor γ:

$$\sigma_{x,y}^2 = \frac{\epsilon_N^{x,y} \beta^*}{\gamma} \tag{7.5}$$

where γ is strictly connected to the Energy at which the beams are accelerated:

$$\gamma = \frac{E}{0.938\, GeV} \tag{7.6}$$

The luminosity L is proportional to the total number of colliding bunches (N_b) in the machine and their frequency revolution around the LHC ring ($f_{rev} = 11245\,\text{Hz}$). As a general rule, to maximize the luminosity L it is desirable to have very small values for the β^*-function, for the normalized beam emittance and for the crossing angle. In addition, very high values for the number of bunches in the machine and the Energy are desired. However, limitations play a contransting role in the achievable values for the parameters just described. For example, the beam-beam effect may become worse if the β^*-function and the crossing angle are too small, and it is proportional to the number of bunches. The beam-beam effect is an effect which happens when the protons from one beam interact with the protons of the other beams while reaching the location of the interaction. The β^*-function is a function which is applied to bunches at the interaction point to squeeze the bunches transversally. The crossing angle is the effective angle at which the two beams collide at the interaction point of an experiment.

It is here important to note that the application of a crossing angle to the beams at the interaction region is to avoid unwanted collisions in the neighbouring time-space region. Figure 7.1 shows how applying a crossing angle at the IP allows separating the neighbouring bunches tansversally. Without crossing angle, the

neighbouring bunches would collide at the same time as the main colliding pair at a position shifted with respect to the nominal interaction point. This may create difficulties in reconstructing the events since particles coming from the the neighbouring collisions would travel the detector in time with the main colliding pair or they would happen in the middle of the LHCb detector. It is important to note that the crossing angle reduces the luminosity by a factor which is proportional to the angle. This is because geometrically the effective area of interaction is reduced with respect of *head-on collisions*. In LHCb, the crossing angle is applied in the horizontal plane.

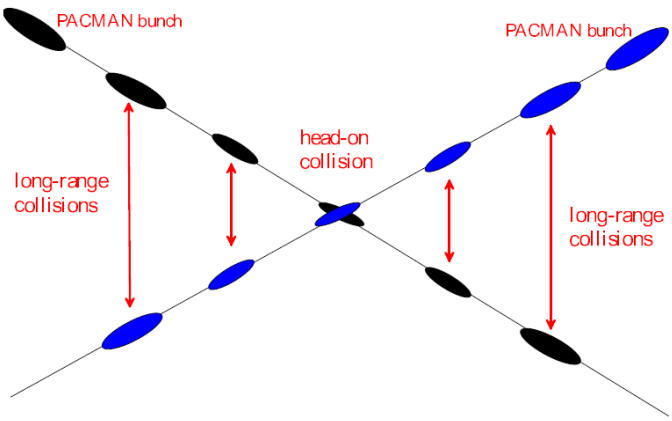

Figure 7.1: Schematic drawing of the crossing angle at the IP for a bunched beam.

The beams characteristics have to be chosen by balancing the mentioned effects and therefore they have to be monitored extremely precisely in order to understand any possible anomaly in the luminosity behaviour. At the same time, quantifying the various parameters provides an absolute luminosity measurement.

The LHC machine has developed numerous tools to monitor and measure the luminosities and beams parameters. However, luminosity calibration have become part of regular operation. These calibrations are performed together with the experiments since they depend on the beam characteristics at each interaction point. Here a brief description of the luminosity calibration methods in LHCb is given.

Two methods are used:

- the measurement of the beam size by scannning the beams. This is done via LHC wire scanners in point 4. The drawback of this method is that the beam size have to be transferred from the scanned positions to the IP loctions by means of the β^*-function. Hence, the β^*-function must be known extremely precisely.

- the calibration with the known cross section for process with small scattering

angle. This is done by LHC experiments by looking at a dedicated physics process. The main drawback of this method is that the beam currents must be known precisely in order to normalize the cross section with the intensity of each bunch in each beam.

The measurement of the intensity of each bunch is provided by the LHC Direct Current Bunch Current Transformers (DCBCT), which give the beam current per beam, and by the LHC Fast Bunch Current Transformers (FBCT), which give the current for each bunch in each beam. These systems are complemented by the BPTX systems dedicated to the experiments (Chapter 4.2.1). However, the precision response of the BPTX system is not as precise as the one from the FBCT, whose aim is to measure each bunch current to a precision level of a percent.

The intensity of each bunch is important for the estimation of the *specific luminosity*:

$$L_{spec} = \frac{\Sigma_{i=1}^{N_b} \frac{L_i}{N_{i,1} N_{i,2}}}{N_b} \tag{7.7}$$

The specific luminosity is the average of the instantaneous luminosity of each colliding pair normalized by the population of protons of each colliding pair. It gives an estimation of the luminosity independently from the currents in the beams. Therefore different LHC Fills can be compared to study possible anomalies or effects.

In the LHCb experiment, the particular physics scope and the detector shape (forward arm spectrometer) allowed the direct measurement of the cross section for luminosity measurement in two different ways:

- Beam gas imaging method [49] and [50]. The method relies on the measurement of beam gas interaction vertices for determining the individual beam shapes and the beam overlap integral.

  $$L = \Sigma_{i=0}^{N_b} N_{i,1} N_{i,2} f_{rev} \int \rho_{i,1}(x,t) \rho_{i,2}(x,t) d^3x dt \tag{7.8}$$

  The aim of the method is to measure the time-dependent bunch densities ρ_1 and ρ_2 which enters the integral of the luminosity formula for beams which do not have the same Gaussian shape. This method is unique to LHCb as it is based on the detection of beam-gas vertices. The position of the beam-gas interactions vertices can be used to determine the beam angles, profiles and relative positions by analysing offline the selected events. Therefore the trigger fires on beam interacting with the gas in the vacuum chamber.

- Van der Meer scan method [51] and [52]. This method relies on the fact that if the density distributions in the horizontal and the vertical plane are uncorrelated and stable, the effective transverse beam size can be measured

by sweeping one beam stepwise across the other while measuring the collision rate R as a function of the beam displacements. For Gaussian distributions, the luminosity L as a function of the transverse offset can be determined by another Gaussian:

$$L = L_0 exp(-\frac{\delta x}{2(\sigma_{1x}^2 + \sigma_{2x}^2)} - \frac{\delta y}{2(\sigma_{1y}^2 + \sigma_{2y}^2)}) \tag{7.9}$$

where σ_x and σ_y are the individual RMS of the beam sizes and δx and δy the transverse offsets. Ultimately, measuring the collision rate allows determining the beam sizes and hence an absolute measurement of the luminosity. In fact, the effective tansverse area A_{eff} in which the collisions take place can be rewritten as a function of the beams displacements:

$$A_{eff} = \frac{\int R_x(\delta x) d\delta x}{R_x(0)} \frac{\int R_y(\delta y) d\delta y}{R_y(0)} \tag{7.10}$$

where $R_u(\delta x)$ are the measured collision rates for a displacement in x or y and the $R_u(0)$ are the collision rates at the optimal colliding point. It is here to be noted that the cross section σ_p of a process of rate R and the effective transverse area A_{eff} are related by:

$$L = \frac{R}{\sigma_p} = \Sigma_{i=1}^{N_b} \frac{N_{i,1} N_{i,2} f_{rev}}{A_{eff}} \tag{7.11}$$

From an operational point of view, the Van der Meer scan is entirely automated between the machine and the LHCb experiment thanks to the online framework for global operation described in Chapter 5.1. The main driving force is the LHC machine, which is responsible to initiate the scan and to effectively displace the beams according to a well defined procedure. In practice, this is done by simply changing the magnetic field of the corrector magnets around the LHCb interaction region. The number of steps and the beams displacement per step are agreed upon the beginning of the scan. When the scan is started, an information via the common data exchange software [38] is received by the LHCCOM project. This information comprises the plane in which the scan is performed (Horizontal or Vertical), the step number and the beam displacement. These information are archived for offline purposes. The LHCb collision rate is transmitted to the machine for real-time feedback during the scan. Events are recorded throughout the whole scan and a step number is appended to the ODIN data bank of each event. A reduced version of the Van der Meer scan, usually referred to as *optimization scan*, is performed at the beginning of an LHC fill in order to find the best settings at which the instantaneous luminosity is maximized. The automation of such procedure allows finding the best settings in a very short amount of time minimizing global inefficiencies.

A first result was recently published [53] on the direct measurement of the total visible luminosity cross section at 3.5 TeV energy within the LHCb acceptance. This resulted to be $\sigma_P = 61.6 \pm 6.2\,\mathrm{mb}$. This measurement was obtained by an average of the beam gas imaging method and the Van der Meer scan method.

7.1 LHCb *pileup*, μ and online luminosity measurement

The LHCb experiment was built to operate at an average instantaneous luminosity of $2 \times 10^{32}\,\mathrm{cm}^{-2}\,\mathrm{s}^{-1}$ with one interaction vertex per visible event on average. In LHCb, the visible events are those proton-proton interactions which contain at least two tracks through the VELO.

Here a formulation of the pileup and *mu* with respect to luminosity is given, as they are important operational parameters of the LHCb experiment. From a statistical point of view, the number of proton-proton interaction vertices per visible event is commonly defined as *pileup* and it is strictly related to the beam characteristics. The pileup is mathematically related to the μ, which is the average number of proton-proton interactions per bunch-bunch crossing. Taking into account that the cumulative probability P of having collisions with a certain number (n) of proton-proton interactions follows the Poisson law, we have:

$$P(n) = \exp^{-\mu} \frac{\mu^n}{n!} \tag{7.12}$$

and the pileup is defined as follows:

$$pileup = \frac{\Sigma_{n=1}^{\infty} \frac{n\mu^n \exp^{-\mu}}{n!}}{\Sigma_{n=1}^{\infty} \frac{\mu^n \exp^{-\mu}}{n!}} = \frac{\mu}{1 - \exp^{-\mu}} \tag{7.13}$$

The *visible fraction* of events is 1-P_0 :

$$P_0 = \exp^{(-\mu)} = \frac{f_{rev} * N_b - R_{bb}}{f_{rev} * N_b} \tag{7.14}$$

where P_0 is defined as the probability of having an event with a pileup = 0 or *non-visible* event and R_{bb} is the bunch-bunch crossing rate with at least one interaction. For example, for $\mu = 1$, the visible fraction of events is 63%. These events will contain a poissonian ditribution of number of vertices: 37% of events will contain 1 vertex, 18% of events will contain 2 vertices, 6% of events will contain 3 vertices, etc. Hence, μ is:

$$\mu = -lnP_0 = -ln(1 - \frac{R_{bb}}{f_{rev} * N_b}) \tag{7.15}$$

The *visible rate* of events at the LHC is therefore $\mu\,\mathrm{f}_{rev}\,\mathrm{N}_b$, where $\mathrm{f}_{rev} = 11.245\,\mathrm{kHz}$ and N_b is the number of colliding bunches:

$$R_{pp} = pileup * R_{bb} = \mu * f_{rev} * N_b \tag{7.16}$$

Therefore, the online instantaneous luminosity formula becomes:

$$L = \frac{R_{pp}}{\sigma_p} = \frac{pileup * R_{bb}}{\sigma_p} \tag{7.17}$$

It is here important to note that there is no mathematical relation between the instantaneous luminosity and μ or pileup. This is because the two parameters only depend on the characteristics of the beams and on the parameters described in the previous section.

In order to evaluate the μ in a given period of time during an LHC Fill it is enough to observe the *non-prescaled MinimumBias LHCb L0 Trigger rate* from the Calorimeter sub-detector and apply the Eq. 7.15. A measurement of the instantaneous luminosity can be obtained by correcting the non-prescaled L0 Trigger rate R_{bb} with the pileup obtained from Eq. 7.13 and by applying Eq. 7.16 to Eq. 7.17.

Finally, the cross section is corrected for the efficiency of the MinimumBias (MB) LHCb L0 Trigger, which was initially estimated via simulation in MonteCarlo and set to 90%.

The online estimation of luminosity at LHCb it is possible thanks to the central role of the LHCb Readout Supervisor, which is able to collect all the trigger rates information and produce run statistics online.

Complete tables of values of μ and pileup at LHCb is given in reference [54].

7.2 Independent source of relative instantaneous luminosity measurement

In order to have redundancy in the online estimation of the LHCb instantaneous luminosity, the LHCb scintillator system is used. It was shown in Chapter 4.1.1 that the scintillator system is highly sensitive to very low angle scattering particles because of its position just around the beam pipe. However, the scintillator system can only provide a relative online estimation of the luminosity since no absolute luminosity calibration was ever attempted in simulation.

The calibration of the system is done online, by simply evaluating the acceptance of the scintillator system with respect to the acceptance of the LHCb detector. A correction factor c is applied to the luminosity formula for the scintillator system:

$$L_{BLS} = \frac{R_{BLS} * pileup_{BLS} * c}{\sigma_p} \tag{7.18}$$

where R_{BLS} is the trigger rate as measured by the scintillator system gated in the colliding crossing. A study on the acceptance of the scintillator system is given in Chapter 8.7.

The advantage of having a redundant system for the online estimation is that whenever the LHCb detector is not ready to record physics data during the *stable beams* period, the instantaneous luminosity is given by the scintillator system. Reasons by which the LHCb detector maybe not be ready to take data are mostly due to reconfiguration of some electronics in the detector that lost synchronization or communication, reconfiguration of some farm nodes or change of trigger configuration. If some of this reconfiguration have to be done while the LHC is performing the optimization scans at the beginning of the physics period of an LHC Fill, having redundancy allows the LHC machine to perform the optimization scans even though the LHCb detector is not ready to take data. The luminosity estimation in this case is provided by the scintillator system.

The scintillator system is the only system in LHCb which provided online bunch-by-bunch luminosity measurement during the 2010 physics data taking. This was achieved by programming the FPGA with a 2808-words deep memory and gating the trigger rates with each of the colliding bunches. In fact, loading the LHC filling scheme automatically in the FPGA code via the online framework for global operation allows the FPGA code to associate a particular trigger to a specific bunch crossing. Plots of the luminosity bunch-by-bunch can be found in the LHCb Operation Webpage for all the LHC physics fill during 2010. An example of an analysis of the luminosities bunch-by-bunch provided by the scintillator system is given in Chapter 8.8.

Summary

In this Chapter, an overview of the main luminosity parameters and calibration methods was given. Particular attention was directed to those figure of merits which are used later on and to a newly independent source of relative luminosity measurement in LHCb.

Chapter 8

Analysis results

In the previous Chapters, the motivations, architecture and implementation of a full system for beam, background, luminosity monitoring and global operation of the LHCb detector were given. A first implementation was already ready at the beginning of the proton collision runs in 2010. However, the question for improved monitoring of beam, background and luminosity pushed new implementations and upgrades of the system during the whole year. At the time of publishing the thesis, the system was mature and complete. The full system showed good performance and heavily contributed in the commissioning the LHCb detector. Many analyses were requested by the LHC machine in order to understand new or undesired effects, in particular in the region around the LHCb experimental site.

In this Chapter and in the following sections, examples of analyses performed with the use of the described system are presented. Only selected topics are shown here, with the intention of demonstrating the high performance of the system and presenting results which were taken into account in order to improve the performance of the LHCb detector and the LHC machine. These analyses are finalized and are based on data taken during the first year of proton collisions at 7 TeV centre-of-mass at the LHC.

8.1 Study of the beam injection dynamics in LHCb

The LHCb detector is located near the injection line of beam 2. This has some operational consequences, mostly due to the high level of particles showers which may occur whenever the proton bunches are injected in the LHC accelerator. A quest for discovering the origin of this phenomenon was performed using the LHCb scintillator system and the Beam Conditions Monitors together with information from the machine. The system helped the LHC machine to commission the LHC elements around the injection region and find the best settings which minimize the particles showers at injection.

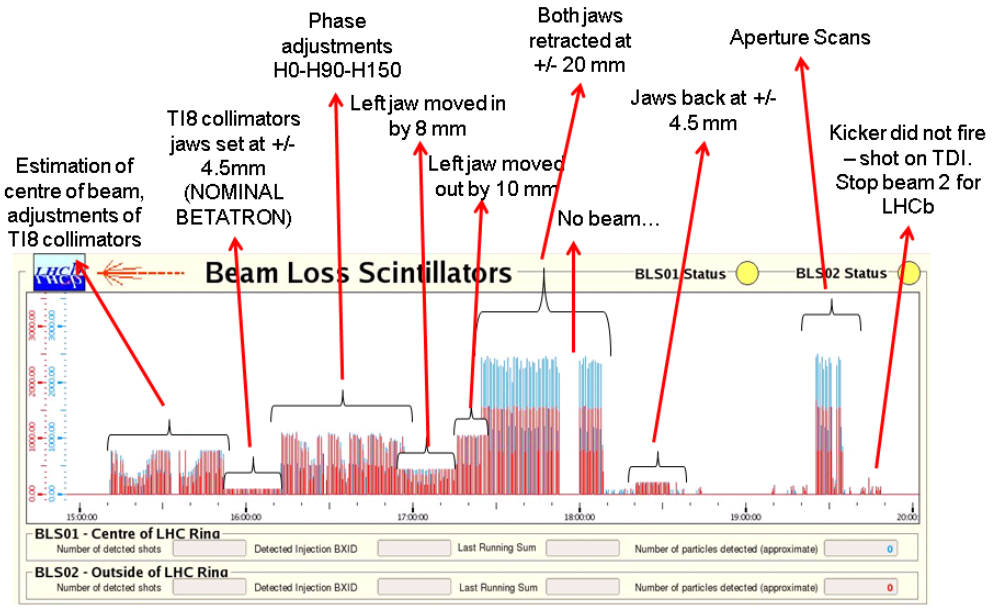

Figure 8.1: Graphical description of the commissioning of the injection collimators near LHCb. In blue, BLS01 or BLS C-side which is located towards the centre of the ring. In red, BLS02 or BLS A-side which is located towards the outside of the ring. The flux of particles losses changed according to different setting of the TDI collimators. Moreover, it was confirmed that losses in the C-side are much worse than losses on the A-side for geometrical reasons.

A first test was performed in October 2009, during the machine commissioning period. The test aimed at finding the best settings for the TDI collimators with the use of the scintillator system. It was an opportunity to commission the scintillator system as it had just been installed. Figure 8.1 shows graphically the various steps of the commissioning of the settings of the TDI jaws. Each spike corresponds to a loss measured by the scintillator system. The whole test gave a clear indication of which settings could be used to minimize beam losses around the LHCb detector.

The LHCb scintillator system is composed of two scintillators located in the horizontal plane around the beam pipe, *BLS01* or *BLS C-side* and *BLS02* or *BLS A-side*. From the experiment point of view, C-side is towards the centre of the LHC ring, while A-side is towards the outside of the ring. From the loss pattern, it can be concluded that the losses at injection were worse in the C-side with respect to the A-side. This was expected as it is due to the geometrical tilt of the injection line of beam 2.

The same test was useful to correlate the dynamic range of the scintillator system with respect to the Beam Condition Monitors system (BCM). In fact, the BCM system is meant to protect the LHCb experiment by dumping the beams whenever losses are measured above a set of well defined thresholds. The BCM system is therefore less sensitive to beam halo, but more sensitive to big fluxes of particles. The scintillator system instead is be able to record fast losses and give an estimate of the halo of the beams. Figure 8.2 shows well the correlation between the two systems. It shows that the BLS system is more sensitive to particles fluxes than the BCM. The BLS scintillators in fact saturate when the particle fluxes reach about 30% of threshold level in the BCM system. The BCM system is instead insensitive to small fluxes of particles, whereas the BLS system detects them. Different voltage settings can be used in the scintillator system for the injection phase and the circulating phase of an LHC fill in order to adapt the dynamic range to the expected flux of particles.

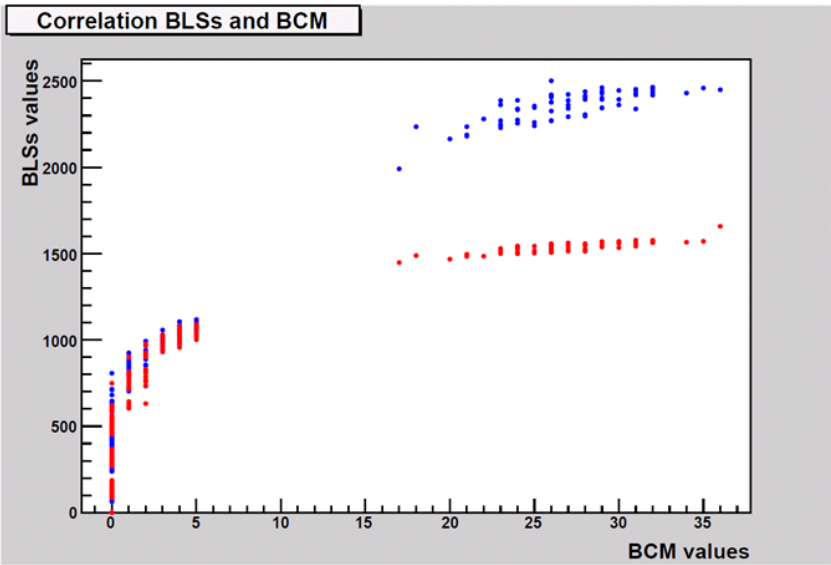

Figure 8.2: Correlation plot between the BCM system and the two scintillators of the BLS system. Data is taken from the commissioning of the injection collimator test. BLSs values are in arbitray units, BCM values are in percent of threshold. In blue, BLS C-side. In red, BLS A-side.

Later during the year, another set of tests was performed in order to investigate the origin of big fluxes of particles which were seen during the injection of many trains of bunches from the SPS to the LHC. Figure 8.3 shows graphically a typical pattern of beam losses whenever beam 2 was injected in the machine. Every time an injection of bunches or trains of bunches was performed, losses were seen in the scintillator system. Worse losses are still seen towards the centre of the ring - in the Figure in blue, BLS01 or BLS C-side.

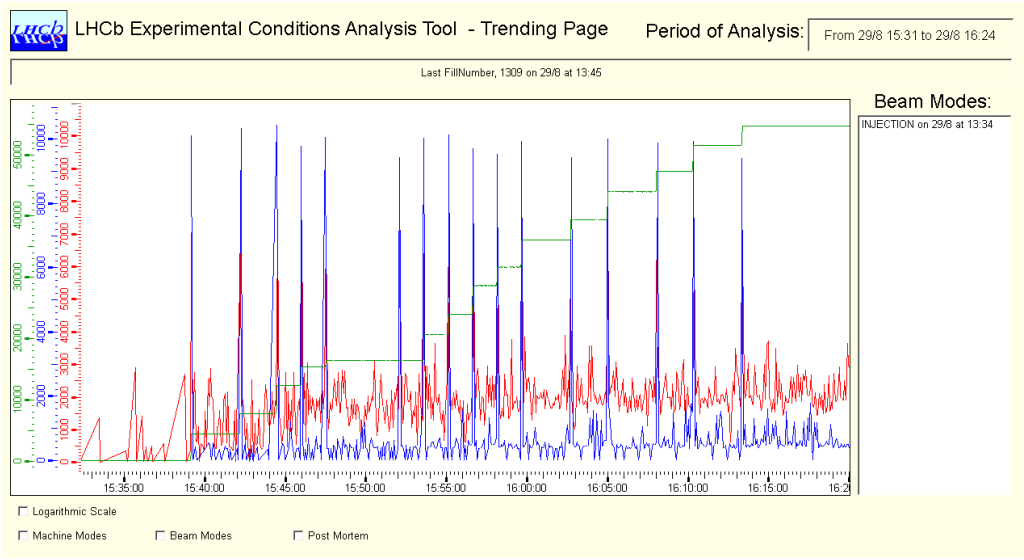

Figure 8.3: Graphical example of beam losses around the LHCb experimental area whenever beam 2 is injected in the machine. In green, the intensity of the beam is shown. Each time a new bunch or train of bunches is injected, a step in the total beam intensity is clearly visible. The scale for beam intensity is 10^8 ppb. In blue, BLS C-side and red, BLS A-side. The scale is in arbitray units.

It was possible to understand the main cause of these losses by correlating the bunch crossing information from the BLS system and the information from the machine. It was noted that the worst losses seen by the BLS system were consistently about 700 ns in advance with respect to the expected bunch crossing which was effectively injected. Other losses of lower intensity were seen about 100 ns in advance and 9 μs after the first bunch in a train of successfully injected bunches. This information was precise enough to understand that the losses were synchronized with the injection pulse of the MKI kicker. The MKI kicker is a magnet whose purposes are to deflect the beam of protons into the LHC accelerator from the injection line and to sweep a pilot bunch whenever a high intensity batch of bunches is injected. The functioning of the MKI is described in Fig. 8.4. In order to do so, a 7.85 μs long pulse is applied to the kicker, excluding rising and falling time. This pulse must be synchronized to the bunch crossing of the first bunch in the injected train. The length of the pulse corresponds to the maximum

time interval in which bunches can be injected. Bunches of protons which are outside this time interval are swept against the TDI collimators in order to avoid the particles to shower the LHCb detector and the triplet magnets around the injection region. Instead, particles that are within the rising and falling time of this pulse are grazed against the jaws of TDI and the effect is a particles shower that can reach the LHCb experimental area.

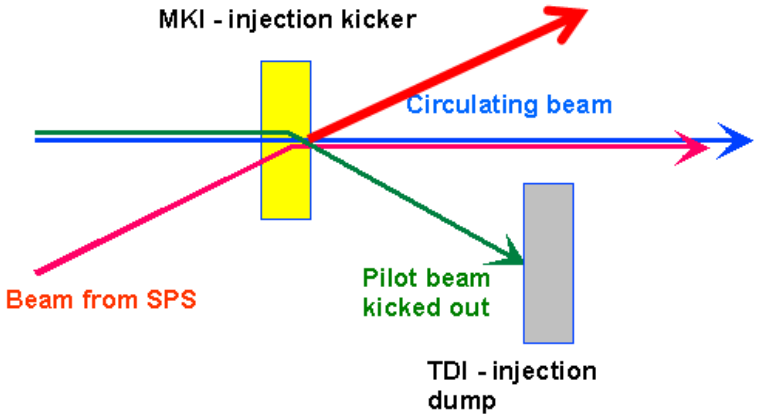

Figure 8.4: Graphical explanation of the functioning of the MKI. Whenever a high intensity beam is injected in the machine, the pilot is swept against the lower jaw of the TDI. The upper jaw of the TDI is used to protect the experiment in case of malfuctioning of the MKI.

Figure 8.5 shows graphically the MKI pulse with the corresponding losses seen by the BLS system. All the losses corresponds to the grazing of particles lying in the rising or falling edge of the MKI pulse. After an accurate analysis of the bunch crossing information it was concluded that:

- losses at -700 ns were due to uncaptured beam (de-bunched beam or ghosts) which is already in the machine at the time of the injection of new bunches.
- losses at -100 ns were due to satellite bunches generated already in the SPS and grazed against the TDI by the rising edge of the MKI pulse.
- losses at $+9\,\mu$s were due to satellite bunches generated already in the SPS and grazed against the TDI by the falling edge of the MKI pulse.

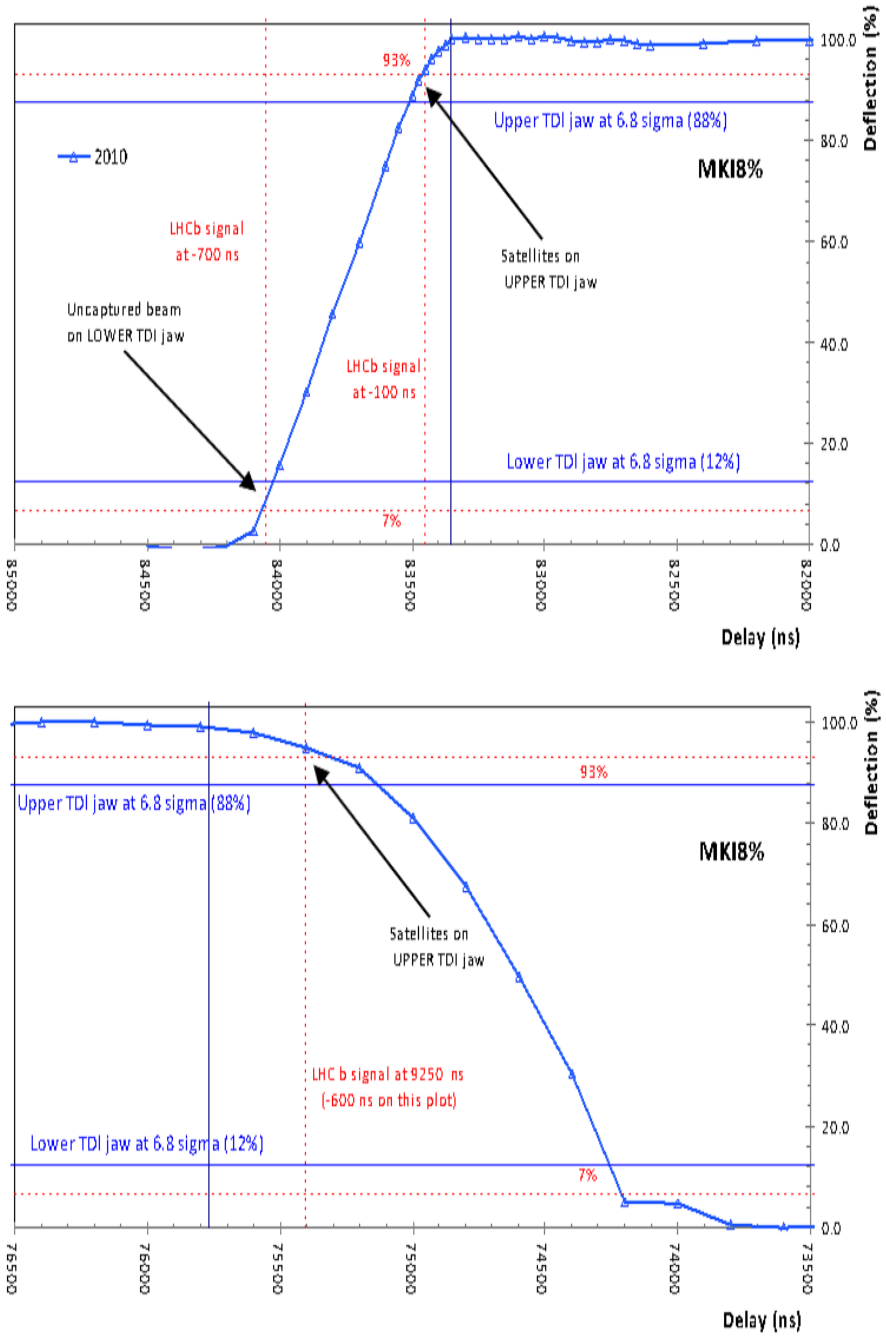

Figure 8.5: Graphical explanation of the losses seen at LHCb due to ghosts or satellite which are grazed against the TDI by the MKI pulse. *Courtesy B. Goddard, BE department.*

8.2 Vacuum test at LHCb during lead ions fills

During the month of November 2010, the LHC proton physics programme was taken over by the LHC lead ions physics programme. For the type of physics studying with heavy ions, the LHCb experiment did not participate in the programme. However, the beam and background monitors were kept on, mostly for safety reasons and for particular requested tests.

One of these tests was performed between the LHC Fills 1534 and 1535. The pressure of the vacuum of the VELO detector were changed and the beam-gas rates from lead ions beams were monitored with the LHCb scintillator system (BLS, Chapter 4.1.1). The final aim is to observe quantitatively the effect of the VELO vacuum pressure on the beams by comparing beam gas rates between two Fills.

The VELO vacuum pumps were turned off after Fill 1534 and the pressure changed from 1×10^{-9} mbar to around 7×10^{-9} mbar and remained stable during Fill 1535. Beam gas rates were monitored with the two scintillators of the BLS system. Figure 8.6 shows the trend of the test over time. Four Fills are plotted for completeness (1532, 1533, 1534 and 1535 from left to right), but only the last two are taken into account for the analysis in this section. It is already qualitatively clear from the trend how the increase in the pressure degrades the characteristics of the gas around the LHCb interaction region.

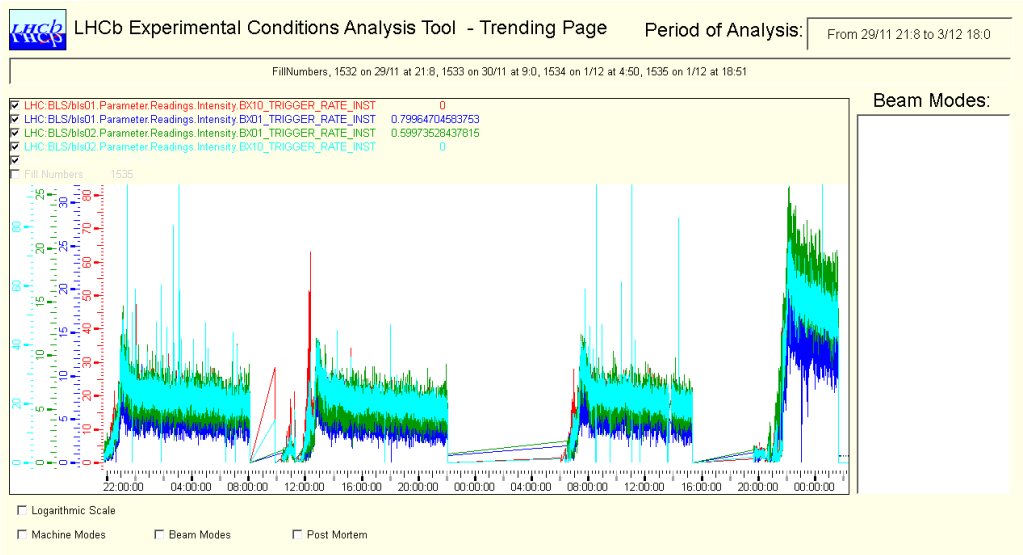

Figure 8.6: Trend of beam gas rates as seen by the BLS system during Fills 1532, 1533, 1534 and 1535 from left to right. The trend was generated with the Experimental Conditions Analysis Tool described in Chapter 5.1.4.

In order to have a quantitative measurement of the beam gas rates, only the

period between the *FLAT TOP* and *DUMP* beam modes was considered. The beam gas rates are then plotted for the two scintillators and for the two fills. Moreover, the beam gas rates were normalized to the total intensity of the beams, since between different LHC Fills the total current can change and therefore can affect the observed rates. A linear fit is applied to the normalized plots, obtaining the tilt parameter (p1) of the linear fit and the interception (p0) with the y-axis. Finally, the ratio between the p1 parameters between two different fills for the same scintillator gives the quantitative degradation of beam characteristics. This is done for both beams.

The plots are shown in Figure 8.7 for the BLS located in the C-side of the beam pipe and in Figure 8.8 for the BLS located in the A-side. Some observations can be done. The linear fits on normalized beam gas rates are flat within errors. However, a slight difference between the non-normalized beam gas rates and the normalized ones can be observed. This is due to the degradation of the beam currents throughout the length of an LHC Fill. Normalizing the data with the beams currents allows having a measurement which is independent from the degradation of the beam currents.

Moreover, the beam gas rates for beam 1 and beam 2 are different by a factor 3. This is explained in the Chapter 4.1.2 and it is only due to the timing of the beams with respect to the main clock.

Ultimately, four ratio are then found. Errors are quadratically calculated.

$$ratio_{Cside}^{Beam1} = \frac{p1^{1535}}{p1^{1534}} = 2.76 \pm 0.20 \qquad ratio_{Cside}^{Beam2} = \frac{p1^{1535}}{p1^{1534}} = 2.73 \pm 0.11 \quad (8.1)$$

$$ratio_{Aside}^{Beam1} = \frac{p1^{1535}}{p1^{1534}} = 2.85 \pm 0.20 \qquad ratio_{Aside}^{Beam2} = \frac{p1^{1535}}{p1^{1534}} = 2.51 \pm 0.11 \quad (8.2)$$

The beam gas rates increased by a factor 2.7 in average with a change of pressure of about 7×10^{-9} mbar. This information will be taken in consideration for the proton running in 2011/2012 and a similar test will have to be performed in case degradation of beam gas rates will be observed.

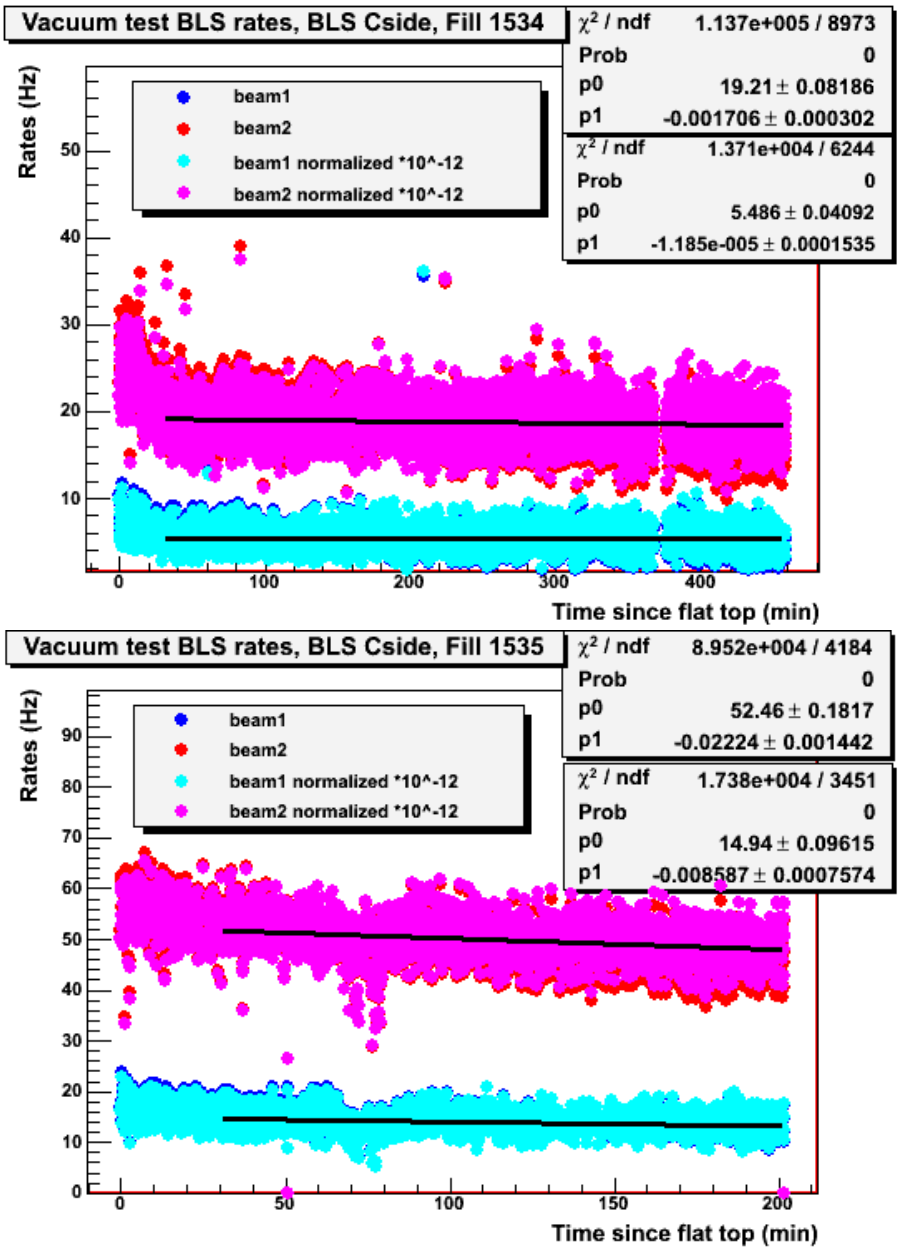

Figure 8.7: Plots for the BLS scintillator located on the C-side for Fills 1534 and 1535. Beam gas rates for each beam, in blue for beam 1 and red for beam2, and normalized beam gas rates to the total beams currents, in cyan for beam 1 and magenta for beam2, are plotted. The tilt (p1) of the linear fit shows how the normalized rates were constant throughout the whole fill.

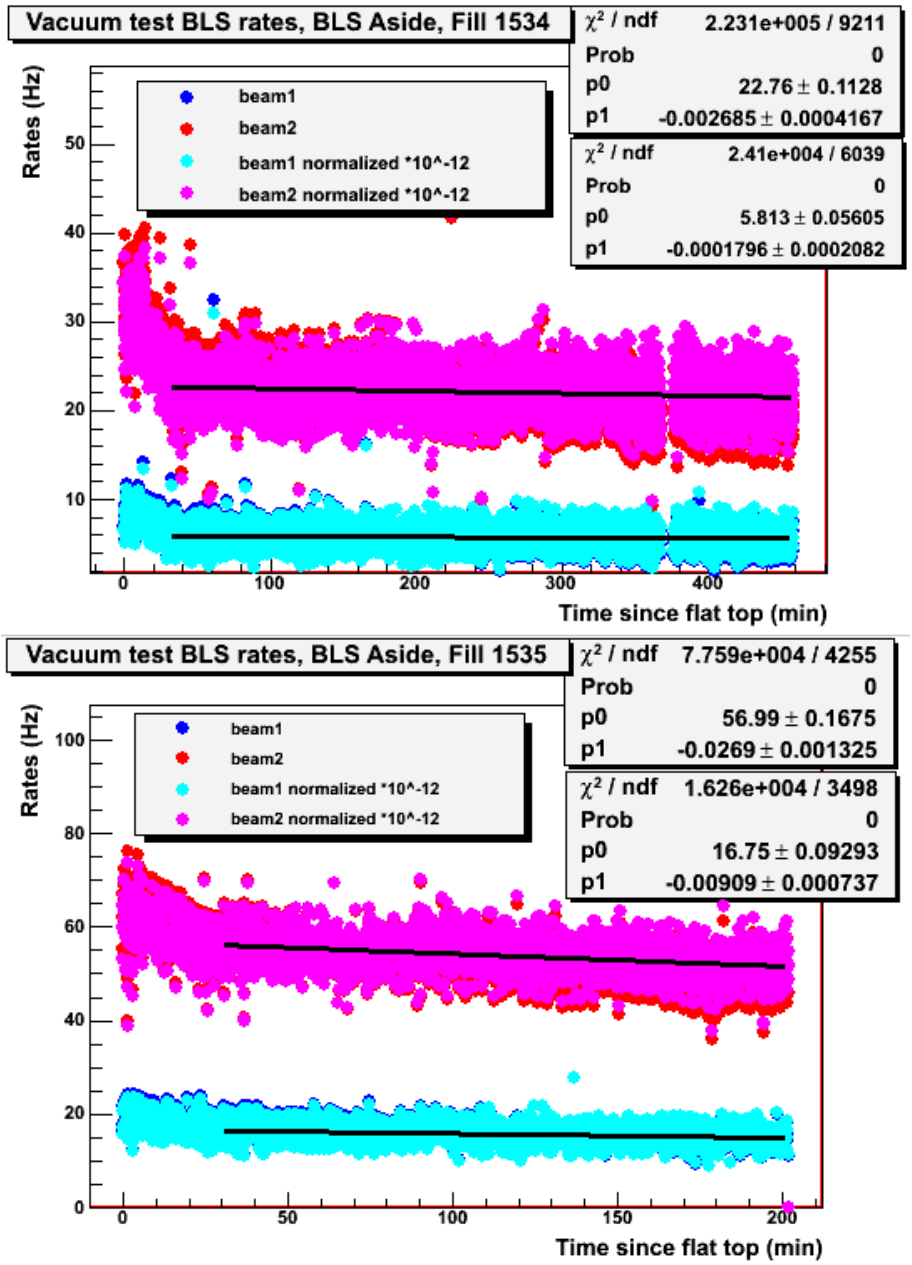

Figure 8.8: Plots for the BLS scintillator located on the A-side for Fills 1534 and 1535. The color coding is the same as in Figure 8.7.

8.3 Beam Intensity calibration with the LHCb general purpose electronics boards

In order to calibrate the measurement of the intensity of the beams with the BPIM system and correct for any non-linearity, measurements were first performed with only the BPIM readout board in the lab using a very fast signal generator. The input pulse generated by the signal generator had the same shape as the pulse generated by the BPTX during the passage of the beam, and the phase of the pulse was set up in order to perform the integration of the pulse in the exact same conditions as during normal beam operation. A calibration curve of the area of the pulse measured in V × ns using an oscilloscope was plotted against the raw ADC values and fitted, as shown in Figure 8.9. The fit was made with a third-order polynomial.

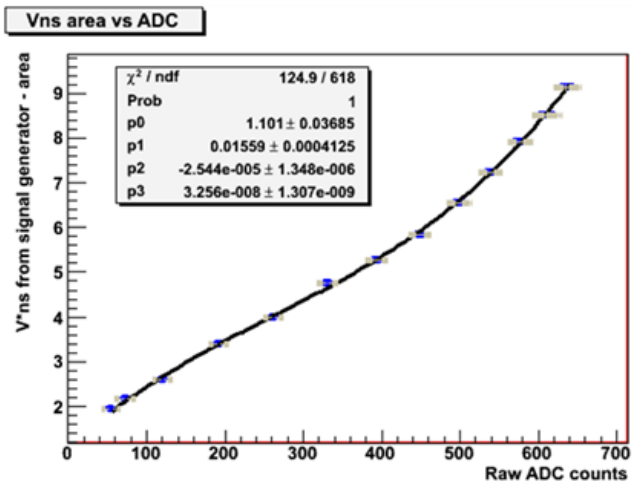

Figure 8.9: Calibration plot for the measurement of the intensity performed with a signal generator.

Also, a fudge factor was determined in order to convert the corrected ADC counts to a proper measurement of the bunch and beam intensities expressed in protons per bunch. This was performed in Fill 1250 by comparing with the LHC Direct Current Bunch Current Transformers which provide continuous measurements of the total beam intensities. Figure 8.10 shows the intensities measured by the DCBCT for beam 1 and beam 2 as a function of the BPIM ADC counts. The plots were fitted with the calibration curve of the integrator circuit in order to obtain the global conversion factor to intensity. The dynamic range of the ADC results in an intrinsic resolution of 1.8×10^8 pppb/ADC count for BPIM1 and 3.5×10^8 ppb/ADC count for BPIM2. As the baseline subtraction is about 20 ADC counts, the minimum intensity which can be measured by the BPIM is about 4×10^9 ppb for beam 1 and about 6×10^9 ppb for beam 2.

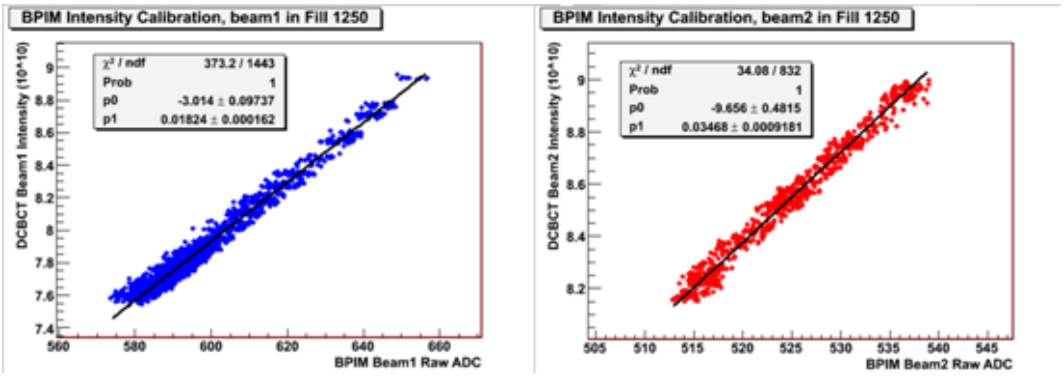

Figure 8.10: Determination of the conversion factors for the intensity measurement of beam 1 and beam 2 using a linear approximation of the integration circuit.

It should be noted that the understanding and calibration of the DCBCT evolved during 2010 and that the calibration is in progress. Nevertheless, in order to get an indication of the error on intensity measurement, Figure 8.10 shows the spread of the measurements around the fitted values. The error is therefore about 1.6×10^7 ppb for beam 1 and 9.2×10^7 ppb for beam 2.

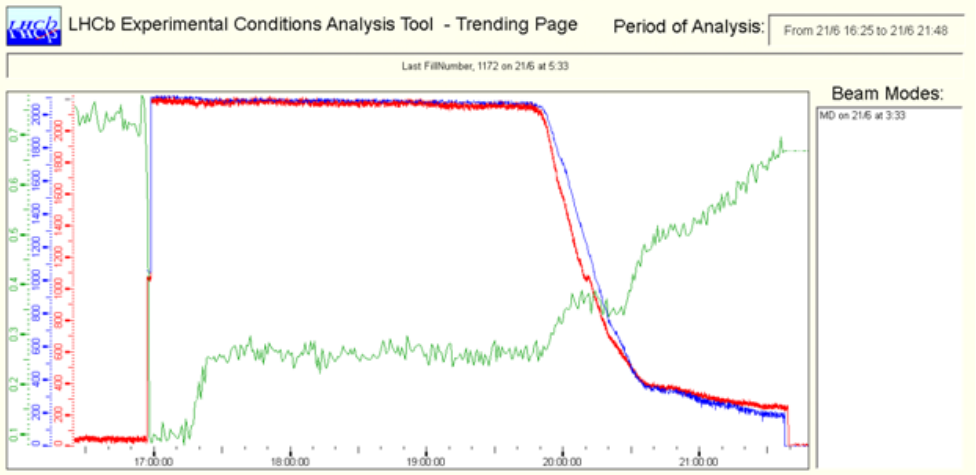

Figure 8.11: Trend of the phase measurement during a scraping test by the LHC from 1.1×10^{11} ppb down to 2.2×10^{10} ppb. From top to bottom: beam 1 intensity as measured by the LHC DCBCT. Beam 1 intensity as measured by the LHCb BPIM (blue). Beam 1 phase with respect to clock edge as measured by the LHCb BPIM (green).

During Fill 1172, the LHC machine performed a test in which beam 1, containing two bunches, was scraped from a high intensity of about 1.1×10^{11} protons per bunch to a low intensity of about 2.2×10^{10} protons per bunch. Figure 8.11 shows

the trends of the raw intensity values. This provided an opportunity to check the linearity correction over a wide range of intensities and check the assumption that the energy of the bipolar pulse of the BPTX pickups is directly proportional to the bunch intensity.

The intensity conversion function obtained from the data in Figure 8.9 and Figure 8.10 was used to correct the data obtained with the BPIMs during the scraping test, and check how well the correction apply to the BPIM data. In Figure 8.12, the intensity measurement from the LHCb BPIM for beam 1 is plotted against the intensity measurement from the LHC DCBCT. The corrected data with the conversion function are also compared to the non-corrected data, i.e. the raw BPIM data from the scraping test. The corrected data are finally fitted with a linear function to show how that the slope is almost unitary and the offset is almost zero. This confirms that the calibration curve can be used to correct real data and obtain a linear relation between the LHC measurement and the LHCb measurement.

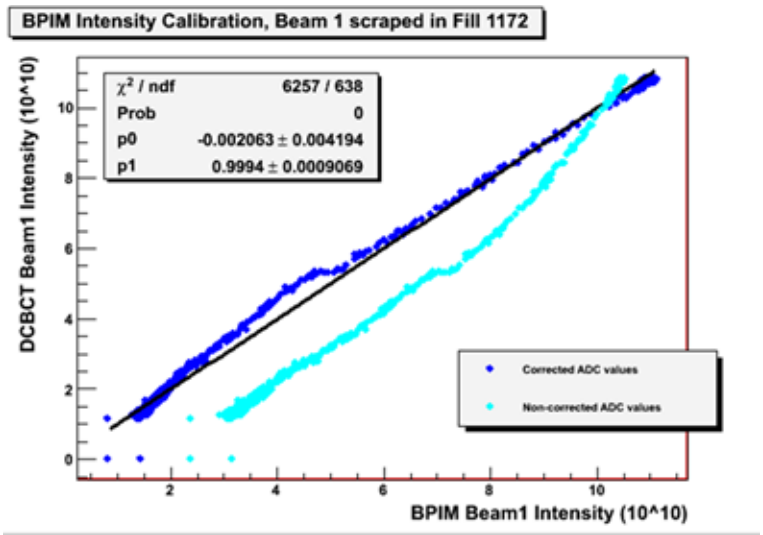

Figure 8.12: The corrected data (dark blue) with the calibration curve is compared to a linear fit and to the non-corrected data (light blue). The non-linearity improves with the correction factors, even though some non-linearity is still present.

It is however important to note that even though the calibration curve applied to data improves drastically the intensity relation, some non-linearity is still clearly visible. Also a jump is present during which the DCBCTs detected no change in intensity while the BPIMs did. To a large extent these effects are attributed to a change in the bunch shape and to de-bunching which takes place during the beam scraping. The effect of changes in bunch length on the pick-up signal is shown in Figure 4.9. An effect is visible in the phase measurements at this point.

8.4 Commissioning of the LHCb timing monitoring system with first 3.5TeV colliding beams

The commissioning of the full LHCb timing monitoring system has been performed during the first month of operation at the LHC with beams at 3.5 TeV, between the 30 March and the 7 of May 2010. During this period the phase of the beams with respect to the clock edge as measured by the BPIMs-BPTX were compared to the drift time in the LHCb Outer Tracker detector and to three stations of the LHCb Muon detector. Figure 8.13 shows the trend over the considered period, where outliers due to calibration runs are removed and where the measurements were normalized to the initial phase at the 30 March. On 7 of May, the global LHCb clock was shifted back by 2.5 ns in order to re-centre the sampling point of the detector.

In the plot, a discrepancy between the BPIM system and the timing of the Outer Tracker and Muon stations is observed. This is due to internal time alignment of the LHCb sub-detector which was performed during a Technical fill dedicated to this purpose.

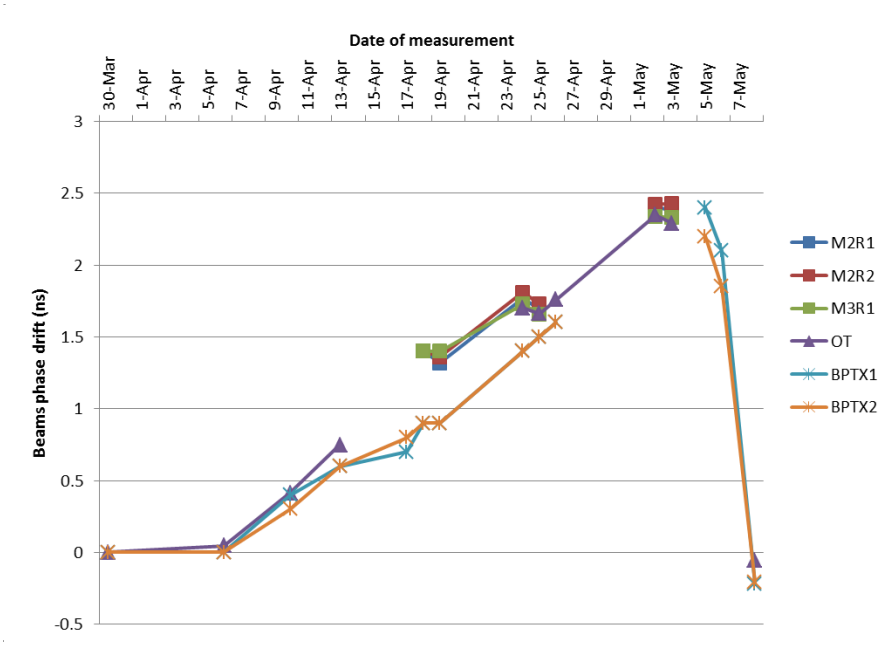

Figure 8.13: Trend of the clock phase drift as measured by the BPIM, the LHCb Outer Tracker and the Muon Chambers. At the end of the commissioning phase, the global LHCb clock was shifted back by 2.5 ns via the RF2TTC clock receiver card.

The commissioning test together with the LHCb detector proved the good performance of the system. It proved that the system can be used reliably to

monitor the global timing of the LHCb detector with respect to time arrival of each beam at the LHCb interaction region. The advantage of having a completely independent system allows for quick monitoring and control of the global time alignment of the detector during physics fills.

8.5 Clock phase drift evolution

The phase of the bunches in each beam with respect to the clock edge varies with the outdoor temperature. Fill 1222 allowed quantifying the drift as it lasted for more than 11h and there was a strong temperature change in the morning. The calculated ΔT was stable and no particular beam losses were observed meaning that the shift was entirely due to temperature drifts. Figure 8.14 shows the comparison between the measured zero-shift phases and the temperature during the *Stable beam* period. The temperature went from 20 °C to about 28 °C in 5 hours and the phases shifted by about 100 ps during the same interval.

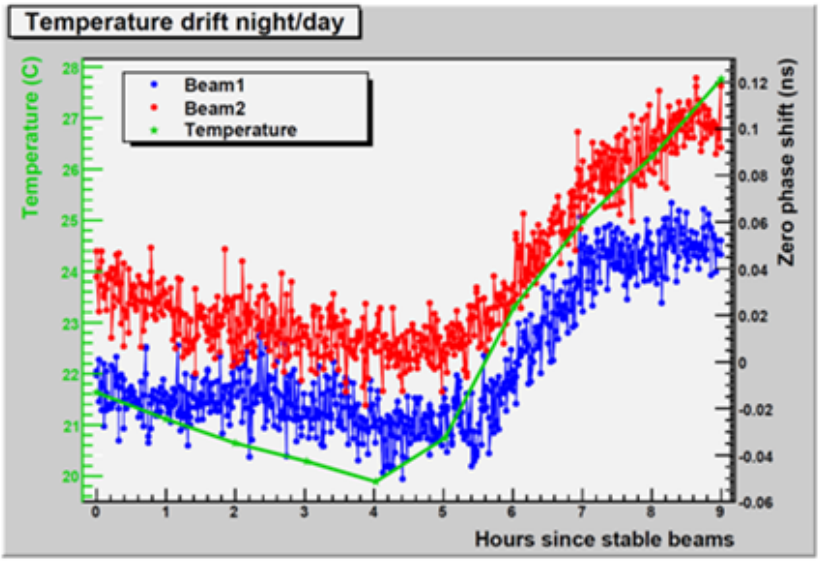

Figure 8.14: The trend plot comparing the zero-phase shifts of beam 1 (blue), beam2 (red) and temperature (green). The temperature changed by about 8 °C in 5 hours and the zero-shift phases varied by about 100 ps. This means that the clock edge was late by 100 ps with respect to the arrival time of each bunch of each beam at the end of fill with respect to the beginning of fill.

Figure 8.15 shows the zero-phase shift and the temperature drift over a period of about 90 days from the beginning of May to mid-July 2010. During this period the global LHCb timing has been shifted seven times, each of them by 0.5 ns in order to compensate against the timing drift. The zero-phase shifted by a total amount or 4 ns, while the average temperature went from 10 °C to about 25 °C. This corresponds to a shift of about 260 ps/deg over the 13 km of fibres that connects LHCb to the LHC global clock distribution system.

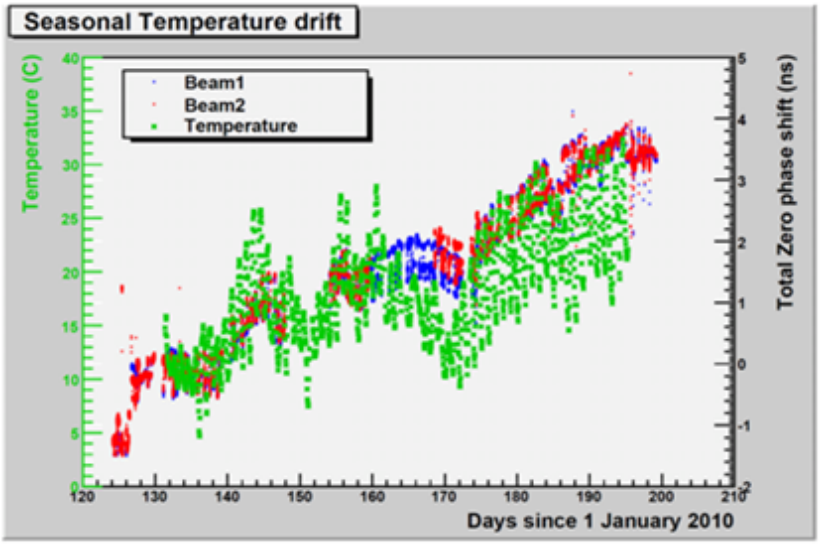

Figure 8.15: Temperature (green) and phase drifts during a period of 3 months.

8.6 Longitudinal scan of LHC beams

During Fill 1455, a so called *longitudinal scan* test was performed. The test aimed at displacing the beam in the longitudinal axis. This means that the beams were displaced along the LHCb Z-axis, which is the axis along the beam pipe and along the LHCb detector. The aim of this test was to search for asymmetries in the geometry of the optics of the LHC machine around the experiments, to search for ghost bunches lying outside the main LHC filled bucket and to test the timing monitoring systems of the four experiments and the LHC machine. Each beam had five bunches and one pilot bunch (low intensity bunch), with only one bunch colliding in LHCb. The polarity of the LHCb spectrometer magnet was such that the crossing angle at LHCb was about 740 μ rad.

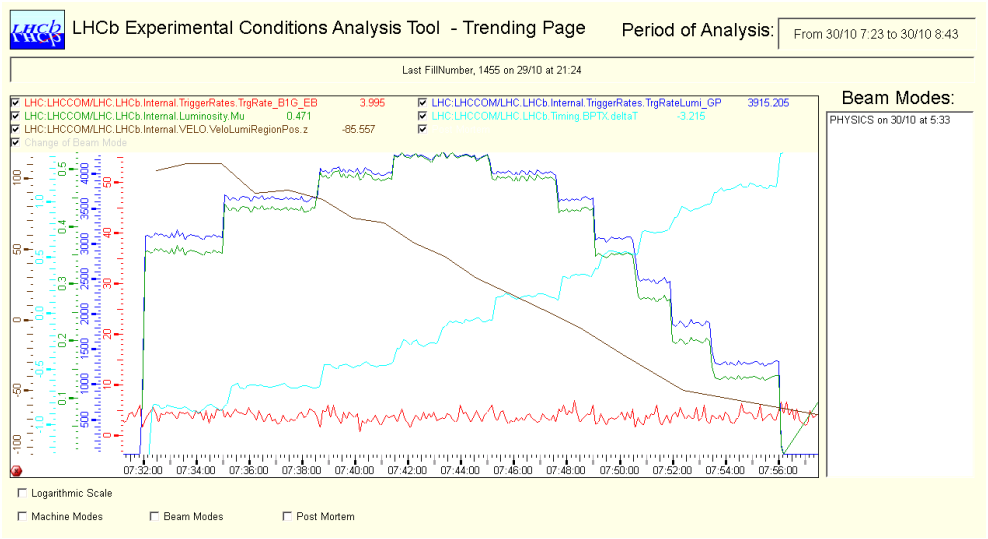

Figure 8.16: Trend of the parameters monitored during the longitudinal scan test when the timing of beam 1 was shifted from -1 ns to +1 ns. In red, beam gas due to Beam1. In dark blue, the trigger rate of collisions. In green, the μ. In light blue, the ΔT. In brown, the Z centroid of the luminous region as measured from the VELO.

In practice, the test was driven by the CERN Control Room, where the phase of beam 1 was shifted according to a predefined set of steps: from -15 ns to +15 ns in steps of 5 ns and from -1 to +1 in steps of 0.2 ns. Each experiment was monitoring the trigger rate of collisions, the trigger rate of beam gas due to beam 1, the average number of interactions per visible bunch crossing μ, the difference of the arrival time of the beams at the LHCb IP ΔT and the measured Z centroid of the luminous region from the VELO. In Figure 8.16, the test is drawn in a trend plot using the LHCb Experimental Analysis Tool.

Some conclusions can be already drawn from the trend plot. The beam gas rate

due to beam 1 stayed constant and at a low level throughout the whole test. This means that there was no significant beam degradation during the test and that the amount of parasitic charge lying around the LHC accelerator was very low. This can be deducted by considering that the bunches in beam 1 were shifted along Z, basically scannning for possible filled buckets around the main bucket.
The fact that beam 1 was shifted along Z can be seen by the VELO measurement of the Z centroid. It moved from 100 mm to -100 mm linearly, proving the fact that the center of the luminous region at the interaction region in LHCb was moving coherently with the phase shift. Moreover, whenever the time arrival of the beams at the LHCb IP was 0, the VELO measures a Z centroid at 0. Therefore, the alignement in time and in space of the two beams was good.
However, the trigger rate due to collisions show asymmetried. This was not expected and a more thorough analysis of this effect was performed in order to understand the cause of it.

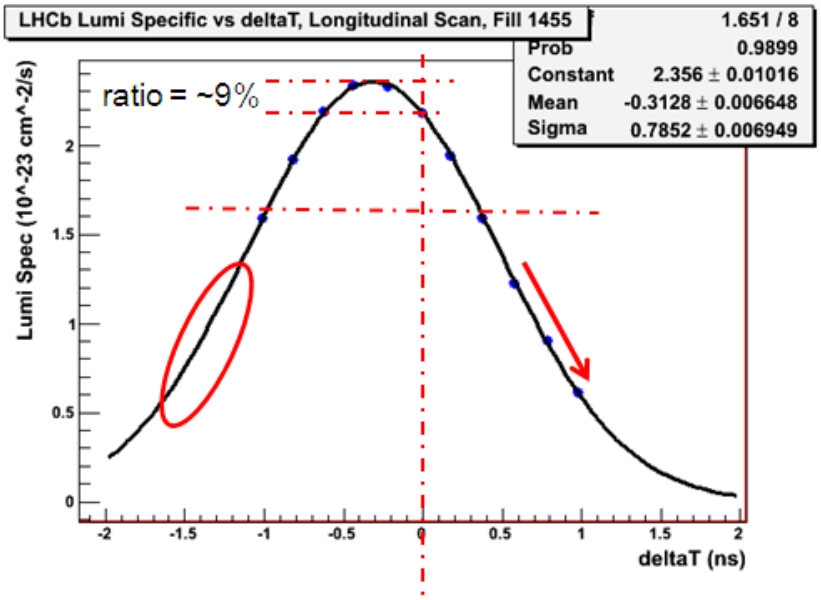

Figure 8.17: Plot of the LHCb specific luminosity against the measured ΔT during the scan between -1ns and +1ns. Whenever the phase of beam 1 was shifted by more than 1 ns (positive and negative direction), the rate of collisions was 0. These points were therefore not used in the analysis. It clearly visible the asymmetry of the plot and the maximum of the gaussian fit does not correspond to the expected 0 ns, but it is shifted by about 0.3 ns. The ratio of specific luminosity between the maximum and the value at $\Delta T = 0$ ns is about 9%.

Figure 8.17 contains the plot of the LHC specific instantanous luminosity against the ΔT as measured by the LHCb BPIM timing monitoring system. The asymmetry is clear considering the line corresponding to $\Delta T = 0$ ns. The plot was fitted with a gaussian function and the maximum of the fit is at about $\Delta T =$ -0.3 ns. The

ratio between the specific luminosity at $\Delta T = 0$ ns and the specific luminosity at $\Delta T =$ -0.3 ns is about 9%.

It is important to note that the trigger rate used for the luminosity measurement is a non-prescaled MinimumBias trigger rate from the Calorimeter detector. This means that there is no efficiency effect to be taken into account, because the travel time of the particles from collisions is compensated by the delay (positive or negative) of beam 1. It is important to note that the IP position at LHCb was optimized with a so called Luminosity Scan.

This phenomena can have different explanations:

- the squeezing β^* function at the LHCb IP does not have its minimum at Z = 0 (so called *hourglass effect*)
- the LHCb IP is shifted by about 10 cm along Z with respect to its designed position
- a small transverse shift (of about 30 μm) occurred during the scan due to geometrical effects of the LHCb crossing angle

It has been agreed that this test will be performed again during the 2011 physics run to investigate more in detail the effect of this phenomena. Since the ratio between the luminosity at the maximum and the luminosity at $\Delta T = 0$ ns is about 9%, this could have a big impact in the total integrated luminosity calculation.

8.7 The LHCb scintillator system acceptance

The LHCb scintillator system was used as an independent source of relative luminosity measurement in LHCb during the 2010 physics data taking. The scintillator system was used as a source of luminosity only during periods in which the LHCb detector could not provide a measurement of online luminosity because not ready for data taking or reconfiguring.

In order to calibrate the acceptance of the system with respect to the acceptance of the LHCb detector, a correction factor c is introduced in the luminosity formula for the scintillator system (BLS):

$$L_{BLS} = \frac{R_{BLS} * pileup_{BLS} * c}{\sigma_p} \tag{8.3}$$

The cross section used is the LHCb one corrected for the calorimeter efficiency ($\sigma_p = 57700\,\mathrm{mb}$). The pileup is calculated from the collision rate R_{BLS} and the beam characteristics as in Eq. 7.15. Three physics fills out of the 2010 data taking were considered. These fills 1440, 1450, 1453 had all the same LHC filling scheme, with 368 injected bunches per beam and 344 colliding bunches at LHCb. During these fills the maximum instantaneous luminosity of $1.7 \times 10^{32}\,\mathrm{cm}^{-2}\,\mathrm{s}^{-1}$ was achieved at LHCb.

The correction factor c was calibrated such that $\mathrm{L}_{BLS} = \mathrm{L}_{LHCb}$. Figure 8.18 shows the distribution of the correction factor c for the three fills in consideration. The mean values are compatible within errors, so c can be measured as the average of the three fills:

$$c = 5.95 \pm 1.87 \quad acceptance_{BLS} = 16.8\% \pm 5.3\% \tag{8.4}$$

From the distributions in 8.18, a poissonian contribution to the correction factor c is present. This is due to the pileup contribution to c at the beginning of an LHC Fill, when the pileup is higher and the collision rate as measured by the scintillator system is insensitive to high values of pileup.

The dependance of c from the pileup and the low acceptance value of the scintillator system with respect to the LHCb detector are two of the main reasons for an upgrade of the system for the 2011-2012 physics data taking as described in 4.1.4.

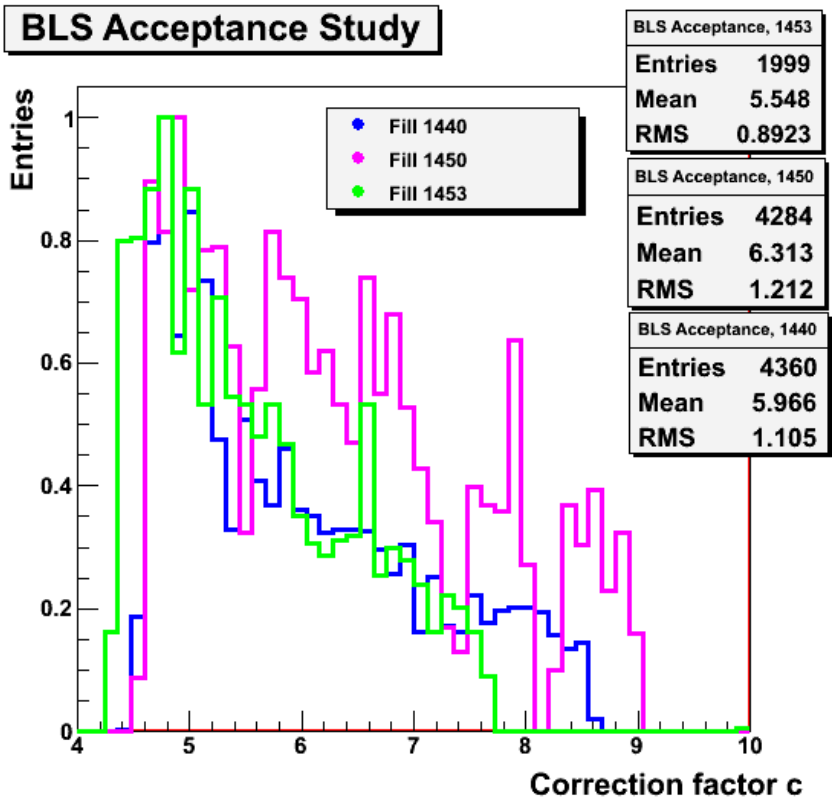

Figure 8.18: Distributions of the correction factor c for the LHC Fills 1440, 1450, 1453. Mean values are compatible within errors. However, a poissonian distribution is visible in the distributions. This is due to the dependence of the correction factor c to the pileup, especially at the beginning of an LHC Fill, when the pileup is higher.

8.8 Analysis of an LHC physics Fill using the bunch-by-bunch luminosities from the scintillator system

Figure 8.19 shows the bunch-by-bunch instantaneous and specific luminosities as measured by the scintillator system for Fill 1303. This physics fill was chosen because it is the first physics fill in which luminosity levelling was performed in LHCb. The beams were displaced vertically jsut after the beginning of the fill in order to limit the value of instantaneous luminosity and μ. Each step towards a higher value of the luminosity corresponds to a reduction of the beam separation and therefore a relative increase of luminosity. With this method, the specific luminosity was kept basically constant throughout the whole fill as the specific luminosity is independent from the bunch currents. It is therefore possible to observe possible degradation of the beams characteristics during the period in which they are spatially separated. Plots and trends in this section are generated using the software tools for experimental conditions described in 5.1.4.

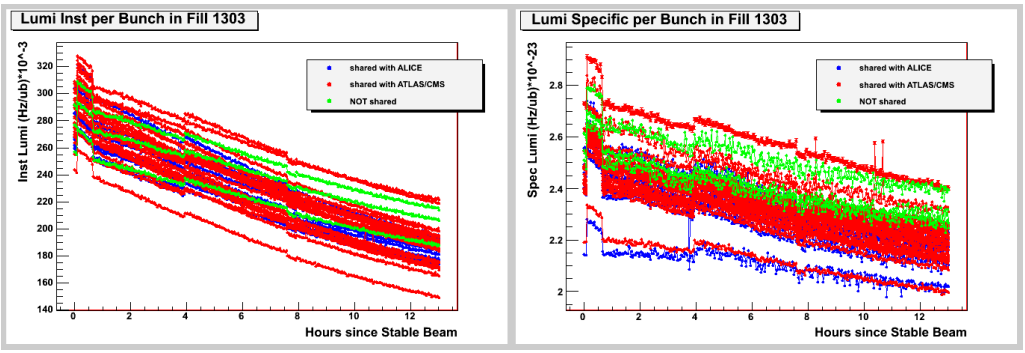

Figure 8.19: Trend of the instantaneous luminosity and specific luminosity per bunch as measured by the scintillator system during Fill 1303.

Figure 8.20 shows the LHCb Run Summary for the luminosity measurements. The peak μ in this physics fill was about 1.5 while the peak pileup was about 2. The total integrated delivered luminosity from the LHC was about $120\,\mathrm{nb}^{-1}$ and the total integrated recorded luminosity by LHCb was about $113\,\mathrm{nb}^{-1}$. The number of colliding bunches in LHCb was 32.

A consequence of the luminosity levelling is that the trigger rate did not change too much for the duration of the fill. This has some operational advantages as the trigger configuration does not change and the events are all similar in terms of complexity and multiplicity. Therefore the processing time is the same throughout the whole fill and increases the stability of the whole system. This helps the offline analysis of signals since a single cut can be chosen for all the events in the fill. The operational stability is shown in Figure 8.21 where the LHCb Run Summary for efficiencies is given.

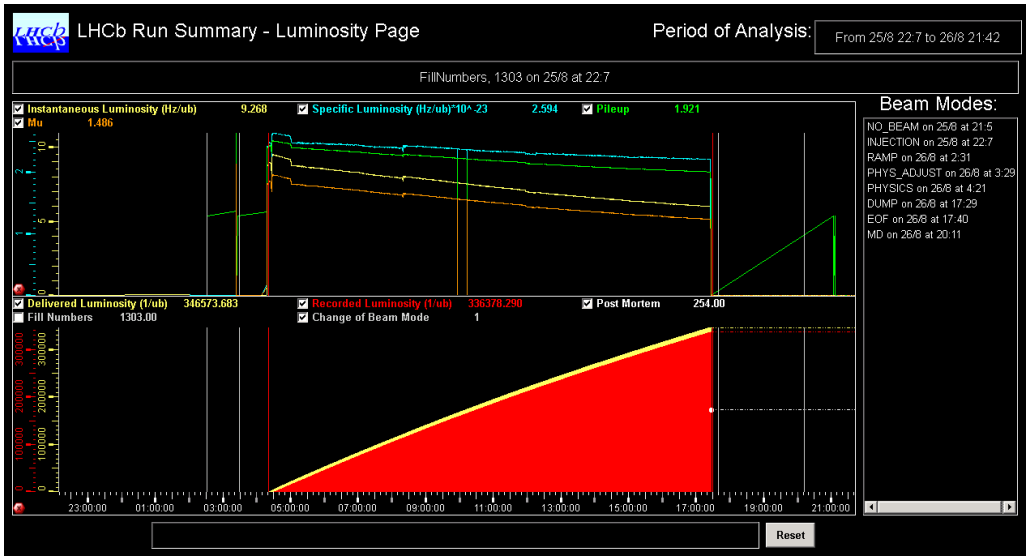

Figure 8.20: Luminosity Run Summary for Fill 1303.

Returning to Figure 8.19, the different colliding bunches are divided in three color codes according to the experiment in which they were colliding. In fact, because the LHCb experiment and the ALICE experiment are not located in a symmetric position with respect to each other and they are not located symmetrically with respect to ATLAS and CMS, some colliding bunches were colliding in ALICE, other were colliding in ATLAS/CMS and some of them were exclusively colliding in LHCb. Dividing the bunches in different color codes allows observing the different behaviour of the bunches. As expected, the bunches which were colliding exclusively in LHCb (green) and those who were shared with ALICE (blue) have a better luminosity lifetime with respect to the bunches which were shared with ATLAS/CMS. In fact the bunches shared with ATLAS/CMS collides three times per LHC turn, while the others once (LHCb exclusive) or twice (shared with ALICE). This confirms the good behaviour of the scintillator system as a source of bunch-by-bunch luminosity.

Moreover as shown in Eq. 7.7, the specific luminosities are normalized to the product of the population of the colliding pair of bunches. Therefore, the ratio between the instantaneous luminosity and the specific luminosity allows studying the emittance of the beams bunch-by-bunch over time throughout the entire fill. As shown in Eq. 7.4 and 7.5, the ratio between the instantaneous luminosity and the specific luminosity gives the product of the population for each colliding pair. In reality, the simple ratio results in the product of the emittance of each bunch times a geometrical factor due to the beams separation. For simplicity reasons, the geometrical factor is not considered in the analysis here presented. Knowing the β^*-function and the Lorentz factor γ allows studying the emittances per bunch by simply comparing them to the instantaneous luminosity. Figure 8.22 shows the

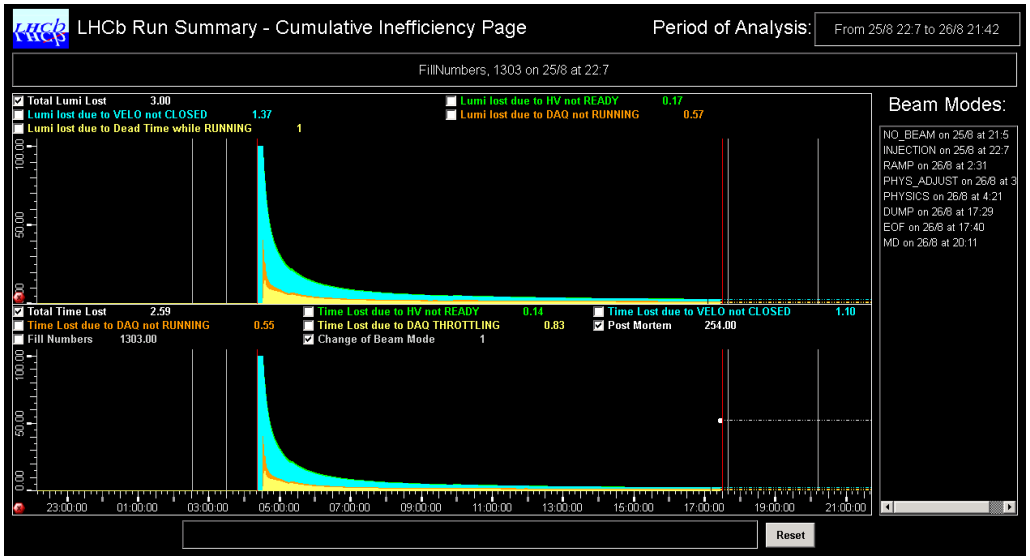

Figure 8.21: Efficiency Run Summary for Fill 1303.

trend of the emittance per bunch during the fill. The emittance grew by about 10% during the stable beams period. When the separation of the beams was 0 at the beginning of the fill, the starting value of the emittance was about 2.5 μm, which was a typical value througout the whole 2010 physics run. The same observations can be done on the trend for the intensities per bunch during the same fill, as shown in Figure 8.23, where each bunch lost about 15% of intensity during the stable beams period. The relative loss trend confirms that the bunches exclusively colliding in LHCb and those shared with ALICE have a better intensity lifetime than the ones shared with ATLAS/CMS as the relative loss throughout the whole fill is worse.

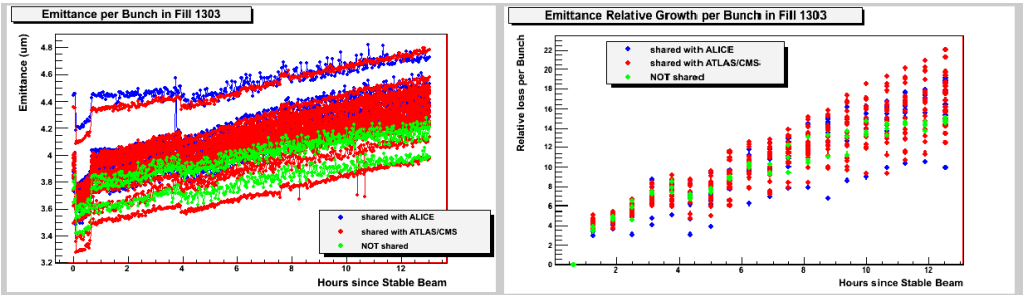

Figure 8.22: Example of a trend of the emittance per bunch and relative emittance growth as measured by the scintillator system during Fill 1303.

Correlating the information together, the bunches which are shared with ATLAS/CMS and colliding at LHCb have a worse luminosity lifetime, mostly due to

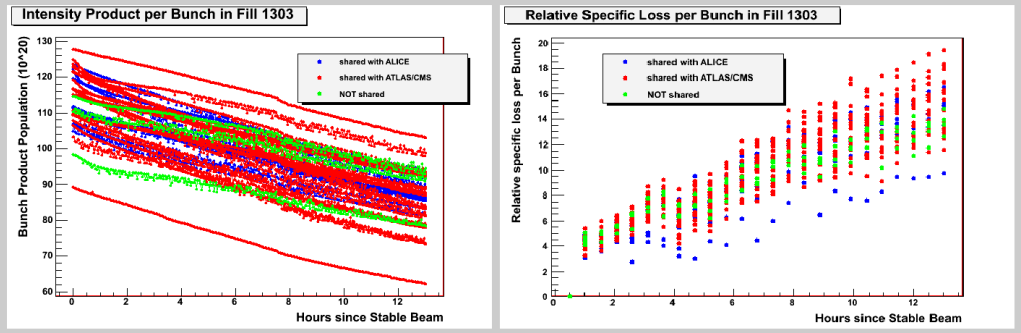

Figure 8.23: Example of a trend of the intensities per bunch during Fill 1303 and their relative loss.

intensity degradation. It can be concluded that the beam separation did not affect the beam characteristics. However, the beam characteristics were not extreme since the emittance was $3.5\,\mu$m, there were only 32 colliding bunches and μ was 1.4. Luminosity levelling will be extensively used during the 2011-2012 physics data taking as the machine intends to reach an instantaneous luminosity value which is above the design specification of the LHCb experiment. The analysis shown in this section can be therefore repeated in order to study beam characteristics during the separation with filling schemes which are more challenging in terms of beam characteristics (lower emittance, 50ns or 75ns scheme).

8.9 Global performance of the LHCb detector during $\sqrt{s} = 7$ TeV collisions in 2010

In this Chapter, a review of the global performance of the LHCb experiment is given. The plots used in this Chapter are generated automatically within the Online framework for global operation and control described and they are published publicly in the Operation Webpage.

The LHCb experiment was designed to run at an average instantaneous luminosity of $2 \times 10^{32}\,\mathrm{cm}^{-2}\,\mathrm{s}^{-1}$ with an average number of visible proton-proton interactions per bunch crossing μ of 0.4 at $\sqrt(s) = 7\,\mathrm{TeV}$. These conditions can be nominally achieved by injecting 2622 bunches per beam, with 1.15×10^{11} ppb, a squeezing function $\beta^* = 10\,\mathrm{m}$ and a normalized emittance $\epsilon_N = 3.75\,\mu\mathrm{m}$ at the LHCb interaction point. However, the running conditions in 2010 were different thanks to the outstanding performance of the accelerator. In fact, LHCb reached almost 80% of its nominal luminosity with 8 times less colliding bunches (344) and challenging beam characteristics ($\beta^* = 3.5\,\mathrm{m}$, $\epsilon_N = 3.5\,\mu\mathrm{m}$) with respect to the nominal LHC conditions.

Figure 8.24 shows the trend of the instantaneous peak luminosity over the LHC Fill Number. The maximum was about $1.7 \times 10^{32}\,\mathrm{cm}^{-2}\,\mathrm{s}^{-1}$. In particular, μ constantly stayed above the nominal LHCb design value and even reached the maximum of 2.5, which is almost six times the design value. In practice this meant that each proton-proton interaction increased complexity as number of tracks and number of interaction vertices as a function of the LHC Fill Number. Due to the main focus on the commissioning of the LHC machine in its first year of operation, LHCb had to face with preparations without knowledge about the ultimate parameters. However, the main LHCb operational objective to explore the experiment physics potential, by running in extreme conditions which were very different from the nominal ones, was completely fulfilled. The detector, the trigger and the readout performance could be tuned more efficiently and their potential explored more rapidly as a function of integrated luminosity.

Nevertheless, running as such $high - \mu$ could have non-negligible impacts on operational aspects:

- Events at $high - \mu$ have higher effective colliding rate per bunch crossing and they are more complicated, because they contain more than one interaction vertex. This saturates the available bandwidth of the LHCb readout system if events are not selected properly.

- Events with more than one interaction vertex contain more tracks. The track finding algorithm in the HLT takes naturally more time to process the event in this condition and therefore reducing the available processing power.

- Events with many tracks have higher particle flux which influences the per-

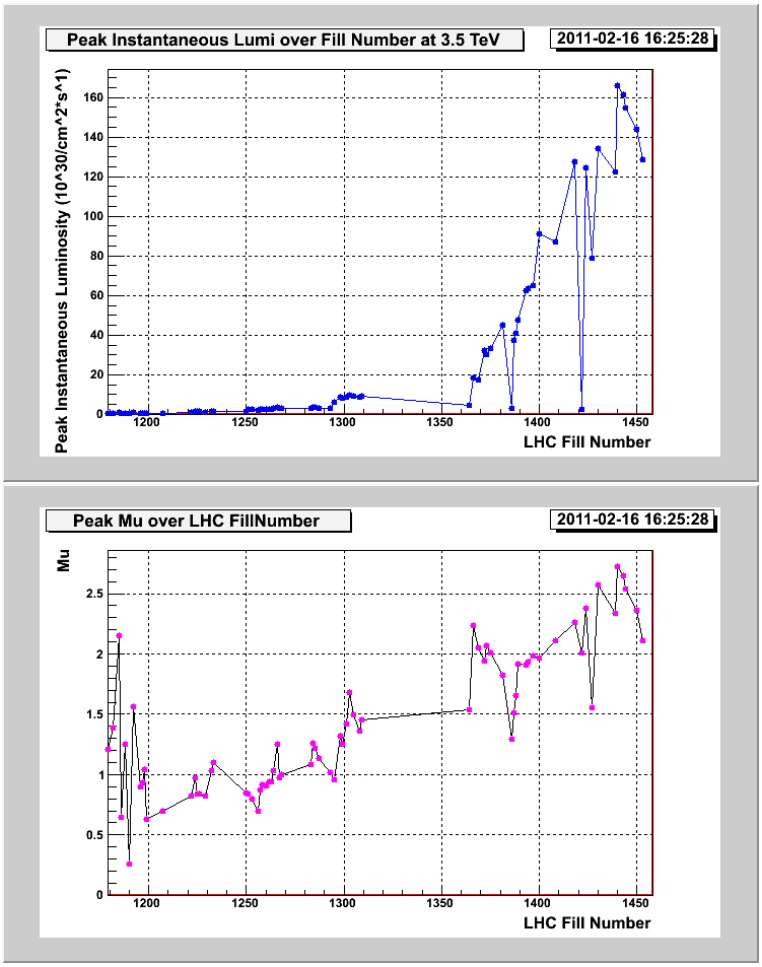

Figure 8.24: Trend of the instantaneous peak luminosity (left) and μ (right) over the LHC Fill Number as measured in LHCb during the 2010 physics data taking.

formance of the trigger. Eventually Global Events Cuts (GEC) on events would be needed in order to select only the very interesting events. Having a higher particle flux has a long-term impact on accumulated radiation doses and has an impact on the efficiency of each LHCb sub-detector and trigger.

The challenges of running an experiment for the first time in an new commissioned machine like the LHC together with the difficulties of running at six times the design parameters were overcome by the LHCb experiment. During the full 2010 physics run, the LHCb detector worked with more than 99.5% active channels (total of 544063) and the detector hardware behaved extremely well throughout the whole year 2010. $37.7\,\mathrm{pb}^{-1}$ of luminosity was recorded out of $42.2\,\mathrm{pb}^{-1}$ of delivered luminosity at LHCb with an overall efficiency just above 90%. Even though the main objective of LHCb was to explore the LHCb physics potential

and detector performance, the choice to follow the increasing instantaneous luminosity allowed LHCb to follow the same luminosity trend of ATLAS and CMS, which are designed to cope with two order of magnitude higher luminosities and one order of magnitude of μ in average. Figure 8.25 shows the integrated delivered and recorded luminosity as a function of the LHC Fill Number. More than 50% of the total integrated luminosity was collected in the last few physics fills which happened in the last week of physics runs. This had evident impact on the LHCb operation and trigger strategy as described just before, as the complexity of events grew quickly while most of the luminosity was being delivered. In the Figure, the efficiency of the LHCb detector and its breakdown components is described.

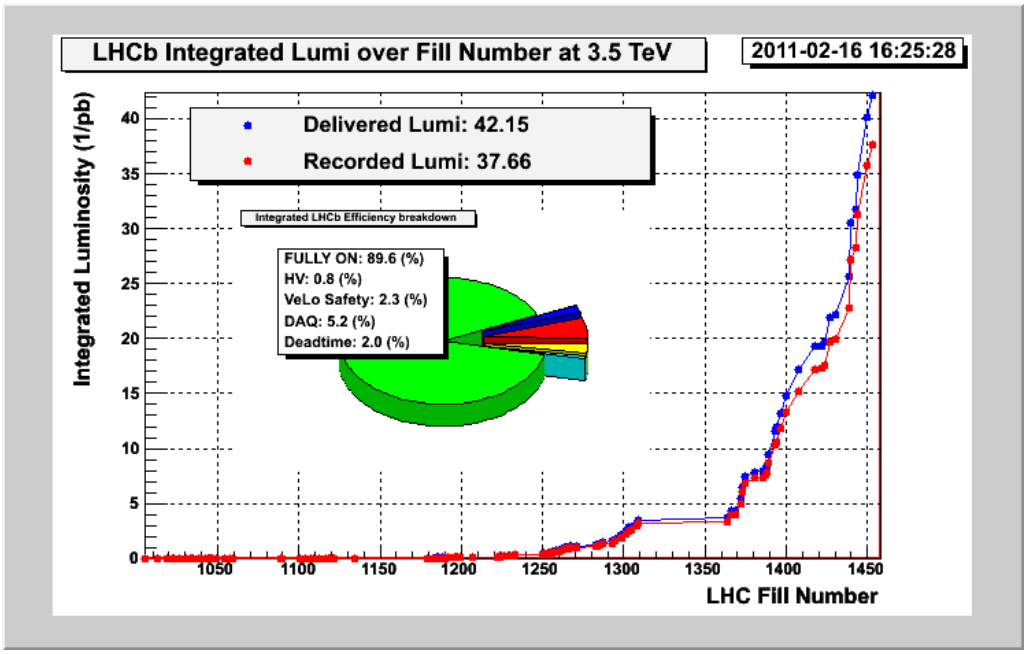

Figure 8.25: Trend of the integrated delivered (blue) and recorded luminosity (red) as measured by the online LHCb luminosity monitors. In the table, the global efficiency and the breakdown of efficiencies are shown.

Chapter 9

Conclusions

Les systèmes conçu, développé et mise au point pendant cette thèse permettent d'étudier les caractéristiques des faisceaux et du bruit de fond, de surveiller la synchronisation globale de l'expérience LHCb et de surveiller en temps réels la luminosité et la plupart des conditions expérimentales. Ils jouent un rôle clé dans l'optimisation de conditions expérimentales nécessaire à une physique de qualité. Les divers systèmes ont montré leur fiabilité et robustesse. Ils ont fortement contribué à l'efficacité globale de la première prise de donnée pour la physique en 2010.

Quelques concepts importants sont décrits dans cette thèse et montre des solutions possible au LHC, notamment un système de scintillateur pour le surveillance en ligne du faisceau, du bruit de fond et de la luminosité. Ce concept est extrêmement puissant grâce à sa flexibilité et sa simplicité. Il a d'ailleurs été repris par la collaboration ALICE qui a installer le même système que LHCb. La collaboration ATLAS et la machine ont également installer des systèmes semblables.

Un autre concept est l'utilisation d'un système centralisé pour la synchronisation et le contrôle de l'acquisition des données. Avoir accès à toutes les conditions expérimentales possibles de l'expérience LHCb et de la machine simultanément est essentiel. Cette approche requiert une très grande inter-connectivité, mais permet de prendre en compte les corrélation entre les différents systèmes, entre l'expérience et la machine ainsi que entre les différents expérience. Réaliser ces fonctionnalités nécessite un cadre logiciel très complexe pouvant accéder et manipuler à toutes les informations disponibles. Il permet aussi de produire des résumés afin de donner à tous moment un vue synthétique de la prise de données.

L'impact de cet outils logiciel sera bien plus important pendant la prise de données 2011/2012 car les conditions expérimentales dépendront fortement de l'organisation des paquets de protons dans la machine. Le but final est d'atteindre une luminosité instantanée constante pendante toutes la durée de la prise des données.

Ce concept a été aussi repris dans la proposition d'amélioration de LHCb prévue en 2018.

Chapter 10

Thesis main contributions

Here a list of the main publications is given. The *Main contributions* section includes publications to which I had a direct and heavy contribution and they sustain the concepts described in the thesis.

10.1 Main contributions

"LHCb global timing and monitoring of the LHC filling scheme"
F. Alessio, R. Jacobsson and Z. Guzik
LHCB-PUB-2011-004, LHCb Public Note, January 2011

"Operation and performance of the LHCb experiment"
F. Alessio on behalf of the LHCb Collaboration
Submitted to Journal of Physics, Talk presented at *Kruger2010* Conference, Kruger Park, South Africa, December 2010

"The LHCb Online framework for global operation control and experiment protection"
F. Alessio, R. Jacobsson and S. Schleich
Submitted to Journal of Physics, Talk presented at *CHEP2010* Conference, Taipei, Taiwan, October 2010

"An LHCb general purpose acquisition board for beam and background monitoring at LHC"
F. Alessio, R. Jacobsson and Z. Guzik
Journal of Instrumentation, 2011 JINST 6 C01001, Talk presented at *TWEPP10* Conference, Aachen, Germany, September 2010

"A Beam Loss Scintillator system for background monitoring at the LHCb experiment"
F. Alessio, R. Jacobsson, G. Corti, A. Bobrov, V. Talanov, R. Dzhelyadin
Proceedings of the *RuPAC2010* Conference, Talk presented at the *RuPAC2010*

Conference, Protvino, Russia, June 2010

"A 40 MHz trigger-free readout architecture for the LHCb experiment"
F. Alessio, R. Jacobsson and Z. Guzik
Proceedings of the *TWEPP09* Conference, Poster presented at the *TWEPP09* Conference, Paris, France, September 2009

"A 40 MHz trigger-free readout architecture for the LHCb experiment"
F. Alessio, R. Jacobsson and Z. Guzik
Proceedings of the *16th IEEE-NPSS Real Time* Conference, Talk presented at the *16th IEEE-NPSS Real Time* Conference, Beijing, China, May 2009

"Timing and fast control and readout electronics aspects of the LHCb Upgrade"
F. Alessio, R. Jacobsson and Z. Guzik
LHCB-PUB-2008-072, LHCb Public Note, December 2008

"An Experimental Conditions Analysis Tool for the LHCb experiment"
F. Alessio and R. Jacobsson
LHCb Public Note in preparation

"An LHCb scintillator system for beam, background and online luminosity monitoring"
F. Alessio, R. Jacobsson and Z. Guzik
LHCb Public Note in preparation

10.2 Other publications

"Electronics Architecture of the LHCb Upgrade"
K. Wyllie et al.
LHCB-PUB-2011-011, LHCb Public Note, March 2011

"The LHCb Run Control"
C. Gaspar et al.
Journal of Physics, Conference Series Vol. 219, Part 2, 022009

"The LHCb readout system and real-time event management"
R. Jacobsson et al.
IEEE TNS No. 57, pg 663-668

"LHCb Online event processing and filtering"
N. Neufeld et al.
Journal of Physics, Conference Series Vol. 119, Part 2, 022003

Chapter 11

Acknowledgements

The work presented in this thesis is the result of four years of intense and exciting work side by side with Richard Jacobsson. I would like to thank him for the support and tireless teaching he provided me during my Doctoral Student period at CERN. He was not only a guide in the learning process in the biggest scientific research center of the world but he was also a friend with which we surely lived one of the most exciting and unforgettable times in the history of science and physics, and of our lives. It will be hard to forget the nights spent up in the LHCb Control Room developing and fixing new implementations with passion, curiosity and love for culture and science in the unique environment of the LHC. The excitement for the LHC start-up and the excitement for the first proton-proton collisions will be also hard to forget.

I would also like to thank Renaud Le Gac as the Director of this thesis, for his fruitful and stimulating suggestions and for the unique opportunity to support my PhD at the Centre de Physique des Particules de Marseille at the Université de la Mediterranée.

I would like to thank the whole LHCb Online Team for their support and for having created a fruitful work environment where young students can express their abilities, competences and enlarge their knowledge without feeling the pressure of a big experiment. In this regard, the LHCb Collaboration has also given me the unique opportunity to work and study in a big physics experiment at CERN and to participate in fruitful discussions about physics, upgrade technologies and the operation of the experiment. I was proud to represent the LHCb experiment presenting the first operation and performance results in a conference in South Africa.

I would like to thank the referees Tiziano Camporesi and Rudiger Schmidt for having accepted the heavy duty of revise the work presented in this thesis which will surely gain value thanks to their experience and knowledge in the fields of science and physics.

Another big thank goes to Emily for her support, patience and interest in my work during this great exciting times at CERN. Surely this period will be remembered also for the time spent and for the moments of joy we lived together .

Il ringraziamento finale, forse il più importante, va a mia madre Adriana per avermi aiutato in tutti i modi a partecipare a questo grande avventura e progetto e ad avermi supportato con affetto, dignità e stima. Senza di lei, niente di tutto questo sarebbe stato possibile.

Appendix A

The details of the TFC system

Readout Supervisor: ODIN

Figure A.1 shows logically the principal blocks of functions of the LHCb Readout Supervisor. The TTC encoder circuit receives directly the LHC clock and the LHC orbit signal via a RF2TTC board. The clock is distributed on the board in a star fashion and is transmitted to all synchronous components of the LHCb readout system via the TTC system.

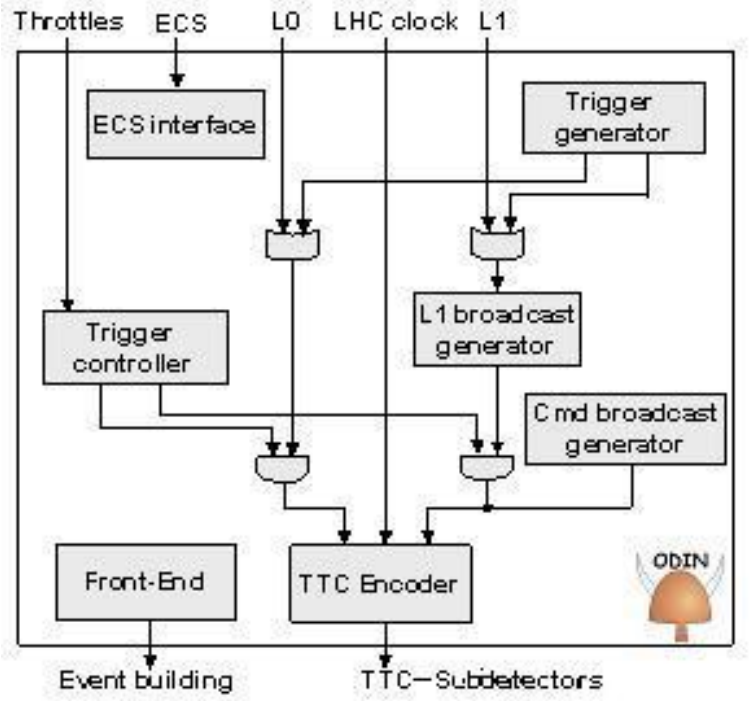

Figure A.1: Simplified logical diagram of Readout Supervisor.

The Readout Supervisor receives the L0 Trigger decision from the L0 Decision Unit (L0DU), together with the Bunch Crossing ID. In order to adjust the global latency of the entire L0 Trigger path to a total of 160 cycles, the Readout Supervisor has a pipeline of programmable length at the input of the L0 Trigger. Provided no other changes are made to the system, the depth of the pipeline is set once and for all during the commissioning with the first timing alignment. The Bunch Crossing ID received from the L0DU is compared to the expected value from an internal counter in order to verify that the L0DU is synchronized. ODIN controls the trigger rates according to the status of the buffers in the system in order to prevent overflows. Due to the distance and the high trigger rate, the L0 FE buffer occupancy cannot be controlled in a direct way. However, as the buffer activity is completely deterministic, ODIN has a state machine to emulate the occupancy.

In case an overflow is imminent, ODIN throttles the trigger, which in reality is achieved by converting trigger accepts into rejects. The slower buffers and the event-building components feed back throttle signals via the dedicated throttle network to ODIN, as described in Figure 2.10. Data congestion at the level of the High Level Trigger farm is signaled via the Experimental Control System (ECS) to the onboard ECS interface, which can also throttle the triggers. For monitoring and debugging, ODIN has history buffers that log all changes on the throttle lines.

ODIN also provides several means for auto-triggering. It incorporates a uniform random generator of L0 Triggers according to a Poisson distribution, a unit running several state machines synchronized to the LHC orbit signal for periodic triggering of a single or a specified number of consecutive bunch crossings (for timing alignment), triggering at a programmable time after sending a command to fire a calibration pulse, triggering at a given time on command via the contol system interface. ODIN can also transmits various reset commands, like the Bunch Counter Resets, Event Counter Resets, L0 FE electronics resets and ODIN can be programmed to send the commands regularly or solely on demand via the ECS interface. ODIN also incorporates a series of buffers analogous to a normal Front-End chain to record local event information and provide the DAQ system with the data on an event-by-event basis. The ODIN data block contains the *true* bunch crossing ID, the Event Number, the time trigger source, and it is merged with the other event data fragments during the event building. Information about bunch crossing, bunch intensity and bunch phase from the Beam Phase and Intensity Monitor are fed into the ODIN data block.

ODIN is able to assign and broadcast MEP destinations according to the MEP Requests of the farm nodes; ODIN can also send calibration events to a special part of the farm and determines the MEP factor on the fly according to the event types or trigger types by interleaving triggers and destination assignments to the Readout Boards.

The MEP Destination Assignment scheme is all implemented in an FPGA, as well as all the other functions of the board. In total ODIN has four different

FPGAs which can be easily programmed via a Software Interface. The choice of using custom-made electronics, in particular FPGAs, to control the entire readout of the LHCb detector was mostly due to have the possiblity to program and implement new functions with time. Counters and custom-made logic, such as trigger rates counters, luminosity counters, buffer occupancy counters, trigger types counters and deadtime counters are used for online run statistics and *live* display of information. These information are stored in a Database for offline analysis.

TFC Switch: THOR

The TFC Switch (Figure A.2) realises the partitioning of the TFC system [17]. It is a programmable patch panel that allows the distribution of the TFC information to the different parts of the Front-End electronics.

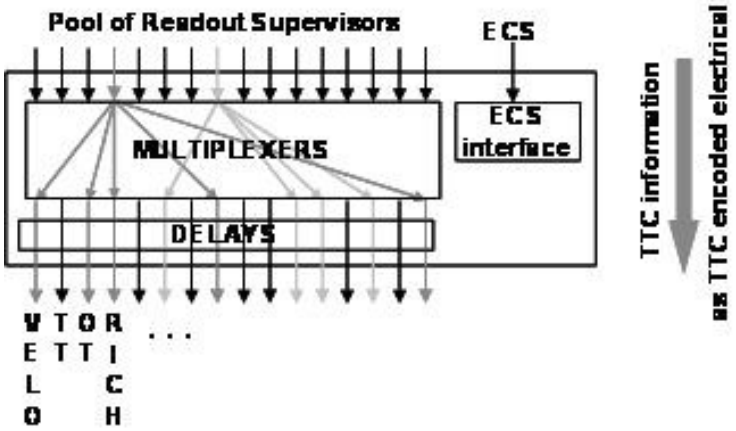

Figure A.2: Simplified TFC architecture to illustrate partitioning.

From the architecture of the TFC system, it follows that the Front-End electronics that is fed by the same output of the TFC Switch is receiving the same timing, trigger and control information. The connectivity provided by the board is not necessarily one-to-one: the TFC Switch should allow setting up several partitions, by associating a number of partition elements (e.g. sub-detectors), to several Readout Supervisors in order to accomplish different tasks. For example while the main ODIN is controlling a set of the detectors for data taking, the optional Readout Supervisors have the possibility of controlling separately other detectors for tests and debugging purposes. The TFC Switch has been designed as a 16x16 switch and thus allows the LHCb detector to be divided in 16 sub-systems. The TFC switch configuration setup is done remotely by software via the control system interface.

Throttle Switch and OR: MUNIN and HUGIN

Opposite to the control information flow provided through the TFC Switch, a Throttle Switch [18] (Figure A.3) has been designed with the aim of providing backward paths of throttle signals in case of imminent buffer overflows from the end buffers in the Readout Boards to the appropriate Readout Supervisor. The functionality of this module is the reverse to the one used in the TFC Switch: the signals from a set of subsystems forming a partition are OR'ed to produce a single output signal. The Switch has 16 inputs and 16 outputs. The inputs exist in both electrical and optical to allow galvanic isolation from the subsystems. Besides providing the ORing and the routing of the throttle signals the Throttle Switch also trace the behaviour of all input and output signals with a good time resolution.

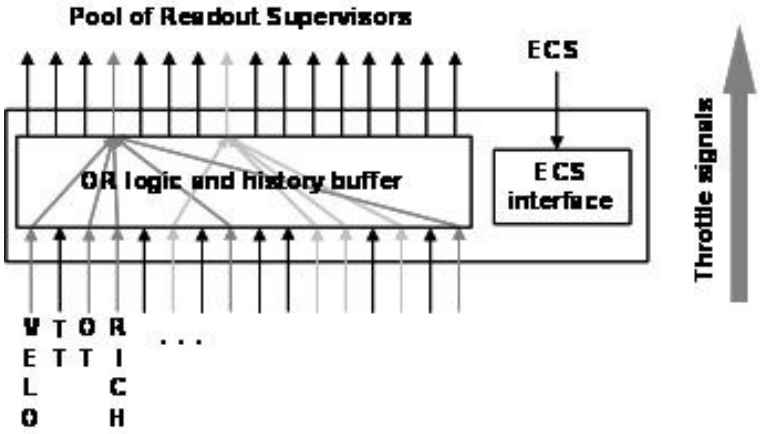

Figure A.3: Diagram of the Throttle Switch.

In addition to the Throttle Switch, a Throttle OR [18] has been designed to group throttle lines belonging to the same partition elements. It is identical to the Throttle Switch in all aspects except that it ORs 20 throttle inputs and transmits the result on a single output. The Throttle Switche and OR are also software configurable via the control system interface.

Appendix B

Introduction (in English)

The work presented in this thesis is here introduced. It is important to note in first instance that the topics covered in this thesis are extremely interconnected with each other. Most of the work was done as part of the global operation of the LHCb experiment during the first year of physics data taking at the LHC.

There are two main central topics in the thesis: the LHCb beam, background and luminosity monitoring systems and the LHCb optimization systems of experimental conditions. These systems are heavily connected to each other, as improving the machine beam, background and luminosity conditions will automatically improve the LHCb global operation by maximizing the ratio of luminosity recorded over signal background. At the same time, improving the operation of the experiment will help improve luminosity, by studying more accurately the beam and background conditions and therefore improving the LHC machine settings. In this thesis, the systems to accomplish the requirements of these two main topics are described in detail.

In Chapter 2, the accelerators complex and the LHC machine are briefly described. Then, the attention is moved to the LHCb experiment, its various subdetectors and their technologies, the LHCb readout system and the Timing and Fast Control (TFC) system. Particular care is given to the very complex experimental conditions at LHCb in Chapter 3 as they drive the motivations for the work presented in this thesis. In particular, the beam and background conditions in the region around the LHCb experiment and the LHCb global timing reception and distribution were the chosen topics. The Chapter includes a brief description of the modes and procedure of an LHC fill as seen from the LHCb experiment point of view.

The requirements and motivations for a complete system for beam, background and online luminosity monitoring at LHCb as well as for LHCb global operations are listed and described in Chapter 3.4. A state of the art is also given in order to frame the work presented in the thesis within the more general LHC environment.

Comparisons with other experiments are also provided as they add value to the choices of methods and implementations for the developed systems. Chapter 3.4 is a central chapter in this thesis as it contains the basis of the work presented here.

In order to satisfy the requirements a set of different hardware and software systems was developed. They are described in Chapters 4, **??**, 6 and 7.

Chapter 4 contains the description of the complete framework developed for beam, background and online luminosity monitoring at LHCb and touches briefly on the instrumentations involved. Amongst the systems described in this Chapter, an LHCb scintillator system is highlighted and described in details as it plays a central role in the beam, background and online luminosity framework at LHCb. This system is commonly referred to as the LHCb Beam Loss Scintillators system. The LHCb beam intensity and LHC filling scheme monitoring system is also described. These two systems are hardware systems and they are both implemented with a common general purpose LHCb readout eletronics board which is also described in this Chapter. The same board is also used for the global timing monitoring and control system which is described at the beginning of Chapter **??**.

The second part of Chapter **??** is dedicated to the description of the system optimizing the experimental running conditions of LHCb. It also includes the complete online software framework developed for LHCb global operations, machine protection and data exchange, with particular attention to the various software tools developed for these purposes: LHCb Experimental Analysis Tool, LHCb Run Summary, Operations Webpages and LHC Programme Coordinator automatic files exchange. Its integration within the PVSS-based LHCb Experiment Control System (ECS) is also described.

In order to manage all the systems described before and control the readout of the LHCb experiment, a centralized timing, trigger and readout control system was developed in LHCb. The beginning of Chapter 6 is dedicated to the description of this system and its central role in the LHCb global operations. A detailed proposal for an upgraded system for timing, trigger and readout control is outlined in the second part of the Chapter. This work is inserted in the more general work of the LHCb upgrade.

The LHCb timing, trigger and readout control is also responsible to monitor the online luminosity at LHCb, amongst many other functionalities. The theory behind the measurement of luminosity and the methods used in LHCb for the first year of running are given in Chapter 7. An alternative method for online luminosity measurement is also given at the end of the Chapter. Here, it is important to note that monitoring the online luminosity depends heavily on the beam and background characteristics. However, it drives directly the operations of an experiment, in particular the LHCb experiment which is designed to run at particular running conditions.

The final Chapter is entirely dedicated to presenting results obtained from the

first year of running at 3.5 TeV proton collisions at the LHC. Different analyses are presented, and their impact on machine commissioning, LHCb global operations and understanding of beam and background conditions are underlined. The presented analyses touches topics like the injection dynamics, the beam gas rates and their relation with vacuum, LHCb dedicated beam intensity calibration, timing monitoring results and clock phase drift due to temperature effects, luminosity per bunch and emittances per bunch, longitudinal scan of the LHC beams. A separate study on the scintillator system acceptance is also presented as the system was used as a source of online luminosity measurement which was independent from the LHCb detector. Finally the last section highlights the LHCb global performance during the 2010 physics data taking showing the good performance and implementation of the systems described above.

Appendix C

Conclusions (in English)

The work described in this thesis was developed, implemented and completely put in operations during the first year of physics data taking at the LHC. It was shown that it is aimed at studying beam and background characteristics, monitor the global timing of the experiment, monitor online the luminosity at LHCb and monitor most the experimental conditions which can affect the LHCb physics data quality. The many functionalities of the presented systems have been outlined in great detail and some selected topics of analysis have been presented in order to validate the good performance. The various systems in fact showed high reliability, completeness and robustness and hence it heavily contributed to the global efficiency of the LHCb experiment and also contributed directly to the commissioning and running of the LHC machine for first physics runs.

Some important concepts were also brought to attention in the thesis as possible solutions to be taken into account at the LHC. A scintillator system for beam, background and online luminosity monitoring system at LHC was described. The concept, even if not new, of monitoring beam and background characteristics and evaluating the luminosity with a scintillator based system proved to be extremely powerful, thanks to its flexiblity and simplicity. The concept in fact was also taken in consideration by the ALICE experiment, the ATLAS experiment and the LHC machine which are installing similar systems to the one in LHCb.

Another important concept which was presented is the importance of a centralized system for timing, trigger and readout control. The global timing of the LHCb experiment is centrally managed as well as the readout control. Moreover, having access to all possible experimental conditions from the LHCb experiment and the LHC machine allows for an extreme level of interconnectivity. This would allow also for possible correlation between different systems of an experiment and between different experiments with the LHC machine. It was shown that in order to achieve these functionalities a very complex software framework should be developed in order to have access to all possible information. The development of dedicated software tools is also essential in order to analyse, produce summaries

and files summaries for offline and post-mortem analysis.

This online framework will become even more important during the 2011/2012 physics data taking as the LHCb experiment running conditions will strongly depend on the beam and machine settings. The final aim is to reach a steady running performance, maximizing the recorded luminosity and the quality of data.

Finally, the concept of a centralized timing, trigger and readout control was also considered in the proposal of an upgraded readout control system for the upgrade of the LHCb experiment. In this thesis, the proposal for such an upgraded system is presented, with the functionalities, implementations and technologies involved. In this context, the use of FPGA also allows having extreme flexibility and high readout speed complying with the extreme specifications of an upgraded LHCb detector within the upgrade of the LHC accelerator.

Bibliography

[1] CERN Website [online], http://www.cern.ch

[2] LHC Machine Website [online], http://lhc-machine-outreach.web.cern.ch

[3] LHCb Collaboration, "Road Map for selected key measurements of LHCb", *LHCb-ROADMAP-1*, 2009

[4] LHCb Collaboration, "The LHCb Detector at the LHC", *2008 JINST 3 S08005*, 2008

[5] LHCb Collaboration, "LHCb Technical Design Report", *CERN-LHCC 98-4*, 1998

[6] LHCb Collaboration, "LHCb Online System Technical Design Report", *CERN-LHCC 2001-40*, 2001

[7] LHCb Collaboration, "LHCb Trigger System Technical Design Report", *CERN-LHCC 2003-31*, 2003

[8] J. Christiansen et al, "Requirements to the L0 front-end electronics", *CERN-LHCC 2001-14*, 2001

[9] G. Haefeli et al, "TELL1 - Specification for a common read out board for LHCb", *CERN-LHCb 2003-007*, 2003

[10] P. Koppenburg et al, "HLT Exclusive Selections Design and Implementation", *CERN-LHCC 2005-15*, 2005

[11] A. Barczyk et al., "The New LHCb Trigger and DAQ Strategy: a system architecture based on Gigabit-Ethernet" , *IEEE TNS, vol. 51, no 3*, 2004

[12] R. Cornat et al, "Level-0 decision unit for LHCb", *CERN-LHCb 2003-065*, 2003

[13] R. Jacobsson et al, TFC website [online], http://lhcb-online.web.cern.ch/lhcb-online/TFC/default.html

[14] S. Baron et al, TTC upgraded system website [online], http://ttc-upgrade.web.cern.ch

[15] Z. Guzik and R. Jacobsson, "LHCb Readout Supervisor 'ODIN' with a L1 Trigger - Technical reference", *EDMS 704078-V1.0*, Aug 2005

[16] R. Jacobsson, "Controlling the Multi-Event Packet Distribution in the 1 MHz Readout", Technical Note in preparation

[17] R.Jacobsson et al, "The TFC Switch specifications, *CERN-LHCC 2001-018*, 2001

[18] R. Jacobsson et al, "Driving the LHCb Front-End Readout", *IEEE-TNS*, 2004

[19] R. W. Assmann et al, "The final collimation system for the LHC", *LHC-PROJECT-REPORT-919*, 2006

[20] R. B. Appleby et al, "Simulation of Machine Induced Background in the LHCb Experiment: Methodology and Implementation", *LHCb-PROC-2010-072*, 2010

[21] Ch. Ilgner et al, "The Conditions Monitor of the LHCb Experiment", *TNS-00807-2009*, 2010

[22] F. Alessio, R. Jacobsson, Z. Guzik, "An LHCb scintillator system for beam, background and luminosity monitoring at the LHC, *CERN-LHCB-PUB-2011-xxx*, 2011

[23] F. Alessio, R. Jacobsson, Z. Guzik, "LHCb global timing and monitoring of the LHC filling scheme", *CERN-LHCB-PUB-2011-004*, 2011

[24] M. Agari et al, "Radiation Monitoring System for the LHCb Inner Tracker", *CERN-LHCb 2007-062*, 2007

[25] LHCb Collaboration, "LHCb VELO: Technical Design Report", *LHCb-TDR-5*, 2001

[26] LHCb Collaboration, "LHCb calorimeters: Technical Design Report", *LHCb-TDR-2*, 2000

[27] R. Dzhelyadin, "The injection beam monitor counter", *CERN EDMS 935193*

[28] L. Roy, "BLS long distance cables", *CERN EDMS 1123302*

[29] B. Jost et al, "The use of Credit Card-sized PCs for interfacing electronics board to the LHCb ECS", CERN-LHCb 2001-147

[30] D.P. McGinnis, "The design of beam pickups adn kickers", *Technical Report, FNAL, 1994*

[31] C. Ohm, "Phase and Intensity Monitoring of the Particle Beams at the ATLAS Experiment", *THESIS-LITH-IFM-EX-07/1808-SE*

[32] F. Alessio, R. Jacobsson, Z. Guzik, "An LHCb general purpose acquisition board for beam and background monitoring at the LHC", *Journal of Instrumentation, 2011 JINST 6 C01001*, 2010

[33] LHC Logging Project [online], http://lhc-logging.web.cern.ch/lhc-logging/

[34] ACAM Electronics, "Ultra-high Performance 8 Channel Time-to-Digital Converter", *TDC-GPX technical datasheet*

[35] F. Alessio, R. Jacobsson, S. Schleich, "The LHCb Online framework for global operation control and experiment protection", *submitted to Journal of Physics, to be published*

[36] ETM PVSS website [online], http://www.pvss.com

[37] R. Schmidt, "Safe LHC parameters generation and transmission", *LHC-CI-ES-0004*, *CERN EDMS 810607*

[38] E. Tsesmelis, "Data to be exchanged between the LHC machine and the experiments", *CERN EDMS 701510*

[39] CAEN website, "V1718 controller card" [online], http://www.caen.it/nuclear/product.php?mod=V1718

[40] C. Gaspar, "DIM, A distributed Information Management System" [online], http://dim.web.cern.ch/dim/

[41] Z. Guzik and R. Jacobsson, "Glue Light - A Simple Programmable Interface between the Credit Card PC and Board Electronics", CERN-LHCb 2003-056

[42] R. Jacobsson, "Building Integrated Control Systems for Electronics Boards"', *IEEE TNS, vol. 55, no 1*, 2008

[43] LHCb Collaboration, "Expression of Interest of an LHCb upgrade", *CERN-LHCC 2008-007*, 2008

[44] LHCb Collaboration, "Letter of Intent for an LHCb upgrade", *CERN-LHCC-2011-001*

[45] K. Wyllie, F. Alessio, R. Jacobsson and N. Neufeld, "Electronics Architecture of the LHCb Upgrade", *CERN LHCb-PUB-2011-011*

[46] P. Moreira et al, "The GBT : A proposed architecture for multi-Gb/s data transmission in high energy physics", *TWEPP07 proceedings, pp 332-336*

[47] ALTERA website [online], http://www.altera.com/

[48] W. Herr and B. Muratori, "Concept of luminosity", *CERN Accelerator School pp 361-378*, 2003

[49] M. Ferro-Luzzi, "Proposal for an absolute luminosity determination in colliding beam experiments using vertex detection of beam gas interactions", *Nucl. Inst. Methods A 553, 3*, 2005

[50] P. Hopchev, "The beam-gas method for luminosity measurement at LHCb", *CERN-LHCb-PROC 2010-015*, 2010

[51] S. Van Der Meer, "Calibration of the effective beam height in the ISR", *ISR-PO-68-31, KEK-68-64*, 1968

[52] S. White, H. Burkhardt, "Luminosity Optimization", *Evian Workshop, pp 71-74*, 2010

[53] M. Ferro-Luzzi, "Determination of the luminosity at the LHC experiments", *ICHEP Proceedings*, 2010

[54] LHCb Collaboration, "Nu, Mu and Pile-Up. The LHCb definitions of what we see and what we don't see" [online], https://twiki.cern.ch/twiki/bin/view/LHCb/NuMuPileUp